Characterisation of Leucine-Rich Repeat Kinase-2 regulation and kinase function.

Laura Dunn

Thesis submitted in fulfilment of the degree of Doctor of Philosophy

Institute of Neurology
Department of Molecular Neuroscience
Queen Square
London
WC1N 3BG

DECLARATION

I, Laura Mary Dunn confirm that the work presented in this thesis is my own. Where information has been derived from other sources, I confirm that this has been indicated.

ACKNOWLEDGEMENTS

I would firstly like to thank my primary supervisor Prof. John Hardy for giving me the opportunity to work in his lab. Without his support, this work would not have been possible and for that I am extremely grateful. Thanks also to my secondary supervisor Dr. Patrick Lewis. Massive thanks to Dr. Selina Wray on both a professional and personal level. Submission of this thesis would not have been possible without your support and comments and as a friend, I am very lucky that you came to work in our lab. Big thanks also to my work wife Dr. George Allen for thesis comments and generally being legendary and supportive. I am grateful for the comments and support from Dr. Julia Fitzgerald and I'm glad we remained friends since you left. Thank you also for the input and friendship of so many people on the 9th floor, especially Abi Li. I look forward to your viva especially, it has been a long road!

Many thanks to Dr. Mark Cookson for allowing me to spend the first few months of my PhD at the NIH and especially to Dr. Elisa Greggio for taking me under her wing. You showed me great kindness during my time in DC and I will always appreciate everything you did for me. Thanks to Dr. Helene Plun-Favreau for help and advice regarding signaling cascades and to Dr. Emma Deas for the advice and help (often involving radiation!) in trying to get the gatekeeper technique to work. I am grateful for the work of Dr. Wendy Heywood at the ICH Mass spectrometry service and to Miss Daniah Trabzuni for running my RNA samples on Agilent chips. Thank you to everyone at the IoN and Royal Free involved in the collection and generation of fibroblasts from the LRRK2 mutation patients. I am incredibly grateful to the individuals who donated their skin cells. Finally, thank you to Dr. Kirsten Harvey, Dr Rosa Sancho, Dr. Daniel Berwick and Mr Bernard Law at the School of Pharmacy, for the collaboration involving DVL and TUBB5.

I would like to thank my family for the support they have given me throughout this process, in particular my Mum and Dad. I acknowledge in particular my partner, Robina, who has shouldered me through this whole process. I am sorry for the time I have spent explaining my work to you on napkins in restaurants, thank you for putting up with me!

ABSTRACT

Mutations in Leucine-Rich Repeat Kinase 2 (LRRK2) are one of the most common causes of genetic Parkinson's disease (PD), with mutations thought to account for around 5% of all familial cases. LRRK2 is a large protein with a kinase and GTPase domain and multiple protein-protein interaction domains. Regulation of this protein is complex, with GTPase activity known to regulate kinase activity. Similarly, LRRK2 can autophosphorylate and is thought to form a dimer when active. Mutations in LRRK2 are numerous, with the most prevalent mutations occurring in the enzymatic core of this protein.

This thesis describes work done to characterise the regulation and functioning of LRRK2, in order to further contribute towards understanding how mutations in this protein can lead to the pathogenesis of PD. Using BlueNative PAGE and glycerol gradient centrifugation, the quaternary structure of LRRK2 was assessed. *In vitro* kinase assays were used to characterise kinase activity of recombinant LRRK2 and a number of putative kinase substrates were also investigated. Identification of new kinase substrates was attempted and immunoprecipitation of LRRK2 to identify novel binding partners was also performed.

Results of these experiments showed that familial mutations do not affect the ability of LRRK2 to form complexes. Instead, some mutations are affecting the enzymatic activity of LRRK2. Dephosphorylating LRRK2 showed that dimer formation is dependent on phosphorylation. Dephosphorylated forms of LRRK2 were more likely to be monomeric and displayed lower kinase activity than higher molecular weight forms. *In vitro* kinase assays to evaluate LRRK2 kinase substrates showed that α-synuclein is phosphorylated at low levels by G2019S but not wild-type LRRK2. Attempts to identify novel kinase substrates and binding partners of LRRK2 were unsuccessful, however evaluation of putative kinase substrates *in vitro* showed that DVL3 and TUBB5 may be good candidates for further investigation, as they were robustly phosphorylated by LRRK2. These results contribute towards our understanding of how LRRK2 functions and future studies based on these results may prove useful in aiding our understanding of how LRRK2 can cause PD pathogenesis.

CONTENTS

LIST OF EQUATIONS

LIST OF FIGURES

LIST OF TABLES

ABBREVIATIONS

α-syn	α-synuclein
4E-BP	4E-binding protein
AADC	Aromatic L-amino acid decarboxylase
AD	Autosomal dominant
ADP	Adenosine diphosphate
Akt	Protein kinase B
ANK	Ankyrin-repeats
ANOVA	Analysis of variance
AR	Autosomal recessive
ATP	Adenosine triphosphate
AV	Autophagic vacuole
BAD	Bcl-Xl and Bcl-2 associated death promoter
Ben-ATP	N^6- (benzyl)-ATP
BN	BlueNative
bps	Base pairs
BSA	Bovine serum albumin
CCCP	Carbonyl cyanide m-chlorophenyl hydrazone
cDNA	Complementary deoxyribonucleic acid
cGMP	Cyclic guanosine monophosphate
CK1	Casein kinase 1
COMT	Catechol-O-methyltransferase
COR	C-terminus of ROC
C_T	Cycle threshold value
Da	Daltons
DAPK1	Death-associated protein kinase 1
DDM	N-Dodecyl-ß-maltoside
DMEM	Dulbecco's modified Eagle's medium
DMSO	Dimethyl sulfoxide
ΔN-LRRK2	N-terminally truncated LRRK2, residues 970-2527
DNA	Deoxyribonucleic acid
dNTPs	Deoxynucleosides

DPBS	Dulbecco's PBS
DVL	Dishevelled protein
ECL	Electrochemiluminescent
ER	Endoplasmic reticulum
ERK	Extracellular-regulated kinase
ESI-QTOF	Electrospray ionisation quadrupole-time-of-flight
FBS	Fetal bovine serum
Foxo	Forkhead Box O
FPLC	Fast protein liquid chromatography
GAD	G-protein activated by nucleotide-dependent dimerisation
GAPDH	Glyceraldehyde 3-phosphate dehydrogenase
GBA	Gene encoding glucocerebrosidase
GCR	GTPase co-regulator
GDP	Guanosine diphosphate
GEF	Guanine exchange factor
GFP	Green fluorescent protein
GRK2	G-protein-coupled receptor kinase 2
GSK3β	Glycogen-synthase kinase 3β
GST	Glutathione-S transferase
GTP	Guanosine triphosphate
Hek293T	Human embryonic kidney 293T cells
HLPC	High-performance liquid phase chromatography
HSP90	Heat-shock protein 90
IAP	Inhibitor of apoptosis
IBR	In-between RING domain
IoN	Institute of Neurology
JNK	c- Jun N-terminal Kinase
KD	Kinase dead
KO	Knockout
L-DOPA	L-3,4-dihydroxyphenylalanine
LBs	Lewy bodies
LC	Locus coeruleus
LDH	L-lactic dehydrogenase

LDS	Lithium dodecyl sulfate
LRRK1	Leucine-rich repeat kinase 1
LRRK2	Leucine-rich repeat kinase 1
LRRs	Leucine rich repeats
MAO	Monoamine oxidase
MPP+	1-1-methyl-4-phenylpyridinium ion
MPTP	1-methyl-4-phenyl-1,2,3,6-tetrahydropyridine
mRNA	Messenger ribonucleic acid
MSA	Multiple system atrophy
mTOR	Mammalian target of Rapamycin
NDPK	Nucleoside Diphosphate Kinase
NO	Nitric Oxide
p-	Phospho-
PAGE	Polyacrylamide gel electrophoresis
PD	Parkinson's disease
PBS	Phosphate buffered saline
PBS-T	PBS supplemented with 1% (v/v) Tween
PCR	Polymerase chain reaction
PE-ATP	N^6-(2-phenylethyl)-ATP
PINK1	PTEN induced kinase 1
PKC	Protein kinase C
PRKN	Gene encoding parkin
PSP	Progressive Supranuclear Palsy
RIPK	Receptor interacting protein kinase
RIPK5	Receptor interacting protein kinase 5
RNA	Ribonucleic acid
ROC	Ras of complex proteins
ROS	Reactive oxidative species
RT	Room temperature
RT-PCR	Reverse-transcriptase PCR
SDS	Sodium dodecyl sulfate
SNCA	Gene encoding α-synuclein
STE	Serine/ threonine kinase

SNpc	Substantia Nigra *pars compacta*
TAE	Tris base, acetic acid and EDTA buffer
TAP	Tandem affinity purification
TDP-43	TAR DNA-binding protein 43
TH	Tyrosine hydroxylase
TLC	Thin-layer chromatography
TUBB5	β-tubulin isoform 5
UPDRS	Unified Parkinson's disease rating scale
UPS	Ubiquitin proteasome system
Wnt	Wingless and int
WT	Wild-type
x g	Relative centrifugal force
Y2H	Yeast II hybrid

PUBLICATIONS ARISING FROM THIS THESIS

-Li Y, **Dunn L**, Greggio E, Krumm B, Jackson GS, Cookson MR, Lewis PA, Deng J. (2009). The R1441C mutation alters the folding properties of the ROC domain of LRRK2. *Biochim Biophys Acta*. **1792**(12):1194-7.

-Deas E, **Dunn L** (2010). Unraveling LRRK2 pathogenesis: common pathways for complex genes? *J Neurosci.* **30**(5):1577-9.

1. INTRODUCTION

1.1 SYMPTOMS OF PARKINSON'S DISEASE

1.1.1 Clinical symptoms

Parkinson's disease (PD) was first described by James Parkinson in his 1817 paper, 'An Essay on the Shaking Palsy' (Parkinson, 1817). The symptoms described in the paper were notably those displayed by 6 men, 3 of whom he saw "casually in the street." The traits characteristic to all six men were that they displayed "involuntary tremulous motion... with a propensity to bend the trunk forwards, and to pass from a walking to a running pace: the senses and intellects being uninjured." These accurate observations led to the disease being named after Parkinson by French neurologist Jean Martin Charcot in the 1850's (Lees, 2007). Clinical diagnostic criteria for PD have since been established, the most commonly used being the Queen Square Brain Bank clinical diagnostic criteria (Table 1.1).

Inclusive Criteria	Exclusive criteria
	-MPTP exposure
	-History of strokes with progressive step-wise parkinsonian features
	-Repeated head injuries
-Bradykinesia	-Cerebellar signs
	-Supranuclear gaze palsy
Plus one of the following,	-Sustained remission
	-Oculogyric crises
-Muscular rigidity	-Unilateral symptoms after 3 years
- 5-7 Hz resting tremor	-Neuroleptic treatment at the onset of symptoms
-Postural instability	-Early severe autonomic involvement
	-Babinski sign
	-Cerebral tumour or hydrocephalus
	-Negative response to L-DOPA
	-More than one affected relative

Table 1.1. Summary of the inclusive and exclusive criteria for a diagnosis of Parkinson's disease to be upheld. (Adapted from Litvan *et al*. 2003).

According to the criteria outlined in Table 1.1, PD is characterised clinically by symptoms of bradykinesia and accompanied by either muscle rigidity, tremor at between 5-7Hz and/or postural instability, which are responsive to the dopamine precursor L-DOPA. Idiopathic, or sporadic PD is known to affect about 2% of the European population aged over 65, with the prevalence increasing as the population gets older (De Rijk *et al.* 1995).

The clinical features of PD are caused by the death of dopaminergic neurons in the Substantia Nigra pars compacta (SNpc), although many different cell types die in PD (reviewed in Surmeier *et al.* 2011). Symptoms are thought to show when neuronal loss reaches about 80% and it has been estimated that disease progression takes 14 years to reach a wheelchair-bound state, from initial onset (Hoehn, 1987). The progression of PD has been shown to occur in distinct stages, and is often quantified in terms of the Hoehn and Jahr scale (Hoehn *et al.* 1967) or the unified PD rating scale (UPDRS) (Fahn, 1987), which place symptoms in stages according to the restrictive effects that are placed on the life of a patient. Additionally the motor deficits characteristic of PD are accompanied by secondary symptoms and although these differ between patients, those most commonly observed are pain, impaired olfaction, personality change, mild executive cognitive deficits, dementia and depression (Quinn, 1997).

1.1.2 Treatment of PD

The discovery that dopamine depletion in mice results in parkinsonism, by Arvid Carlsson (Utley *et al.* 1965) and the discovery by Oleh Hornykiewicz that PD sufferers have a dopamine depletion in the striatum (Hornykiewicz, 1962), were instrumental in the development of drug therapies for PD. Use of the dopamine precursor L-3,4-dihydroxyphenylalanine (L-DOPA) in the 1960's, showed that this drug can alleviate many PD motor symptoms (Birkmayer *et al.* 1962, Cotzias *et al.* 1968, Anden *et al.* 1970). The addition of the peripheral aromatic L-amino acid decarboxylase (AADC) inhibitor benserazide to L-DOPA preparations prevents peripheral conversion of L-DOPA to dopamine by AADC, as benserazide cannot cross the blood brain barrier. Instead conversion to dopamine occurs in the brain,

minimising side effects in the peripheral nervous system and allowing the maximal amount of dopamine to be targeted to the basal ganglia (Birkmayer *et al.* 1967, Papavasiliou *et al.* 1972).

L-DOPA therapy is accompanied by many side effects. Dyskinesias often occur with higher doses of L-DOPA and the 'on/off' cycling of medication efficiency means that patients spend periods of time when their medication is not having any effect. As such, modern contributions to PD therapy aim to ensure that the effects of medication are exerted as evenly as possible, while trying to balance the dyskinesias induced by excessive dopamine. To this effect, L-DOPA is frequently co-prescribed with dopamine agonists such as ropinirole hydrochloride, which work by directly mimicking the action of dopamine by directly agonising dopamine receptors (Jenner, 2003). Dopamine agonists are common in PD therapy, however they have recently been associated with a number of additional side effects including pathological gambling, hypersexuality and addictive behaviours (reviewed in O'sullivan *et al.* 2009). PD treatment plans also often include monoamine oxidase-B (MAO-B) inhibitors, which act by stopping the breakdown of dopamine after it has been released into the synapse and prolong the effects of L-DOPA. Catechol-O-methyl transferase (COMT) inhibitors are a more recent addition to the medications available to PD patients and also increase the availability of dopamine by inhibiting its breakdown (reviewed in Varanese *et al.* 2010).

1.2 PATHOLOGY

Macroscopic changes in the brains of PD sufferers are visible as pallor of the SNpc and Locus Coeruleus, due to the death of dopaminergic neurons containing the pigment neuromelanin (Greenfield *et al.* 1953). It has been shown that neuronal death in PD always starts with the SNpc and follows a very specific pattern, namely that neurons in the venterolateral tier die preferentially (Gibb *et al.* 1990). The SNpc contains neurons involved in the nigrostriatal pathway, a descending pathway that is afferent to the striatum and serves as the main input to the basal ganglia. Loss of these neurons in the nigrostriatal pathway, means that

dopaminergic input to the striatum is diminished and output dampened in turn, resulting in the motor deficits that present in PD (Hurtig *et al.* 2000).

Postmortem, a diagnosis of PD is upheld if Lewy bodies (LBs, see Figure 1.1) are found in the SNpc and LC (Hughes *et al.* 1992). LB accumulation and distribution has been shown to occur prescriptively, starting in the dorsal motor nucleus at the glossopharyngeal and vagal nerves, and anterior olfactory nucleus and/or intermediate reticular zone (stage I), cumulating in neocortex and premotor cortex deposition in severely affected individuals (stage VI). It is according to this staging that individuals are often classified post-mortem (Braak *et al.* 2003). Cortical LBs are frequently seen, but are thought to be indicative of secondary cognitive symptoms such as dementia (Hurtig *et al.* 2000). LBs are cytoplasmic, proteinaceous inclusions (Lewy *et al.* 1912) which stain positively for ubiquitin and consist predominantly of the 134 amino acid peptide α-synuclein (α-syn) (Ueda *et al.* 1993).

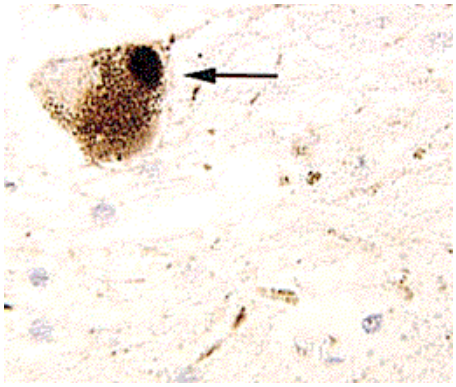

Figure 1.1. Lewy body stained for α-synuclein in the Substantia Nigra. Taken from (Spillantini *et al.* 1997).

α-Syn is a cytoplasmic protein that has been shown to exist both in membrane bound form (Zhu *et al.* 2003), and free in the cytosol (Kahle *et al.* 2000). α-Syn is abundant in the synapse and localisation of this protein to presynaptic vesicles has been shown (Withers *et al.* 1997). Although the exact function of α-syn is unknown, the peptide has been implicated in a number of functions including SNARE formation (Chandra *et al.* 2005), regulation of dopamine transmission

(Perez *et al.* 2002) and recently as a ferrireductase (Davies *et al.* 2011), however there is still much debate about the physiological role of this protein in cellular functioning. α-Syn is reported to share a 40% sequence homology with the 14-3-3 proteins and interactions with the 14-3-3 proteins, protein kinase C (PKC) and the apoptosis related BAD protein, have been shown (Ostrerova *et al.* 1999), as well as binding to synphillin-1 (Engelender *et al.* 1999).

α-Syn is unstructured when in the cytosol but has been shown to form α-helices when membrane bound (Jao *et al.* 2004). Atomic force microscopy has shown that α-syn structure forms an equilibrium between α-helical, unstructured and β-pleated sheet conformation when in solution (Sandal *et al.* 2008). An abundance of β-sheet folding can cause hydrogen bonding between polypeptide strands and the aggregation and formation of fibrils. The self-assembly of a fibril is thought to occur in stages which involve intermediates of possibly dimeric, or various forms of multimeric protofibril and are thought to be toxic (Lashuel *et al.* 2002). In PD, accumulation of these aggregates has been shown to cause Golgi fragmentation and impairment of cellular trafficking (Gosavi *et al.* 2002).

1.3 SELECTIVE VULNERABILITY OF DOPAMINGERGIC NEURONS IN PD

Studies comparing the bioenergetic differences between neuronal types, have shown that dopaminergic neurons are more sensitive to changes in bioenergetic functioning than non-dopaminergic neurons, as they rely more heavily on mitochondrial ATP (Gi-Ryang Kweon *et al.* 2004). The presence of dopamine is also thought to be an important contributory factor to PD neuronal pathogenesis (Stokes *et al.* 1999) as cytosolic dopamine is involved in redox reactions, which can produce reactive quinones, superoxide species and hydrogen peroxidase (H_2O_2) (Graham *et al.* 1978). This potentially exposes dopaminergic neurons to higher levels of oxidative stress than other cell types and means that dopaminergic neurons need to work harder at a basal level to combat oxidative stress (Berman *et al.* 1999).

The importance of alpha-synuclein in the specificity of dopaminergic cell loss has been emphasised by many studies which suggest that α-syn is likely to play a pivotal role in the synthesis and homeostasis of dopamine (reviewed in Lourenco Venda *et al,* 2010). α-Syn has been shown to localise to vesicles (Lee *et al.* 2008) and studies in triple synuclein knockout mice have implicated the synuclein family in SNARE formation (Burre *et al.* 2010). Supporting these ideas are the results from studies overexpressing human α-syn in mouse primary neurons, which has been shown to cause a reduction in the synaptic vesicle pool. This suggests that α-syn could be playing a role in vesicle formation and homeostasis (Nemani *et al.* 2010). Synuclein null-mutations in mice have been shown to cause an increased release of dopamine when neurons are stimulated electrically, with A30P overexpressing mice displaying decreased levels of stored dopamine prior to stimulation (Yavich *et al.* 2004). In this case, changes to the homeostasis of α-syn could be selectively detrimental to dopaminergic neurons.

It is well established that melanin-positive dopaminergic neurons in the SNpc die preferentially in PD (Hirsch *et al.* 1988), however dopaminergic neurons in the nearby ventral tegmental area (VTA) are spared (Dauer *et al.* 2003). The sequestering of dopamine into synaptic vesicles, has been shown to be facilitated by the vesicular monoamine transporter (VMAT) and reuptake of dopamine after release into the synapse, is facilitated by the (DAT) transporter (Henry *et al.* 1994). Interestingly, the DAT:VMAT2 ratio is reportedly higher in SNpc neurons than in those from the ventral tegmental area, suggesting that cytosolic dopamine is higher in SNpc neurons (Lourenco Venda *et al.* 2010). This could explain the selective vulnerability of neurons in the SNpc in PD, as increased oxidative stress caused by increased levels of cytosolic dopamine and dopamine metabolism, could be occurring (Miller *et al*. 1999). Taken together, a combination of impaired vesicle recycling and alterations to the amount of dopamine being released, could all contribute to a higher likelihood of pathological changes in dopaminergic neurons, and may explain the cell loss that is seen in the SNpc. A 'multiple hit theory' has been proposed whereby oxidation of dopamine, combined with an increased sensitivity to mitochondrial damage and disruption of α-syn homeostasis, combine

to cause a selective sensitivity of dopaminergic neurons (Sulzer *et al.* 2007). This theory also emphasises the importance of neuronal structure in PD pathogenesis. SNpc neurons are highly branched, with long poorly myelinated axons and large numbers of dendrites (Braak *et al.* 2006), meaning that they are likely more sensitive to the disruption of axonal transport. These disruptions, which manifest themselves as protein deposition and changes to autophagy in PD, are therefore likely to affect midbrain neurons more acutely than other neuronal subtypes (reviewed in Daniela, 2011).

1.3.1 The role of calcium signaling in dopaminergic cell loss

An important aspect of midbrain neuronal function is calcium signaling. The entry of Ca^{2+} through L-type channels has been implicated in the pacemaker activity of dopaminergic neurons and is thought to result in higher cytosolic calcium levels in these cells (reviewed in Surmeier *et al.* 2010). Studies in rodents lesioned with MPTP and rotenone, have shown that preventing Ca^{2+} entry using channel blockers is protective against these mitochondrial toxins (Surmeier *et al.* 2007). Comparison of dopaminergic neurons from the VTA and SNpc, has shown that addition of the dopamine precursor L-DOPA, results in approximately 3 fold higher accumulation of cytosolic dopamine in SNpc neurons than VTA. Intracellular dopamine levels were shown to correlate to that of intracellular Ca^{2+} and addition of dihyropyridine to inhibit channel activity, caused a reduction of dopamine in SNpc but not VTA dopaminergic neurons, suggesting that calcium is playing an important role in the functioning of this particular subtype of neurons (Mosharov *et al.* 2009). It has also been shown that different L-type calcium channels are expressed in the VTA than those in the SNpc (Rajadhyaksha *et al*. 2004), which is thought to be playing an important role in the pathogenesis of PD in dopaminergic SNpc neurons also.

1.4 PATHOGENESIS OF PD

1.4.1 Protein accumulation

Protein accumulation and subsequent deposition of insoluble aggregates, is observed in most major neurodegenerative disorders (reviewed in Sipe *et al.*

2000). When proteins such as α-syn need to be removed from the cytoplasm, they are tagged with poly-ubiquitin chains at lysine residues by ubiquitin ligases. Chaperone proteins recognise these ubiquitin chains and tagged proteins are then trafficked to the proteasome, where they are unfolded and fed through its barrel-like structure (Lowe *et al.* 1995). Inside the proteasome, proteins are broken down into their amino acid components by proteases. When there is a large build-up of protein, or when proteins become aggregated, this unfolding is not possible, and the proteasome can become overwhelmed, resulting in proteasomal inactivation (reviewed in Hochstrasser, 1995). The presence of highly ubiquitinated α-syn aggregation in PD, suggests that proteasome function is compromised. Indeed proteolytic stress caused by large amounts of protein to be degraded, or proteins that have become aggregated, have been shown to cause inhibition of the ubiquitin-proteasome system (UPS) (Bence *et al.* 2001). This causes protein to accumulate further and can thus trigger a downward spiral in which insoluble aggregates form, which become increasingly difficult to remove.

High levels of misfolded proteins are known to cause an emergency response in which purpose built aggresomes are created by the cell to sequester accumulated protein. (Mcnaught *et al.* 2002). Aggresomes are made by a rearrangement of the intermediate filament protein vimentin, to create a cage-like structure surrounding the perinuclear core. Misfolded proteins are ubiquitinated and transported to the aggresome, where they are proteolysed and sequestered; aggresomes are known to occur in response to proteasome inactivation (Junn *et al.* 2002). LBs are thought to form as a result of aggresome formation (Johnston *et al.* 1998).

1.4.2 Autophagy

When the UPS is impaired, removal by autophagy appears to be a more efficient option (Rubinsztein, 2006). Autophagy is negatively regulated by the mammalian target of rapamycin protein (mTOR) and activated in response to protein aggregation and oxidative stress (Ferraro *et al.* 2007), although this process also functions to maintain normal cellular homeostasis. There are three forms of autophagy, which differ depending on the size of the material to be removed.

Macroautophagy is the main process by which large or aggregated proteins are removed and is the process discussed here (referred to as autophagy hereafter unless otherwise stated). Removal of aggregated protein by autophagy is achieved by sequestering rogue proteins in a double-membraned vacuole, prior to disposal by the lysosome (Martinez-Vicente *et al.* 2007). Autophagic vacuoles (AVs), are known to form randomly in the cytoplasm and then move along microtubules until they dock with the lysosome, either merging fully to form an autophagolysosome, or docking briefly to deliver their contents for degradation in the lysosome (Jahreiss *et al.* 2008). In PD, ultrastructural examination of SNpc neurons from PD patients has shown an upregulation of autophagic vesicles (Anglade *et al.* 1997).

1.4.3 Mitochondrial damage in PD

The accidental synthesis of the synthetic opiod 1-methyl-4-phenyl-1,2,3,6-tetrahydropyridine (MPTP) by a student trying to synthesize 1-methyl-4-phenyl-4-propionoxypiperidine (MPPP) in 1976, was an important step forward in understanding possible mechanisms of neuronal death in PD, (Langston *et al.* 1984), linking mitochondrial dysfunction to the aetiology of this disease. The MPTP metabolite, 1-methyl-4-phenylpyridinium ion (MPP+) is selectively toxic to dopaminergic neurons in the SNpc and has been shown to cause cog-wheel rigidity, resting tremor and problems in initiating movement when injected intravenously (Langston *et al.* 1983). The toxic effects of MPP+ result in a decrease in membrane potential and decreased electron transport chain function due to Complex I damage (Ramsay *et al.* 1986). Analysis of human post-mortem tissue from individuals with PD has also shown Complex I damage, resulting in a reduction of Complex I enzymatic activity (Schapira *et al.* 1990). Similarly, comparison of neurons treated with MPTP and those from patients with PD have been shown that these cells share many common features. Continuous, low-level infusion of MPTP in mice has been shown to result in motor deficits caused by cell death and α-syn and ubiquitin positive inclusions in the SNpc (Fornai *et al.* 2005). Injection of the toxin MPTP into mice has shown an upregulation of α-syn mouse homolog synuclein-1 (syn-1) at the mRNA and protein level and an increase in syn-1 positive aggregates in the SNpc (Vila *et al.* 2000). This increase has been shown in baboons (Kowall *et al.* 2000) and also in primary neuronal cultures from

rodents (Duka *et al.* 2006). Importantly, cells lacking α-syn are insensitive to mitochondrial toxicity induced by MPP+ (Fornai *et al.* 2005) and it has been shown that α-syn could play an important role in mediating MPP+ toxicity, perhaps through regulation of nitric oxide (NO) signaling (Fountaine *et al.* 2008). MPTP and other complex I inhibitors such as rotenone, are commonly used in cell models of PD as a result of the MPP+ phenomenon (Greenamyre *et al.* 1999)

In PD, it has been suggested that the vulnerability of dopaminergic neurons (although other non-dopaminergic neurons die also) is facilitated in part by the presence of dopamine (Stokes *et al.* 1999). The involvement of cytosolic dopamine is involved in redox reactions which can produce reactive quinones, superoxide species and hydrogen peroxidase (H_2O_2) (Graham *et al.* 1978), which is thought to leave dopaminergic neurons more susceptible to oxidative stress (Berman *et al.* 1999). One study has shown an increase in extracellular iron levels in port-mortem SNpc tissue of PD sufferers (Dexter *et al.* 1987). Iron can catalyse oxidation reactions in the presence of dopamine, generating free radicals, which cause tissue damage (Halliwell *et al.* 1985). As such, although the exact etiology underlying PD is currently unknown, there are many strands of evidence suggesting that oxidative stress is a key mechanism in cell death, where oxidative stress in the neurons of PD patients is increased, compared to that of the normal aging population.

1.5 COMMON MECHANISMS IN NEURODEGENERATION

The mechanisms discussed for PD are common to a number of neurodegenerative diseases and emphasise the overlap between the many supposedly distinct disorders. Interestingly, these commonalities occur between motor and cognitive disorders, as well as within groups of symptoms.

1.5.1 Protein aggregation

The aggregation of certain proteins is a common feature of many neurodegenerative diseases and identification of these aggregates, is often part of the diagnostic criteria for post-mortem confirmation (Table 1.2). The prevalence of

deposited protein aggregates in neurodegenerative disease, emphasises the importance of protein turnover and axonal transport in neuronal homeostasis. As discussed, disruptions to autophagy have been found in PD patients and increased numbers of autophagosomes have been documented in a number of neurodegenerative diseases, suggesting that an increased demand for protein degradation could be a common feature of these disorders (Nixon, 2006).

Disease	Protein	Lesion	Reference
PD	α-synuclein	Lewy bodies	Lewy, 1912
Alzheimer's disease	Aβ/ tau	Plaques/ neurofibrilliary tangles	Kidd *et al.* 1963 Nikaido *et al.* 1970
Huntington's disease	Huntingtin	Huntingtin inclusions	DiFiglia *et al.* 1997
ALS/ Motor Neuron Disease	SOD1, ubiquitin	Bunina bodies, skein-like bodies, SOD1 aggregates	Bunina *et al.* 1962
Transmissible Spongiform Encephalopathies	Prion protein	Prion protein aggregates	Prusiner *et al.* 1980
Fronto-Temporal Dementia	Tau/ Aβ	Neurofibrilliary tangles/ plaques	Kidd *et al.* 1963 Nikaido *et al.* 1970
Trinucleotide repeat disorders	Various- often contain CAG repeats	Neuronal intranuclear inclusions	Reviewed in Li, 2010

Table 1.2. Neurodegenerative diseases and their hallmark lesions.

As axonal transport is a key mechanism for protein removal, it is perhaps unsurprising that disruptions to the cytoskeleton in Alzheimer's disease are widely documented (reviewed in Lee *et al*. 2006) and disruptions to the cytoskeleton are thought to precede motor symptoms in motor neuron disease (Bilsland *et al*. 2010). Similarly ALS can be caused by mutations in the motor proteins dynein (Hafezparast *et al*. 2003) and dynactin (Munch *et al*. 2004).

Many reports have shown that there can be considerable overlap between the neuropathological features of different neurodegenerative diseases. A fragment of α-syn, originally termed the non-amyloid β component (NAC) of senile plaques has been shown to form aggregates in Alzheimer's disease (Ueda *et al.* 1993). Similarly, as will be discussed in more detail later, some proteins such as TDP-43 and tau can become aggregated and deposited in both frontotemporal dementia and some forms of PD. The lesions associated with many diseases are also ubiquitin positive, suggesting that there could be mechanisms common to neurodegenerative disease and neuronal death in general. The issue as to whether these lesions are neuroprotective or toxic to the cell is still hotly debated (reviewed in Ali, 2010), however the overlap between fields suggests that potential therapeutic avenues for one disorder may also prove promising for other diseases.

1.5.2 Oxidative stress and mitochondrial damage

The reduced rate of glycolysis in neurons suggests that maintenance of oxidative status is crucial for neuronal survival (Herrero-Mendez *et al.* 2009). As such, the oxidative stress and mitochondrial damage widely documented in a number of neurodegenerative diseases, are likely to be important mechanisms in the pathogenesis of these diseases. Damage to respiratory chain enzymes has been reported in a number of diseases, with Alzheimer's and ALS post-mortem brain samples showing damage to complex IV. Individuals with Hungtingdon's disease and Friedrich's ataxia have been shown to have complex II and III dysfunction (reviewed in Kirkinezos *et al*. 2001) and prion disease is associated with damage to complex II and IV (Siskova *et al*. 2010). Damage to mitochondrial DNA has been reported for a number of neurodegenerative diseases (reviewed in Yang *et al*. 2010) suggesting also that oxidative stress is a common feature of these diseases.

The increasing number of genes shown to cause familial forms of neurodegeneration, have supported the idea that mitochondrial dysfunction is a common cause of many disorders. In ALS, mutations in the superoxide dismutase SOD1, have been shown to cause autosomal dominant forms of the disease (Rosen

et al. 1993) and hereditary spastic paraplegia is commonly caused by mutations in the mitochondrial protease paraplegin (reviewed in Tatsuta *et al*. 2008). In Alzhimer's disease, presenilin and the gamma secretase complex which are mutated in some familial forms of demetia, are localised to mitochondria (Hansson *et al*. 2004) and Aβ has been shown to interact with the mitochondrial protease HTRA2 (Park *et al*. 2004), which has also been linked to PD (Strauss *et al*. 2005). Similarly, huntingtin interacts with transcription factors controlling mitochondrial integrity and apoptosis (reviewed in Sugars *et al*. 2003). Taken together, these studies again suggest that, although the disorders discussed are separate clinically, the mechanisms underlying neurodegeneration in different disease are likely to share many common features that could be exploited as therapeutic avenues.

1.6 GENETIC CAUSES OF PARKINSON'S DISEASE

In 1997 it was shown that a point mutation in *SNCA*, the gene coding for α-syn, is sufficient to cause familial Parkinson's disease (Polymeropoulos *et al.* 1997). The discovery that PD can have a genetic cause has led the way for a wealth of genetic sequencing using PD patient samples and subsequently many more loci associated with familial PD have been identified. Familial PD is thought to make up between 5 and 10% of all cases, depending on the populations in question (reviewed in Hardy *et al.* 2006). To date, there have been a total of 16 reported PARK loci, which are known to associate with genetic forms of PD and Parkinsonism (see Table 1.2).

1.6.1 Autosomal dominant forms of PD

1.6.1.1 α-synuclein

Early onset, autosomal dominant (AD) PD in 41 individuals of a large family from the small Italian village of Contursi Terme (Golbe *et al.* 1996), led to the identification of the A53T point mutation in α-syn (Polymeropoulos *et al.* 1997).

PARK1/4	SNCA	α-synuclein	PD	AD	Un
PARK2	PRKN	Parkin	Parkinsonism	AR	E3 ligase
PARK3	2p13.3-2p13.1	Unidentified	Parkinsonism	Un	Un
PARK5	UCHL1	UCHL1	Parkinsonism	AD	Cytosolic. Ubiquitin tagging
PARK6	PINK1	PINK1	Parkinsonism	AR	Mitochondrial. Kinase?
PARK7	DJ-1	DJ-1	Parkinsonism	AR	Cytosolic. Oxidative stress
PARK8	LRRK2	LRRK2	PD	AD	Cytosolic. Kinase?
PARK9	ATP13A2	ATP13A2	Parkinsonism	AR	Lysosomal
PARK10	1p33-1p32.2	Unidentified	Parkinsonism	Un	Un
PARK11	2q36.1-2q37.3	GIGYF2	Parkinsonism	Un	Cytosolic. Signal transduction?
PARK12	Xq21-q25	Unidentified	Parkinsonism	Un	Un
PARK13	HTRA2	HTRA2	Parkinsonism	Un	Mitochondrial protease
PARK14	18q11	PLA2	Parkinsonism	AR	Lipid metabolism
PARK15	22q12-13	FBXO7	Parkinsonism	AR	Mitochondrial
PARK16	1q32	Unidentified	PD-GWAS hit	Un	Un
-	GBA	Glucocerebrosidase	PD	AD	Ceramide metabolism

Table 1.2. PARK loci and the genes implicated in parkinsonism and PD. Adapted from (Lees *et al*. 2009). AD- Autosomal dominant. AR- Autosomal Recessive. Un-Unknown.

This form of the disease is extremely aggressive in progression, with the average age of PD onset in this kindred at 45, with death occurring approximately 9 years after diagnosis. Two further mutations causing an A30P (Kruger *et al.* 1998) and E46K substitution (Zarranz *et al.* 2004) were subsequently found to segregate in other families and duplications and triplications of the *SNCA* gene have also been shown to cause an aggressive, early onset form of the disease (Singleton *et al.* 2003). The increased expression of α-syn caused by duplications and triplications of *SNCA* is thought to induce accumulation of the protein in a dose-dependent manner, which is likely to cause aggregation and deposition (Singleton *et al.* 2003), (Chartier-Harlin *et al.* 2004) resulting in PD associated pathogenesis and LB formation. Bases changes that result in point mutations have also been shown to result in an increased propensity for aggregation. The A53T substitution is thought to promote beta sheet folding, which are prone to aggregation and the formation of so called 'fibrils' (Lashuel *et al.* 2002), and both A30P and A53T have been shown to change the conformational behavior of α-syn (Li J. *et al.* 2002). These changes are all thought to promote aggregation and deposition of α-syn, resulting in neuronal death. In this way, changes to the gene product of *SNCA* have been shown to cause genetic PD, as well as playing an important role in the progression of sporadic PD.

1.6.1.2 LRRK2

Mutations in the putative kinase LRRK2, were first implicated in PD in 2004 with the discovery of point mutations in five families of Basque descent (Paisan-Ruiz *et al.* 2004) and either point mutations or splice site mutation in two families, one of German-Canadian descent and one kindred originally from Nebraska (Zimprich *et al.* 2004). Zimprich *et al* showed that LRRK2 PD pathology is extremely varied, even between individuals carrying the same mutations. Brain stem degeneration accompanied by a mixture of diffuse LBs was shown in some cases, with nigral degeneration absent from additional histopathology and tau pathology resembling that found in progressive supranuclear palsy shown (PSP). In the Sagamihara kindred, where the PARK8 locus was first implicated, a similar picture was found. Histochemical analysis of postmortem tissue showed pure nigral degeneration

without LBs in six out of eight relatives. LBs were present in one case and MSA-like pathology, characterized by cytoplasmic glial cell inclusions was found in another (Satake *et al.* 2009). Recently, brain tissue from carriers of L1165P or R793M substitutions has broadened the pathology associated with LRRK2 PD, with reports of neurofibrilliary tangles in the hippocampus, and TDP-43 positive inclusions also found (Covy *et al.* 2009). LRRK2 parkinsonism generally presents as PD that is indistinguishable clinically from idiopathic PD (Farrer *et al.* 2005). LRRK2 has been shown to be a component of nigral Lewy bodies and a component of granular inclusions found in the lower brain stem (Alegre-Abarrategui *et al.* 2008).

A common feature of LRRK2 PD is the lack of segregation with some mutations. The most common mutation, G2019S is found in an estimated 6% of Parkinson's patients, with the frequency as high as 40% in some Ashkenazi Jewish and North African Berber populations (Lesage *et al.* 2005) although the actual incidence of PD is considerably lower. In populations carrying the G2019S mutation, penetrance is incomplete (Saunders-Pullman *et al.* 2006) and the substitution is also present in control individuals, of note an octogenarian man with no signs of either motor or cognitive decline, who was shown to be a heterozygous carrier (Kay *et al.* 2005). The risk of developing PD when carrying G2019S has been shown to increase over time, ranging from a 28% likelihood at 59 years of age, to 74% at 79 years (Healy *et al.* 2008) suggesting that there could be other factors contributing to the pathogenesis of this disease.

1.6.2 Autosomal Recessive forms of PD

1.4.2.1 PINK1 and Parkin

Exon deletions in the *PRKN* gene, which encodes the E3 ubiquitin ligase parkin (Shimura *et al.* 2000), were first discovered in two Japanese families (Kitada *et al.* 1998). These deletions spanned five exons in one individual and one exon in four individuals from three separate families. Meta-analysis of parkin mutation carriers suggests that pathogenic alterations to *PRKN* account for up to 50% of AR early onset parkinsonism in some populations (Lucking *et al.* 2000) and *PRKN*

alterations have been found in families from a wide range of ethic origins including European, Japanese and Indian origins (Morrison, 2003). Point mutations in parkin are common, with as many as 34 variants described. Patients have been shown to carry single and compound mutations which can be homo or heterozygous in nature. Homozygous parkin mutations are associated with early onset PD, however heterozygous parkin mutations have been found in sporadic cases of PD and are present in some control individuals (Kay *et al.* 2007). Interestingly, mutations in parkin have also been linked to cancer (Fujiwara *et al.* 2008) and leprosy (Mira *et al.* 2004), suggesting that this gene product plays an important role in the normal functioning of a number of cell types.

The clinical presentation of *PRKN* mutation and deletion carriers is extremely heterologous, with age of onset reported to be between 7 and 58 years of age in one study. These patients presented with bradykinesia in 94% of cases, resting tremor in 74% of cases and showed additional symptoms such as dystonia in over half of all cases (Lucking *et al.* 2000). Psychiatric symptoms, autonomic dysfunction and peripheral neuropathy have been reported in parkin mutation carriers in other studies (Morrison, 2003). Neuropathological examination of individuals with parkinsonism caused by parkin, have shown that neuronal loss in the SNpc is commonly associated with a lack of LBs (Hattori *et al.* 2000), however this is not always the case, with LBs found in some cases (Farrer *et al.* 2001, Pramstaller *et al.* 2005).

Mutations in PTEN induced kinase (PINK1) were found in some cases of AR parkinsonism in 2004 (Valente *et al.* 2004). Genetic sequencing of three families of Spanish and Italian consent who presented with early onset parkinsonism in their third and fourth decades, identified two different homozygous mutations resulting in a point mutation and a nonsense mutation which causes truncation of the PINK1 protein. Since the initial report of PINK1 mutations, there have been numerous variants reported, with one study in Irish patients with early onset parkinsonism, identifying 27 different variants (Rogaeva *et al.* 2004). Mutations in PINK1 are thought to represent ~4% of all early onset cases (Ibanez *et al.* 2006) with the prevalence as high as 10% in some populations (Bonifati *et al.* 2005). These

mutations have been reported in both homozygous and heterozygous form. Rare heterozygous forms of PINK1 are known to be indistinguishable from idiopathic PD (Marongiu *et al.* 2008) and late onset PINK1 cases also resemble the sporadic form of the disease. In most cases, parkinsonism is slow in progression and typical disease presentation includes dystonia and depression as well as the classical symptoms of bradykinesia and rigidity (Ibanez *et al.* 2006). Neuropathological examination of PINK1 mutation carriers has long been absent from the literature, however the recent characterisation of one individual with heterozygous mutations has shown that neuronal loss in the SNpc is accompanied by Lewy bodies and Lewy neurites throughout the brain stem, however the LC was spared from any gross neuronal loss (Samaranch *et al.* 2010).

PINK1 is a putative kinase, which is localised to the inner mitochondrial membrane (Silvestri *et al.* 2005). As the name suggests, PINK1 is involved in PTEN signalling (see Figure 1.4) and has been shown to interact with HTRA2 (Plun-Favreau *et al.* 2007), a protease well known for its involvement in apoptosis, which is liberated from the mitochondria to promote cell death. PINK1 has also been shown to regulate calcium efflux from the mitochondria (Gandhi S. *et al.* 2009). *Drosophila* models suggest that PINK1 and parkin may function in the same pathways to maintain mitochondrial integrity (Park *et al* 2006, Clark *et al.* 2006). Parkin has been shown to bind DNA and repress the tumour suppressor protein p53 on a transcriptional level (Da Costa *et al.* 2009) and studies with mouse embryonic fibroblasts (MEFs) from PINK1 knockout mice, have shown that parkin is unable to localise to the mitochondria, suggesting that the mitochondrial function of Parkin may be dependent on PINK1 (Matsuda *et al* 2010, Ziviani *et al.* 2010). Both proteins have been implicated in autophagy (Narendra *et al.* 2008) and rapamycin activation of 4E-BP independent of autophagy has been shown to prevent parkinsonian dopaminergic neuron loss in PINK1 and Parkin overexpressing *drosophila* models (Tain *et al.* 2009). The overlap of these mechanisms with those associated with idiopathic PD, perhaps suggest a role for PINK1 and Parkin in the pathogenesis of sporadic as well as familial forms of PD.

1.6.2.2 Rare forms of parkinsonism and genetic risk factors

Another, rarer form of AR PD was identified in two consanguineous families from Italy and the Netherlands, who were shown to have deletions in the *DJ-1* gene (Bonifati *et al.* 2003), which codes for a cytosolic oxidative stress signalling molecule, first implicated in cancer (Nagakubo *et al.* 1997). Mutations in this protein cause a loss of function, resulting in oxidative stress, ER stress and proteasome inhibition (Yokota *et al.* 2003). The fourth and rarest genetic form of AR parkinsonism is caused by mutations in the PARK9 locus, in the gene encoding the lysosomal ATPase ATP13A2 (Ramirez *et al.* 2006). Mutations in this gene have been shown to cause early and juvenile onset parkinsonism (onset at < 21 years of age) in a small number of families (Di Fonzo *et al.* 2007).

Five genes with possible involvement in ceramide production have been highlighted as possible genetic risk factors for PD, due to the Lewy body pathology associated with them. Of these, the most common is *GBA*, the gene encoding glucocerebrosidase, which is known to cause Gaucher's disease in homozygotes and PD in heterozygotes (reviewed in (Bras *et al.* 2008). Genome-wide association studies (GWAS) have emphasised the importance of α-syn and LRRK2 in PD (Simon-Sanchez *et al.* 2009, Nalls *et al.* 2011). Furthermore, GWAS consortiums have shown that a number of genes previously unassociated with PD reach significance, suggesting that there are a number of unexplored mechanisms underlying PD pathology. Of these, an interesting result was the association of *MAPT* with PD (Pankratz *et al.* 2009). The *HLA* locus, *BST1* and *GAK* are recent GWAS hits that have been replicated in a number of studies. Meta-analyses have provided identification of six additional genes, including the gene encoding the serine/threonine kinase STK39, which are linked to PD (Nalls *et al.* 2011).

As family history is one of the exclusion criteria for PD, there is much debate about familial forms of PD and the extent to which they can be classified as true Parkinson's diease (Lees *et al.* 2009). The mixed clinical presentations shown in many of the early onset parkinsonism disorders and the mixed pathologies found in individuals carrying these genetic abnormalities, have added to the argument that these diseases may instead represent a spectrum of disorders of which PD is

one. As such, it has been proposed that 3 forms of genetic parkinsonism, namely mutations in *SNCA* (Polymeropoulos *et al.* 1997), *LRRK2* (Paisan-Ruiz et al. 2004, Zimprich *et al*. 2004) and *GBA* (Lwin *et al.* 2004) cause true PD whereas the other PARK loci are thought to produce disorders of which parkinsonism is a feature (Lees *et al.* 2009).

1.7 THE ROLE OF LRRK2 IN PD

1.7.1 LRRK2 domain structure

The varied pathology of LRRK2 mutation carriers, has led to the suggestion that LRRK2 may play a role at the intersection of many of the pathways associated with these pathologies, with a regulatory role in microtubule stability, regulation of transcription and mitochondrial functioning suggested by the presence of tau, TDP-43 and α-syn respectively (Zimprich *et al.* 2004). The fact that LRRK2 PD is indistinguishable from sporadic PD, suggests that the physiological role of this protein may be important for sporadic, as well as genetic forms and as such, investigation of LRRK2 may provide a possible therapeutic avenue as well as an important research target. For these reasons, understanding the relationship between mutations in LRRK2 and the clinical presentation of PD, is seen as an important step towards understanding and finding treatments for sporadic PD.

LRRK2 is a large protein, consisting of 2527 amino acids. It contains a serine/threonine kinase domain, a GTPase domain and multiple protein-protein interaction domains as shown in Figure 1.2.

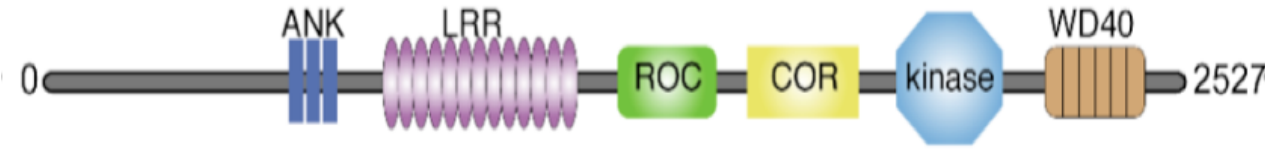

Figure 1.2. Linear representation of LRRK2 domain structure. ANK- Ankyrin repeats, LRR- Leucine rich repeats, ROC-Ras of complex proteins, COR- C-terminal of ROC.

The ankyrin and leucine-rich repeats, and the WD40 domain of LRRK2 are thought to mediate protein-protein interactions (reviewed in Mata *et al.* 2006) and it has been suggested that LRRK2 is a scaffold protein (Liou *et al.* 2008). The enzymatic core of LRRK2 consists of a GTPase domain (Ras of Complex proteins or ROC domain) adjacent to the non-enzymatic COR domain and a kinase domain. This ROC-COR tandem is characteristic of the ROCO family of proteins, a family containing four members in humans which contain the ROC-COR motif, including LRRK2 and its closely related homolog LRRK1 (Bosgraaf *et al.* 2003). The kinase domain of LRRK2 is closest in homology to kinase domains from the RIPK family, a group of predominantly serine/ threonine kinases (reviewed in Meylan *et al.* 2005).

In analogy to the small GTPase Ras, which is known to activate kinase Raf-1 upon GTP binding to its GTPase domain (Maruta *et al.* 1994), kinase activity of LRRK2 is also activated upon GTP binding to the ROC domain. GTP hydrolysis by Ras causes conformational change and the switch to an 'off' conformation, a state which is reversed upon GDP/GTP exchange (Feuerstein *et al.* 1989). Investigation into the functional relationship of the ROC-COR tandem and the kinase domain of LRRK1, showed that GTPase hydrolysis controls kinase activity (Korr *et al.* 2006). Soon after, it was shown that GTP dead forms of LRRK2 lack in kinase activity (Smith *et al.* 2006), and that the kinase activity of full-length LRRK2 overexpressed in mammalian cells, is also controlled by GTP binding to the ROC domain (Ito *et al.* 2007). Binding of GTP appears to stimulate kinase activity, whereas GDP has been shown to inhibit LRRK2 kinase activity. Non-hydrolysable forms of GTP have been shown to increase LRRK2 kinase activity, presumed to be due to an enhanced 'on' state, when GTP is bound to the ROC domain (Li X. *et al.* 2007, Guo *et al.* 2007). These studies support a regulatory role for the ROC domain in controlling LRRK2 kinase activity.

1.7.2 Dimerisation of LRRK2

Accumulating evidence suggests that LRRK2 is able to form dimers. BlueNative (BN) and size exclusion analysis of full length LRRK2 expressed in Hek293T cells

and endogenous LRRK2 from lymphoblasts, have shown that LRRK2 is present in species of ~600 kDa, which likely corresponds to dimeric species. LRRK2 was also present in lower (~300 kDa) and higher molecular weight form (~1.2 MDa) in these studies (Greggio *et al.* 2008, Sen *et al.* 2009). Glycerol gradient centrifugation of overexpressed and endogenous LRRK2 supports these results and suggests that the active form of LRRK2 is dimeric, with kinase activity of higher molecular weight LRRK2 species higher than that of lower molecular weight (Berger *et al.* 2010).

The resolved crystal structure of bacterially expressed fragments of the ROC domain, show that this domain is sufficient for dimerisation. The crystal structure suggests a domain-swap interaction in which residues from one LRRK2 molecule, form associations with those from another, in order to collectively make the active site (Deng *et al.* 2008). Although the legitimacy of this 'domain swap,' has been questioned (Gotthardt *et al.* 2008), crystal structures from other ROCO proteins also support the idea that ROCO proteins are able to dimerise. Crystallization of the ROC/COR tandem from the *C. Tepidium* ROCO protein, has shown that this fragment of the protein can also dimerise. Fragments of the isolated COR domain are able to form dimers and mutating residues at the dimer interface is sufficient to cause separation of the dimer into monomeric species (Gotthardt *et al.* 2008). Yeast II hybrid screens (Y2H) using various fragments of LRRK2 have shown interaction between a number of domains; segments of LRRK2 spanning residues 13-186 (LRRs to ROC), as well as the N-terminus and the WD40 repeats (2084-2217) have all shown the ability to self-interact (Greggio *et al.* 2008).

1.7.3 Regulation of dimerisation

Regulation of kinase activity by the ROC domain is thought to be induced by conformational change dependent on dimerisation of the GTPase domains. This has led to classification of LRRK2 as a 'G protein activated by nucleotide-dependent dimerization (GAD) (Gasper *et al.* 2009).' According to this classification, the active site of the GTPase domain contained within GAD monomers, requires interaction with a complementary active site in order to

function (see Figure 1.3). These proteins have a low nucleotide affinity in the μM range, and it has been shown in other GADs, that the high turnover of GDP/GTP negates the need for a guanine exchange factor (GEF) (Gasper *et al.* 2009). GTP binding studies have shown that the ROC domain of the bacterial ROCO protein from *C. Tepidium* has a low affinity for GTP binding (13.4μM), and a fast dissociation rate (Gotthardt *et al.* 2008) and it is thought that this is also the case for LRRK2. Other features displayed by GADs are shown by the GTPase dynamin, which has been described in terms of its interaction with GTPase co-regulators (GCRs), which are proteins and factors that are necessary to aid GTPase function, but do not have any functional role in doing so. Dynamin interacts with phospholipids and microtubules and according to its classification as a GAD, these accessories are necessary for GTPase activity to function optimally. Similarly, the heat shock protein HSP90 and its interactors have been shown to assist in the GTPase activity of the proteins they interact with (Gasper *et al.* 2009). LRRK2 has been shown to bind to membranes (Hatano *et al*. 2007, Alegre-Abarrategui *et al.* 2009, Berger *et al.* 2010), and the ROC domain has been shown to interact with β and α-tubulin (Gandhi *et al.* 2009). Similarly, association with HSP90 has also been demonstrated (Hurtado-Lorenzo *et al.* 2008), supporting the classification of LRRK2 as a GAD, but also suggesting that there are other factors affecting LRRK2 GTP hydrolysis that have not yet been investigated.

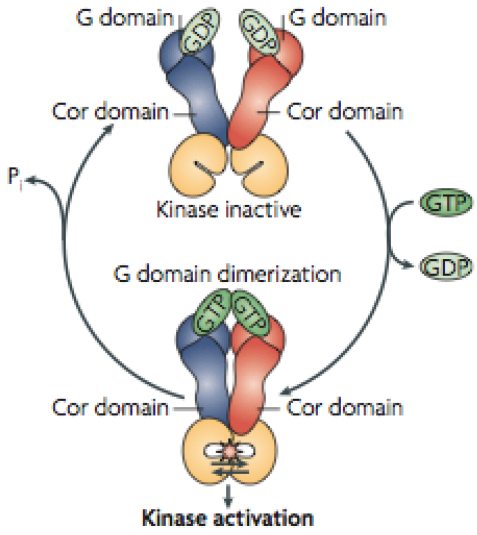

Figure 1.3. Schematic model of LRRK2 activation by dimerisation. Taken from Gasper et al, 2009). The inactive ROC domain of GDP-bound LRRK2 is monomeric. Dissociation of GDP and binding of GTP causes dimerization of the ROC domain, which translates to kinase domain activation through conformational change. Hydrolysis of GTP to GDP causes monomerisation of the ROC domain, and the cycle starts again.

1.7.4 Effect of familial mutations on LRRK2 functioning

In Asian populations, the G2385R mutation situated in the WD40 domain of LRRK2, is thought to be the most common PD causing mutation (Farrer *et al.* 2007). Apart from this, many of the familial mutations known to cause PD, are situated in the enzymatic core of the protein (ROC-COR-kinase) and it has been shown that some of these mutations can affect the enzymatic outputs of LRRK2. This is important for PD, as cellular toxicity of LRRK2 has been attributed to kinase activity (Greggio *et al.* 2006, Smith *et al.* 2006). G2019S, which is situated in the Mg^{2+} binding loop of the kinase domain, has been consistently reported to display increased kinase activity when compared to WT protein (reviewed in Greggio *et al.* 2009) and R1441C, found in the ROC domain, appears to affect GTPase efficiency, decreasing the ability of LRRK2 to hydrolyse GTP (Lewis *et al.* 2007). The crystal structure of the ROC domain purified from bacteria, suggests that R1441 is found

on the interface of ROC-ROC dimers. The cysteine substitution may disrupt hydrogen bonding between the two GTPase domains (Deng *et al.* 2008). Similarly, differential scanning fluorimetry has shown that the R1441C mutation is likely to change the folding properties of the ROC domain (Li Y. *et al.* 2009). As such, this mutation is likely to be affecting GTP hydrolysis by causing subtle structural changes. Recently, Y1699C has also been shown to affect the activity of the ROC domain, causing a decrease in the rate of GTP hydrolysis. This mutation, situated in the COR domain of LRRK2, has been shown to decrease GTPase activity by strengthening the interaction between the ROC and COR domain, which results in a weaker bond between LRRK2 monomers (Daniels *et al.* 2011).

1.7.5 Phosphorylation and autophosphorylation of LRRK2

Ablating kinase activity with the artificial mutation K1906M and GTPase activity with the mutation K1347A (West et al 2007, Gloeckner *et al.* 2006), causes LRRK2 to form higher molecular weight aggregates, presumably due to the stability of this protein being altered. In this case, it would appear that enzymatic activity forms a crucial mechanism to regulate LRRK2 dimer formation (Greggio *et al.* 2008). As LRRK2 is known to autophosphorylate, it is likely that phosphorylation of LRRK2 at certain residues is regulating complex formation. Treatment of transfected Hek293T cells and ΔN-LRRK2 recombinant protein with the kinase inhibitor staurosporine, has been shown to disrupt dimer formation (Sen *et al.* 2009), supporting the idea that autophosphorylation or kinase activity-mediated phosphorylation of LRRK2, provides some regulation over LRRK2 complex formation. Kinase assays using immunoprecipitated LRRK2 separated using FPLC size exclusion, have shown that the kinase activity of higher order LRRK2 species of LRRK2 is higher than that of lower weight LRRK2, suggesting that enzymatic activity is also affected by LRRK2 complex formation.

Overexpressed LRRK2, has been shown to be basally phosphorylated in Cos7 cells (Greggio *et al.* 2007), an idea supported by the analysis of phosphopeptides in cancer cells, which showed phosphorylation of LRRK2 at Y707 (Rush *et al.* 2005). The kinase domain of LRRK2 is highly homologous to that found in serine/

threonine kinases (Declercq *et al.* 2009, Lewis, 2009), and an analysis of LRRK2 consensus motifs for phosphorylation, supports the idea that LRRK2 phosphorylates serine and threonine residues, with a preference for serine phosphorylation (Pungaliya *et al.* 2010). This suggests that phosphorylation of this tyrosine residue is not caused by autophosphorylation, but likely by another interacting kinase. Tyrosine phosphorylation of LRRK2 in general is not widely reported, perhaps due to the reduced stability of tyrosine phosphorylation compared to serine/threonine phosphorylation (Rush *et al.* 2005). The reported membrane association of LRRK2 (Hatano *et al.* 2007, Alegre-Abarrategui *et al.* 2009, Berger *et al.* 2010) could suggest that this phosphorylation is mediated by membrane interaction, due to the high concentration of receptor tyrosine kinases and receptor associated tyrosine kinases at membranes.

Investigation into LRRK2 substrates has reported that LRRK2 is able to interact interact with isoforms of the 14-3-3 proteins, scaffolds involved in numerous signaling cascades, which bind to phosphorylated residues (Dzamko *et al.* 2010, Nichols *et al.* 2010, Li X. *et al.* 2011). Dephosphorylation has been shown to disrupt this interaction and mass spectrometric analysis of phosphorylated residues in LRRK2 has mapped the interaction to two serines at positions 910 and 935. Mutation of these serines to alanines has been shown to disrupt 14-3-3 binding and dephosphorylation of LRRK2 with phosphatase and subsequent rephosphorylation *in vitro*, shows that LRRK2 is unable to autophosphorylate at these residues. This suggests that these residues are instead likely targets for regulation by other kinases (Dzamko *et al.* 2010).

Autophosphorylation of LRRK2 has been shown to cluster in certain, discrete areas of LRRK2, namely the N-terminus, ROC domain and kinase domains. Overexpression of TAP-tagged LRRK2 in Hek293T cells, with mass spectrometry to identify phosphorylation before and after a kinase assay, have shown that up to 20 sites can be identified (see Table 1.3). These sites are found mainly between S850 and S979 in the N-terminus (Gloeckner *et al.* 2010). Additional autophosphorylation targets in the regulatory P-loop of the ROC domain were also identified, namely T1343, S1345 and T1348. Importantly, if these amino acids are

superimposed on the crystal structure of ROCO from *C.Tepidium*, T1410 sits right next to R1441 and T1348 is above. As mutation of R1441 has been shown to decrease GTPase activity (Lewis *et al.* 2007) autophosphorylation of these residues may play a role in the regulation of GTPase activity, and thus provide a feedback mechanism for kinase activity (Gloeckner *et al.* 2010).

Assessment of autophosphorylation in recombinant N-terminally truncated LRRK2 (ΔN-LRRK2) using *in vitro* kinase assays, and full-length FLAG-tagged LRRK2 using the ROC domain as a substrate, has supported the idea of T1343 phosphorylation, as well as T1491 and T2031 (see Table 1.3 for a complete list of LRRK2 autophosphorylation resides to date). When the N-terminus is removed, LRRK2 displays three times higher autophosphorylation activity, suggesting that this segment of LRRK2 is involved in regulation of kinase activity (Greggio *et al.* 2009). Mutation of residues in the active loop T2031, S2032, and T2035, to non-phosphorylatable alanines, does not affect dimerization and importantly, the T2035A mutation is unable to autophosphorylate itself. The finding that WT cannot phosphorylate the kinase dead mutant, suggests that autophosphorylation is likely to occur *in cis,* rather than *in trans* as might be expected, although interacting proteins, absent from these assays may be necessary for trans-phosphorylation of LRRK2.

Residue	Domain	Reference(s)
S850 S858 S860 S865	N-Terminus	Gloeckner *et al.* 2010
S895 S898	N-Terminus	Gloeckner *et al.* 2010
S908 S910 S912	N-Terminus	Gloeckner *et al.* 2010
S926	N-Terminus	Gloeckner *et al.* 2010
S933 S935	N-Terminus	Gloeckner *et al.* 2010
S954 S955 S958	N-Terminus	Gloeckner *et al.* 2010
S971 S973 S975 S976 S979	N-Terminus	Gloeckner *et al.* 2010
T1343 S1345 T1348	ROC	Greggio *et al.* 2009 Gloeckner *et al.* 2010
T1410	ROC	Kamikawaji *et al.* 2009
T1491	ROC	Kamikawaji *et al.* 2009 Greggio *et al*. 2009
T1967	Kinase	Kamikawaji *et al.* 2009
T2031	Kinase	Greggio *et al*. 2009 Li X. *et al.* 2010
T2032 T2035	Kinase	Li X. *et al.* 2010

Table 1.3. Reported LRRK2 phosphorylation sites. (Taken from Gloeckner *et al.* 2010)

Purification and mass spectrometry analysis of phosphorylation sites in ΔN-LRRK2 from Sf9 insect cells has shown phosphorylation at a number of residues in the kinase (T1967) and ROC domains (T1410, T1491). KD mutations in this protein showed a dramatic reduction in phosphorylation at these sites. Conversely, incubation of the protein with ATP increased phosphorylation at these sites, suggesting that these are autophosphorylation sites (Kamikawaji *et al.* 2009). Studies by other groups have confirmed LRRK2 phosphorylation at residues T2031, S2032, and T2035 and perhaps importantly in terms of PD pathogenesis, phospho-antibodies (p-antibodies) against these residues, have shown that there is a 30% increase in phosphorylation when transfected cells are subjected to

oxidative stress due to exposure to H_20_2 (Li X. *et al.* 2010), suggesting that oxidative stress may activate LRRK2.

1.8 PUTATIVE FUNCTIONS OF LRRK2

1.8.1 The role of LRRK2 in signaling cascades-clues from LRRK2 structure

The RIPK family of proteins, have been shown to autophosphorylate and phosphorylate many targets including the mitogen activated protein (MAP) kinases JNK, p38 and extracellular signal-regulated kinase (ERK) (reviewed in Meylan *et al.* 2005) (see Figure 1.4). The ROCO proteins, to which LRRK2 is closest phylogenetically, have also been shown to function as member of signaling cascades. The best-studied member of the ROCO proteins is DAPK1, a well-characterized serine/threonine kinase, which contains a death domain, as well as the characteristic ROC-COR tandem. DAPK1 is known to signal through the ERK pathway and functions upstream of p53 in response to hyperproliferative signals to induce apoptosis by formation of autophagic vesicles and membrane blebbing (Harrison *et al.* 2008). LRRK2 is poorly tolerated by cells made to overexpress the protein, however the closely related homolg LRRK1, which is of almost identical domain structure, is not toxic and overexpression in cells is well tolerated (Korr *et al.* 2006). Recently, it has been suggested that LRRK1 and LRRK2 are able to heterodimerise and genetic analysis of LRRK2 mutation carriers showed that some individuals also carry LRRK1 mutations, which appear to modify the progression of PD (Dachsel *et al.* 2010). Despite this, mutations in LRRK1 alone have not been shown to cause PD and it is generally considered that LRRK1 activity is not toxic (Greggio *et al.* 2007). Apart from differences in sequence, the largest difference between these kinases lies in the N-terminal, a clue perhaps to the cause of LRRK2 toxicity. LRRK2 is 513 amino acids longer and has additional leucine-rich, ankyrin and putative armadillo repeats at this end of the protein, indicating a greater propensity for protein-protein interaction. Indeed studies looking at the role of apoptosis in LRRK2 mediated cell death further emphasise the role of LRRK2 as a scaffold, with the discovery that LRRs and the WD40 domain are essential for

LRRK2 toxicity (Iaccarino *et al.* 2007). In this case, it would seem likely that the toxic effects of LRRK2 are mediated in part by interaction of the N-terminus with binding partners, which mediate this toxicity.

Ankyrin repeats are found in a wide variety of proteins including the DAG kinases and ankyrins, which are known to signal in cell death pathways and function to link cytoplasmic structural proteins to integral membrane proteins in some cases (Bennett, 1982). LRRK2 has been reported to have an affinity for lipid structures in a number of studies. Immunostaining of rat and human brain tissue, and rat primary neurons showed association of LRRK2 with vesicular structures and with the outer mitochondrial membrane (Biskup *et al.* 2006). Similarly, fractionation of mouse primary neurons has showed the affinity of LRRK2 for lipid rafts (Hatano *et al.* 2007) and investigations using a human genomic reporter model, have suggested a role for LRRK2 in membrane microdomains and their associated functions (Alegre-Abarrategui *et al.* 2009). Subcellular fractionation has shown that LRRK2 is in active form when membrane bound (Berger *et al.* 2010), suggesting that there is an important membrane associated protein which activates LRRK2, or as been shown with MAO, that membrane interaction can itself activate LRRK2, perhaps through induced conformational change (Diatlovitskaia *et al.* 1977). This membrane association perhaps supports the idea that LRRK2 could be involved in signaling through transduction cascades.

1.8.2 Function of LRRK2- MAP kinase cascade signaling.

In line with the known functions of RIP kinases and some members of the ROCO proteins, there have been many reports that LRRK2 interacts with proteins and controls functions that involve protein kinase B (Akt) signaling. Activation and perturbation of many MAP kinase pathways has been shown in PD and it is becoming apparent that cell death is not a stand-alone process and is instead the other side of the coin in controlling homeostasis of cellular proliferation. Proliferation must be tightly regulated in order to ensure that this process does not become oncogenic, however, 'applying the brakes' too forcefully, can tip the balance and cause cell death (reviewed in Plun-Favreau *et al.* 2010).

Extracellular stimulation of cell division, is mediated through ligand binding to cell surface receptors and is triggered by stimulants such as growth factors, insulin and other cytokines (reviewed in Rozengurt, 1986). Mitogens, as these ligands are called, stimulate cell division cascades and their related processes, however in post-mitotic neurons, signaling is not allowed to reach the stage where division is initiated-short stimulations promote cell repair functions, however longer durations of pathway activation result in apoptosis (Naetzker *et al.* 2006). Pathways activated by mitogens are characterised by the involvement of kinase cascades to transduce signals. p38, JNK (c-Jun N-terminal kinase), and ERK are MAPKs (Figure 1.4) activated in response to various pro-mitogenic stimuli. Activation of upstream kinases initiates a phosphorylation cascade,

STIMULUS → MAPKKK → MAPKK → MAPK → RESPONSE

which results in their activation and subsequent transcription of required genes. Early interaction studies looking at the possible role of LRRK2 in MAP kinase signaling have showed that it can interact, and phosphorylate some MAPK kinases (MKKs 4, 6 and 7), linking the protein to p38 mitogen-activated protein kinase signaling (Gloeckner *et al.* 2009). Another study looking at this in more detail has shown that LRRK2 can bind to MKKs 3, 6 and 7 through the ROC/kinase domain and control localization of some MKKs. Overexpression of LRRK2 in Hek293T causes the amount of MKK6 localised to the plasma membrane to increase by four-fold, suggesting that the protein-protein interaction domains of LRRK2 may be important here too (Hsu *et al.* 2010). A role for LRRK2 functioning in the MAPK cascade involving ERK 1/2 has been proposed with studies showing that LRRK2-induced neurite shortening (thought to be caused by autophagy), can be partially rescued by utilization of the MEK inhibitor U0126 (Plowey *et al.* 2008). Leukocytes from PD patients with sporadic and G2019S PD show a significant reduction in levels of phospho-Src (p-Src), HSP27 and JNK when compared to normal controls. Interestingly p-Src and p-HSP27 are also reduced in G2019S patients without the clinical symptoms of PD, suggesting that this activation may not necessarily be

disease related, but instead due to the G2019S mutation and LRRK2 itself (White *et al.* 2007).

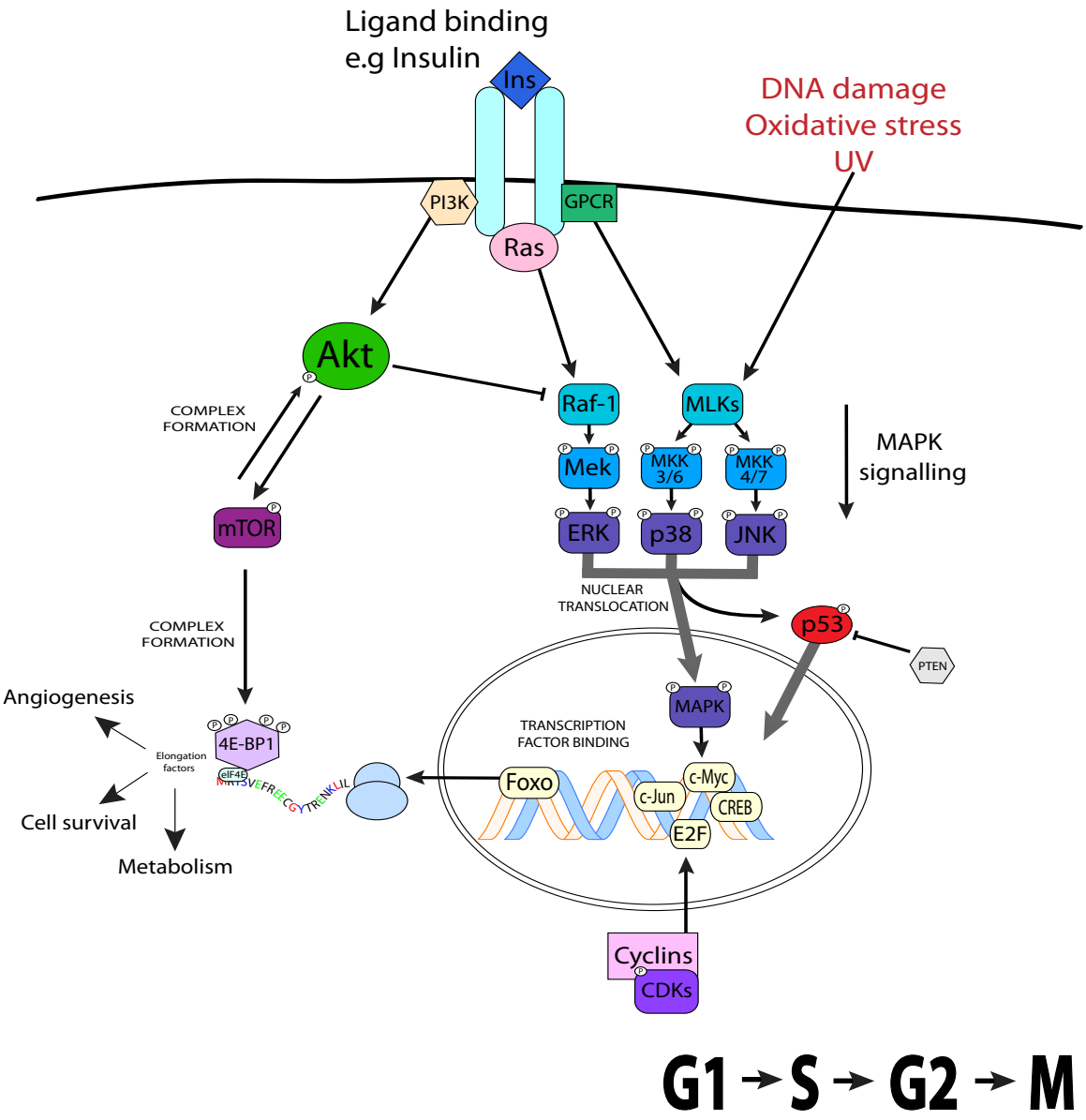

Figure 1.4. Overview of the main pathways that have been implicated in LRRK2 Parkinson's disease.

Hek293T cells transfected with WT and Y1699C LRRK2 have been shown to display reduced basal levels of p-ERK. Treatment of these cells with H_2O_2 after transfection, causes a significant increase in p-ERK levels for WT LRRK2 compared to Y1699C and non-transfected cells, and reduced cell death, again supporting a role for LRRK2 in MAP kinase signaling (Liou *et al.* 2008). The importance of kinase activity for this role has been shown by induction of LRRK2 in transient and stably transfected Hek293T cells which results in increased levels of p-ERK 1/2 that is not seen when kinase dead (KD) LRRK2 carrying the K1906N mutation is expressed (Carballo-Carbajal *et al.* 2010). This activation of ERK can also be seen with G2019S and R1441C, but at decreased levels. When LRRK2 is expressed for extended time periods, R1441C and G2019S show slower activation of ERK, which peaks at 24 and 48 hours respectively, compared to 12 hours with the WT. Importantly, expression of α-syn was also shown to be upregulated by WT LRRK2 to nearly 1.8 times basal levels in this study. For G2019S, this was increased, but at a reduced level of around 1.5 times, suggesting that LRRK2 may play a role in controlling α-synuclein levels through regulation of the ERK pathway. In this, case dysregulation caused by mutations could be a major factor in LRRK2 induced PD pathogenesis.

1.8.3 mTOR signaling and LRRK2

LRRK2 was first linked to mTOR signaling through studies showing that overexpression of G2019S in cells, can lead to upregulation of autophagy (MacLeod 2006Plowey *et al.* 2008). Similarly, LRRK2 has been shown to localise to the endosomal-autophagic pathway in human brain sections and knockdown of *LRRK2* in human cell lines has been shown to upregulate autophagy (Alegre-Abarrategui *et al.* 2009).

Initiation and control of autophagy occurs through mammalian target of rapamycin (mTOR) signaling (Beugnet *et al.* 2003), which regulates the process through G-proteins upon recruitment to autophagic membranes (Garcia-Marcos *et al.* 2011). Mitogen activation of receptors results in upregulation of required gene products. Through the mTOR pathway, this upregulation is controlled at the

translational level. Signalling through Akt results in activation of mTOR and phosphorylation of 4E-BP, an elongation factor, which serves as a negative regulator of translation by binding to translation factors. mTOR is inhibited by the compound rapamycin (Brown *et al.* 1994) and is also regulated by intracellular amino acid levels (especially leucine) and nutrient deprivation (Beugnet *et al.* 2003).

In *drosophila*, LRRK2 has been shown to demonstrate genetic interaction with components of the mTOR pathway, to regulate cell growth and cell size in development (Imai *et al.* 2008). Knockout of the *drosophila* homolog *LRRK* in models overexpressing mTOR pathway components, has shown that LRRK2 can exacerbate developmental defects in flies. Importantly, these phenotypes can be rescued by over-expression of WT but not KD *LRRK*, suggesting that LRRK2 is playing a functional role in these processes. Further investigation into the role of LRRK2 kinase activity and mTOR signaling *in vitro* in these experiments, showed that human LRRK2 overexpressed in Hek293T cells, is able to directly phosphorylate 4E-BP at residues T37 and T46. Western blotting has supported these findings, as flies overexpressing *LRRK* showed increased phosphorylation at these residues. Similarly, *LRRK* knockout flies showed decreased phosphorylation at these residues (Imai *et al.* 2008). Other groups have disputed the idea that LRRK2 is able to phosphorylate 4E-BP directly in humans, with the finding that recombinant 4E-BP is a poor substrate for LRRK2 *in vitro* (Kumar *et al.* 2010). This may mean that LRRK2 plays a different role in humans than in flies. In this case, interaction of LRRK2 and 4E-BP in humans may be indirect and mediated instead by other proteins, or a shared signaling cascade.

Links between 4E-BP and LRRK2 in *drosophila* have been shown at the RNA level, however the differences caused by overexpression of WT and mutant *LRRK2* are not seen at protein level (Kanao *et al.* 2010). 4E-BP expression is reportedly controlled by the forkhead transcription factor (Foxo) (Southgate *et al.* 2007) and investigation into a possible relationship between Foxo and LRRK2 has shown that overexpression of LRRK2 can exacerbate Foxo-mediated developmental defects. *In vitro* kinase assays have also shown that human Foxo can be phosphorylated by

LRRK2 at S319 (Kanao *et al.* 2010). Endogenous phosphorylation at this residue, is increased by overexpression of LRRK2 in WT and mutant flies, but not a triple KD form or when endogenous *LRRK* is knocked out. Further investigation into downstream mechanisms of possible LRRK2 signaling, have shown that LRRK2 induces expression of Hid, (the drosophila homolog of Bcl-2 family member Bim), which plays a mediatory role in apoptosis (Kanao *et al.* 2010).

Recent studies using manipulation of *drosophila* genetics have shown that LRRK2 could be playing a role in the direct regulation of gene transcription and translation (Gehrke *et al.* 2010). Using a microRNA (miRNA) reporter gene-system, knockdown of *LRRK* in *drosophila* has been shown to cause decreased levels of RNA degradation through dysregulation of miRNA mediated degradation pathways. In this model, overexpression of kinase active, but not KD LRRK2 decreases the protein levels of transcription factors E2F1 and DP and reduces initiation of cell proliferation and p53-dependent/independent apoptosis. E2Fs are activating factors which promote cell cycle G1/ S transition (reviewed in Harbour *et al.* 2000). Similarly, overexpression and immunoprecipitation of LRRK2 in Hek293T cells, and immunoprecipitation from *drosophila* head extracts, has shown that LRRK2 can associate with the RNA silencing protein Argonaute. This suggests that, in *drosophila* at least, LRRK2 may play an active role in RNA translation (Gehrke *et al.* 2010). Studies reporting similar results in humans are yet to be published.

1.8.4 LRRK2 and α-synuclein

It has been suggested that the importance of LRRK2 and α-syn in the pathogenesis of genetic PD, points towards common pathways or functions for these proteins (Singleton, 2005) an idea reinforced by both α-syn and LRRK2 being identified in genome wide association studies for idiopathic PD (Tan *et al*. 2010, Satake *et al.* 2009). Indeed, there is mounting evidence to suggest that this may be the case; it has been shown that α-syn and LRRK2 are co-regulated in rodent striatum (Westerlund *et al.* 2008), and overexpression of α-syn and LRRK2 in transgenic mice has shown that α-syn accumulation and deposition is exacerbated by

overexpression of LRRK2 (Lin *et al.* 2009). Ablation of LRRK2 in this model reduced α-syn pathology, although there was no evidence of a direct phosphorylation event (with the double transgenic displaying reduced phosphorylation of α-syn). Overexpression of LRRK2 in cell models has shown that expression of α-syn may be regulated by LRRK2 via involvement of the ERK pathway as increased expression of LRRK2 linked to an upregulation of α-syn (Carballo-Carbajal *et al.* 2010).

Studies in mice have shown that α-syn accumulation and deposition could be dependent on *LRRK2* expression (Lin *et al.* 2009). Double transgenic mice overexpressing human LRRK2 in WT and G2019S form, and α-syn in WT and A53T form, show abnormal somatic accumulation of α-syn that is not seen in single α-syn or LRRK2 transgenic mice. These double transgenic models also displayed fragmentation of the cis- and trans-Golgi, which was shown to correlate with somatic LRRK2 accumulation. Solubility of βIII tubulin was decreased in double transgenic mice compared to single transgenic expressing α-syn or LRRK2 alone. Importantly, double transgenic mice showed neuronal death in the striatum, which was increased by about 50% when compared to A53T overexpressing mice. Importantly, knockout of endogenous LRRK2 was shown to ameliorate the pathological phenotypes and cell death observed in double transgenics overexpressing kinase-active LRRK2. These experiments suggest that LRRK2 may be mediating α-syn induced changes in neurons, through mechanisms involving microtubule dynamics and stability (Lin *et al.* 2009).

1.8.5 LRRK2 and regulation of microtubules

The presence of tau pathology in some familial LRRK2 cases has prompted speculation that LRRK2 may be involved with microtubule regulation. Indeed, there is accumulating evidence to suggest that LRRK2 may play a role, either direct or regulatory, in cytoskeletal modeling and outgrowth. LRRK2 interaction studies have consistently identified cytoskeletal proteins and related structural components, the first published LRRK2 pull down, using overexpression in Hek293 cells identified clathrin heavy chain, and to a lesser degree, vimentin as interactors

of LRRK2 (Dachsel *et al.* 2007). Similarly, a glutathione-S transferase-tagged (GST) recombinant fragment consisting of the LRRK2 ROC domain has been shown to interact directly with α/ β-tubulin heterodimers (Gandhi *et al.* 2008). This interaction was also shown when endogenous mouse LRRK2 was co-purified with β-tubulin in brain and when LRRK2 overexpression was switched on in inducible Hek293T cells (Gillardon, 2009a, b).

Studies to assess LRRK2 kinase substrates, have again supported a role for LRRK2 in cytoskeletal modeling. When the more active G2019S variant of LRRK2 was incubated with protein extracted from whole mouse brain, it was shown that LRRK2 can phosphorylate the actin/ plasma membrane cross-linker, membrane-organizing extension spike protein (moesin) at a known threonine phosphorylation site, T558 (Jaleel *et al.* 2007). Moesin is a member of the so-called ERM family of proteins, which are stereologically regulated by phosphorylation. In an unphosphorylated state, they have a closed, 'inactive' conformation, which is reversed by addition of a phosphate to T558 in the C-terminal domain (Matsui *et al.* 1998). In mice, knock out of *LRRK2* has been shown to decrease phosphorylation of ERM proteins and inducible expression of G2019S causes accumulation of F-actin in the filopodia of developing neurons and increased phosphorylation of ERM proteins (Parisiadou *et al.* 2009).

Drosophila dendritic aborisation neurons overexpressing human *LRRK2*, have been shown to display shorter dendrite lengths and dendritic degeneration, which is more pronounced in G2019S, compared to WT, R1441C and G2385R mutants. In a subtype of these neurons, mislocalisation of tau has also been shown when G2019S but not WT is overexpressed (Lin *et al.* 2009). In G2019S overexpressing models, levels of p-tau (T212/S214) are increased, with mutation of this residue to an alanine shown to confer protection against LRRK2 mediated neurogeneration. GSK3β is known to phosphorylate tau at this residue and overexpression of the *drosophila* GSK3β homolog *sgg* also rescues DA neurons from LRRK2-induced microtubule disruption and dendrite degeneration, suggesting that *sgg* may be mediating some of the effects of LRRK2 mediated pathology in *drosophila*.

Encouragingly, studies in mice have also reported changes to tau when LRRK2 is overexpressed. BAC overexpressing human LRRK2, showed widespread mislocalisation of tau to cell bodies in G2019S mice, with WT LRRK2 overexpressing mice showing a lower amount of tau accumulation in regions with highest LRRK2 expression only. Again WT mice showed lower levels of tau accumulation than the G2019S mice, which was localised to regions with highest LRRK2 expression. In G2019S mice, there was a marked and widespread increase in tau phosphorylation at S202 and S262/356 that was visible in mice aged over 18 months. Interestingly, when tau from G2019S was dephosphorylated, it showed a different migratory pattern than that from non-transgenic mice, suggesting that LRRK2 could be affecting post-translational modification of tau, in ways other than phosphorylation (Melrose *et al.* 2010).

Regulatory roles for LRRK2 in cytoskeletal modeling have been shown in a number of studies. Y2H screens have identified the DVLs as possible interactors of the ROC domain (Sancho *et al.* 2009). The DVLs signal as part of the Wnt signaling cascade in numerous processes, such as neurite outgrowth during development and planar cell polarity during gastrulation (Sussman *et al.* 1994). Of note, GSK3β and CK1, known to phosphorylate α-syn and tau respectively, are involved in this cascade. Studies to identify LRRK2 interactors using endogenous immunoprecipitation have pulled down many components of the actin cytoskeleton. Immunoprecipitation of LRRK2 from NIH3T3 compared to pulldowns from cells treated with LRRK2 RNAi, have identified interactions with actin and numerous actin-asociated proteins, including F-actin capping protein subunits, myosin and tropomyosin isoforms and calmodulin. Co-sedimentation assays showed that LRRK2 seems to bind F-actin and furthermore, that knockdown of LRRK2 in developing dopaminergic midbrain primary neurons, causes neurite shortening (Meixner *et al.* 2011).

Protein microarrays of SH-SY5Y LRRK2 knockdown cells have suggested a link between LRRK2, ARHGEF7 and Cdc42 (Haebig *et al.* 2010). Recently, this study was expanded to examine possible functional roles for these proteins (Haebig *et al.* 2010). It was shown that the GTP exchange factor ARHGEF7, and the Rho-GTPase, Cdc42 which are both involved in the cell division cycle by regulating actin motility

during development (Meyer *et al.* 2002), can co-precipitate when overexpressed in Hek293T cells and when LRRK2 is immunoprecipitated from mouse brain. Interestingly, despite assertion that LRRK2 does not need a GEF due to its classification as a GAD (Gasper *et al.* 2009) ARHGEF7 was shown to double the efficiency of GTP hydrolysis by LRRK2. Most recently, protein microarrays have suggested an interaction between LRRK2 and the STE kinases TAOK3, STK3, STK24, STK25. PKCζ was shown to bind LRRK2, but is not a kinase substrate, however *in vitro* kinase assays showed that PKCζ is able to phosphorylate LRRK2 (Zach *et al.* 2010). This study suggests that LRRK2 may function upstream of tau, via interaction with TAOK/ MARKK, the kinase upstream of microtubule affinity-regulating kinase (MARK), which has been shown to prime tau for phosphorylation by other kinases (Timm *et al.* 2006).

Studies by collaborators, have shown that the β-tubulin isoform TUBB5 (Law and Harvey, unpublished) and dishevelled (DVL) isoforms 1, 2 and 3 (Sancho *et al.* 2009) can cause transcription factor binding when the ROC domain is used as bait in a Y2H screen. Previous studies have shown that LRRK2 can phosphorylate β-tubulin *in vitro* (Gandhi *et al.* 2008, Gillardon 2009a, b), and ROC binding to DVL proteins is thought to be disrupted by familial mutations (Sancho *et al.* 2009). β-tubulin is phosphorylated by a number of kinases including PKC (Chen *et al.* 2002), Cdk1 (Fourest-Lieuvin *et al.* 2006) and the β-adrenergic receptor associated kinase GRK2 (also called β-ARK2) (Yoshida *et al.* 2003) to regulate microtubule extension and cytoskeletal rearrangement. Extension and polymerisation is known to be dependent on GTP hydrolysis by the tubulins, therefore it is a possibility that interaction with the ROC domain serves some functional purpose.

The DVL proteins are also involved in cytoskeletal dynamics as members of the 'wingless and int (Wnt) signalling pathway. This pathway was first discovered in *drosophila* and controls planar cell polarity, with an involvement in neurite outgrowth. LRRK2 has previously been implicated in neurite outgrowth, with overexpression of WT and G2019S LRRK2 in primary neuronal cultures, resulting in a reduction in neurite length and branching. Knockdown of LRRK2 has been

shown to promote the opposite effect, with neurites demonstrating increased length and branching (Macleod *et al.* 2006).

As previously discussed, LRRK2 mutation carriers show different pathologies; some post mortem brains show α-syn deposition, some have TDP-43 positive inclusions, while others have tau pathology, with neurofibrillary tangles and tau positive neurites (Rajput *et al.* 2006). Because of this, it has been suggested on many occasions that LRRK2 could act at the intersection of these pathways, bringing together many different strands of neurodegenerative disease. The Wnt signaling pathway is a good candidate for linking many of these pathways, with CK1 and GSK3β both involved in this signaling cascade. CK1 is known to phosphorylate α-syn and GSK3β is well known for phosphorylating the microtubule binding protein tau, with mutations in tau known to cause Alzheimer's, linking PD with many other movement disorders such as PSP and Pick's disease. Recent studies in *drosophila* have shown that overexpression of LRRK2 can result in recruitment of GSK3β. The DVL proteins interact directly with both CK1 and GSK3β (Sakanaka *et al.* 2000) suggesting a possible mechanism for linking α-syn and tau pathology.

Although the exact role of LRRK2 is currently unknown, the studies that have been published to date are starting to converge with the publication of more data. The discovery that LRRK2 interacts with 14-3-3 (Dzamko *et al.* 2010, Nichols *et al.* 2010, Li X. *et al.* 2011) suggests that binding partners of this protein likely to be numerous, as 14-3-3 is known to function in a wide range of signaling pathways (Bridges *et al.* 2005). In this case, the physiological role of LRRK2 is also likely to span a wide range of functions.

1.9 EXPERIMENTAL AIMS

The discovery that LRRK2 is a cause of autosomal dominant PD, has provided an opportunity to investigate the pathogenesis of this form of the disease from a "bottom-up" perspective. LRRK2 is a good target for investigation, as PARK8-linked PD is indistinguishable from sporadic PD and as such perhaps even a candidate for therapeutic intervention in sporadic PD. A reductionist approach to LRRK2 function poses intrinsic questions about the regulation of this protein due to its domain structure, as well as its regulation by other proteins. The multi-domain structure of LRRK2 with both enzymatic and interaction domains, makes it apparent that there are many layers of regulation controlling the functional outputs of this protein. By understanding how LRRK2 works on a molecular level therefore, we can slowly piece together how this protein controls its outputs and build on this knowledge with the intended result of perhaps understanding more about PD mechanisms in general. To this end, work done in this thesis was focused on three levels of LRRK2 regulation and function, namely

1) Understanding the factors controlling LRRK2 dimer formation.
2) Investigating the regulation of kinase activity.
3) Identification and characterisation of LRRK2 interacting proteins and kinase substrates.

These issues were examined in terms of both WT and mutant LRRK2 functioning. To do this, a number of models of LRRK2 function have been used. The majority of studies looking at internal regulation of LRRK2 kinase activity have been performed in protein immunoprecipitated from cells and likely have some interacting proteins present. In this case it is hard to differentiate intrinsic LRRK2 enzymatic activity, from activity dependent on activation and promoted by other interacting proteins. To address this issue, recombinant LRRK2 has been used as a model of intrinsic LRRK2 activity. As this protein has undergone affinity purification under conditions more stringent than those used when immunoprecipitating overexpressed protein, there is less chance of LRRK2 complexes being intact. To model endogenous LRRK2 complex formation,

fibroblasts taken from LRRK2 mutation carriers with PD and their non-affected siblings were used.

2. METHODS AND MATERIALS

2.1 MATERIALS

2.1.1 Buffers and solutions

Pre-made buffers are listed according to their manufacturer. For all other buffers, components were purchased from Sigma (unless otherwise stated) and are of molecular biology grade.

-1X Anode buffer (*Invitrogen*). Contains 50 mM BisTris, 50 mM Tricine, pH 6.8).

-1X BlueNative transfer buffer (*National Diagnostics*). (25 mM Tris, 192 mM glycine, 20% (v/v) methanol, 0.1% (w/v) sodium dodecyl sulfate (SDS)).

-Cell lysis buffer (*Cell signaling*). Contains 20 mM Tris-HCl (pH 7.5), 150 mM NaCl, 1 mM Na_2EDTA, 1 mM EGTA, 1% Triton, 2.5 mM sodium pyrophosphate, 1 mM β-glycerophosphate, 1 mM Na_3VO_4, 1 µg/ml leupeptin.

-5X Centrifuge buffer. Contains 2.5% (v/v) Triton X-100, 250 mM HEPES (pH 7.4), 450 mM NaCl, 10mM DTT.

-1X Dark blue cathode buffer (*Invitrogen*). Contains 50 mM BisTris, 50 mM Tricine, pH 6.8, 0.02% (w/v) Coomassie G-250.

-Destain solution. 50% (v/v) methanol, 10% (v/v) acetic acid.

-**6X DNA loading buffer.** Contains 30% glycerol (v/v), 0.25% (w/v) bromophenol blue.

-HEPES buffer. Contains 150 mM NaCl, 20 mM HEPES, pH 7.4 and 5 mM $MgCl_2$.

-HiSalt wash buffer. Contains 1% (v/v) Triton X-100, 500mM NaCl made up in 1X PBS.

-Fixing solution. Contains 40% (v/v) methanol, 10% (v/v) acetic acid.

-Kinase buffer (*Cell signaling*). Contains 25 mM Tris-HCl (pH 7.5) 5 mM β-glycerophosphate, 2 mM dithiothreitol (DTT), 0.1 mM Na_3VO_4, 10 mM $MgCl_2$.

-4X LDS loading buffer (*Invitrogen*). Contains 40% (v/v) glycerol, 4% (w/v) lithium dodecyl sulfate (LDS), 4% (v/v) Ficoll-400, 0.8 M triethanolamine-Cl pH 7.6, 0.025% (w/v) phenol red, 0.025% (w/v) Coomassie G-250, 2mM EDTA disodium.

-1X Light blue cathode buffer (*Invitrogen*). Contains 50 mM BisTris, 50 mM Tricine, pH 6.8, 0.002% (w/v) Coomassie G-250.

-1X MES running buffer (*Invitrogen*). Contains 50 mM Tris base, 50 mM 3–(N-Morpholino) propanesulfonic acid, 1 mM EDTA, 0.01% SDS at pH 7.3.

-Phosphate Buffered Saline (PBS). In tablet form. When dissolved contains 0.14 M NaCI, 0.01 M PO_4 Buffer, 3mM KCI.

-PBS-Tween (PBST). 1X PBS, supplemented with 0.001% (v/v) Tween-20.

-1X TAE buffer. Contains 40 mM Tris acetate, 1 mM EDTA.

-1X TLC Buffer. 1.2M Formic acid, 1M LiCl.

-1X Transfer buffer (National Diagnostics). Contains 25 mM Tris, 192 mM glycine, 20% (v/v) methanol.

2.1.2. Cell culture

2.1.2.1 Cell lines used in this thesis

Numerous cell lines have been used for the work done in this thesis. As a model of endogenous LRRK2, human fibroblasts were taken from familial PD patients carrying G2019S R1441G and Y1699C heterozygous mutations and compared to age and sex matched, genetically linked controls (see Table 2.1).

Code	Sex	Phenotype	Details	D.O.B	Age at biopsy	Mutation found
A	F	Unaffected	Sister of D	unknown	70	Unaffected
B	F	Unaffected	Sister of C	28/03/1958	50	Unaffected
C	F	PD	Sister of B	28/05/1956	52	LRRK2 G2019S
D	F	PD	Sister of A	unknown	67	LRRK2 R1441G
E	F	PD	Unrelated	04/11/0936	71	LRRK2 Y1699C

Table 2.1. Details of patient fibroblasts used for this study. All cells were taken from females to minimize sex differences and have an average age of 62 years ±10.17 years. Both controls are non-affected siblings of the G2019S or R1441G mutation carriers.

For overexpression and immunoprecipitation of LRRK2 protein, Hek293T cells were used. Hek293T cells have been used successfully in the literature to express LRRK2 from plasmids and as such, have been used in these studies to generate tagged forms of LRRK2 for immunoprecipitation. To examine the expression levels of LRRK2 in various laboratory cell types, three other adherent human lines were also used, namely HT1080i, a fibrosarcoma line, the neuroblastoma line SH-SY5Y and the 1321N1 astrocytoma line. All non-primary cell lines were purchased from ATCC.

2.1.2.3 Reagents

All cell culture reagents were purchased from Invitrogen unless otherwise stated.

-Complete Dulbecco's Modified Eagle's Medium (DMEM). 1X, contains sodium pyruvate, phenol red, 4.5g/L D-glucose and 4mM L-glutamine. Supplemented with 10% (w/v) Fetal Bovine Serum (FBS).
-DMSO, sterile filtered (*Sigma*).
-Dulbecco's PBS (Without Ca and Mg. Without Phenol red).
-FBS, South American origin (heat-inactivated).
-1X TryPLE EXPRESS, in 1X DPBS, 1mM EDTA. Contains phenol red.

2.1.3 Molecular biology

2.1.3.1 Primers and Constructs

Full-length LRRK2 plasmids with a 2X N-terminal myc-tag (N-myc-LRRK2 hereafter) were used for all experiments. Plasmids were kindly donated by Dr Mark Cookson (Cell biology and expression unit, NIH laboratories, Bethesda). Expression of these plasmids is driven by a pCMV promoter and a kanamycin resistance gene is also contained in the construct. KD forms of the plasmid containing the triple K1906A/D1994A/D2017A mutation were also used.

2.1.3.2 Oligonucleotides

LRRK2 PCR primers were designed by the primer design website http:\www.ncbi.nlm.nih.gov/tools/primer-blast. All primers were designed across exon-exon boundaries to ensure any contaminating genomic DNA present would not be amplified.

Primer	Sequence	Application	Product
LRRK2 forward: LRRK2 reverse:	5'-TCAATATAAAGGCTCGCGCT-3' 5'-TACAAAGCCACTTGGGTTCC-3'	PCR	507 bps
GAPDH forward: GAPDH reverse:	5'-CCATGGCACCGTCAAGGCTGA-3' 5'-GCCAGTAGAGGCAGGGATGAT-3'	PCR	469 bps
M1947A Forward: M1947A Reverse:	5' CCCGGATGTTGGTG**GCA**GAGTTAGCCTCCAAG-3' 5' CTTGGAGGCTAACTC**TGC**CACCAACATCCGGG-3'	Mutagenesis	N/A

Table 2.2. Primers used for DNA amplification. PCR primers were synthesized by MWG Operon and purified by HPSF. Primers for mutagenesis were synthesized by MWG Operon and purified using HPLC. Bases corresponding to the amino acid change for mutagenesis primers are marked in red.

The sequence for GAPDH primers was taken from Poomthavorn *et al.* (2009). Mutagenesis primers were designed to substitute LRRK2 M1947 with an alanine residue, using the primer design program at

http://www.bioinformatics.org/primerx/.

Primer parameters were set so that,

- GC content >40%,
- Primer should terminate in >1 C/G bases,
- Length should be between 25 and 45 bases,
- Melting temperature should be close to or above 78°C.

2.1.3.3 Taqman probes

Pre-optimised probes for LRRK2 and the housekeeper β-Actin, were selected from the Applied Biosystems website www.appliedbiosystems.com (see Table 2.3). These assays were produced with different fluorescent labeling, so that both reactions could be performed in a single well and are the recommended probes for each gene.

Probe number	Exon overlap	Domains spanned	Labelling	Amplicon length
Hs00411194_m1	44 and 45	LRRK2-Kinase/WD40	FAM- Emission 520nm	90bp
Hs01597125_s1	Exon 1	β-Actin	VIC- Emission 552nm	132bp

Table 2.3. Taqman probes chosen for amplification of LRRK2 and GAPDH.

2.1.3.4 Reagents for amplification and replication of DNA

All reagents were purchased from Sigma unless otherwise stated.

-Agarose (molecular biology grade). Gels were made with TAE buffer.
-EcoRI restriction enzyme (*New England Biolabs*).
-Ethanol (Molecular biology grade 200% proof- *VWR*).
-Ethidium Bromide solution (500 µg/mL in H_2O).
-1M D-Glucose.
-Kanamycin solution 50mg/ml in 0.9% NaCl.
-Luria-Bertani (LB) broth (2% w/v). LB broth was made up in double-distilled H_2O (ddH_2O) and autoclaved at 121°C prior to use (*Invitrogen*).
-LB Agar (Lennox) 3.2% (w/v). LB agar was made up in double-distilled H_2O and autoclaved at 121°C prior to use (*Invitrogen*).

-2-Propanol (Molecular biology grade- *VWR*).

-Stbl3 chemically competent E-Coli (*Invitrogen*).

-Taqman gene expression master mix (2X- *Applied Biosystems*).

-TOP10 chemically competent E-Coli (*Invitrogen*).

2.1.3.5 DNA standards

DNA ladder standards were purchased from Promega. Bands ranged from 250 to 10,000 base pairs.

-1kb DNA ladder (DNA concentration 0.1μg/μl in 10mM Tris-HCl (pH 7.4), 1mM EDTA).

2.1.3.6 Kits for DNA/RNA extraction and amplification

Kits were purchased from Qiagen unless otherwise stated.

-Accuprime *Pfx* Supermix (*Invitrogen*).

-HiSpeed Maxiprep kit.

-Miniprep kit.

-QiAshredder cell homogenization kit.

-QuikChange XL mutagenesis kit (*Stratagene*).

-RNeasy Plus, RNA extraction kit.

-Superscript III First Strand Synthesis Supermix (*Invitrogen*).

2.1.3.7 Transfection

-DMEM, serum free. Contains sodium pyruvate, phenol red, 4.5g/L D-glucose and 4 mM L-glutamine (*Invitrogen*).

-Fugene HD (*Roche*).

2.1.4. Biochemical assays

2.1.4.1 Protein extraction and purification

Reagents were purchased from Sigma unless otherwise stated.

-Anti-myc -agarose (clone 9E10).
-Cell lysis buffer (*Cell signaling*).
-c*O*mplete protease inhibitor tablets (*Roche*).
-Glutathione-agarose. Beads were reconstituted in 1X PBS.
-HALT phosphatase inhibitor (*Pierce*).
-Protein G-Sepharose beads.

2.1.4.2 Recombinant Protein

The following recombinant GST-tagged proteins were purchased from Invitrogen and are guaranteed >80% purity. Contained in 50 mM Tris pH 7.5, 150 mM NaCl, 0.5 mM EDTA, 0.02% (w/v) Polysorbate 20, 2 mM DTT, 50% (v/v) glycerol.

-RIPK5
-LRRK2, wild type.
-LRRK2, D1994A.
-LRRK2, G2019S.
-LRRK2, I2020T.
-LRRK2, R1441C.
-LRRK2, Y1699C .

LRRK2 purchased from Invitrogen is lacking the N-terminus to residue 970 and is fused instead to a GST-tag (see Figure 2.1).

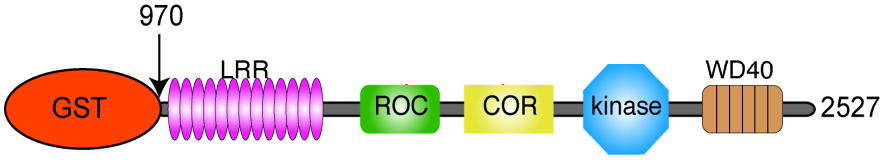

Figure 2.1. Linear representation of the ΔN-LRRK2 recombinant protein. GST-tagged LRRK2, spanning residues 970-2527, was expressed in Sf9 cells.

The following recombinant GST-tagged proteins were purchased from Abnova and are contained in 50 mM Tris-HCI, 10 mM reduced Glutathione, pH 8.0.

-DVL2.
-DVL3.
-TUBB5.

2.1.4.3 Kinase assays and Radiolabelling

The following reagents were purchased from Sigma unless otherwise stated.

-100mM ATP. In H_2O (adjusted to pH 7 with Tris-base).
-32P γ-labelled ATP, 500μCi at 10mCi/ml. In 50mM Tricine pH 7.6 solution (*Perkin Elmer*).
-G50 spin columns (*GE Healthcare*).
-10X Kinase buffer (*Cell signaling*).
-Myelin Basic protein, from mouse (guaranteed purity ≥95%). Lyophilized powder reconstituted in 1X PBS to 200μg/ml.
-Nucleoside Diphosphate Kinase (NDPK). Produced in bakers yeast.
-N^6(2-Benzyl)-ADP 10mM. Sodium salt in aqueous solution (*Biolog*).
-N^6(2-Benzyl)-ATP 10mM. Sodium salt in aqueous solution (*Biolog*).
-N^6(2-Phenylethyl)-ADP 10mM. Sodium salt in aqueous solution (*Biolog*).
-N^6(2-Phenylethyl)-ATP 10mM. Sodium salt in aqueous solution (*Biolog*).

2.1.5 Western blotting

All reagents were purchased from Invitrogen unless otherwise stated.

2.1.5.1 SDS-PAGE electrophoresis

-NuPAGE Bis-Tris gels. 4-12% polyacrylamide. 10 well 1.5mm wide.

-NuPAGE Bis-Tris gels. 4-12% polyacrylamide. 15 well 1.5mm wide.

2.1.5.2 BlueNative PAGE electrophoresis

-NativePage Bis-Tris gels. 3-12% polyacrylamide. 10 well gels 1.0mm wide.

-NativePage Bis-Tris gels. 4-16% polyacrylamide. 10 well gels 1.0mm wide.

-25% DDM (w/v). Made up in 1X PBS.

-Sample Preperation Kit (DDM, Coomassie G-250).

-Novex prestained standard.

2.1.5.3 Protein standards

Protein standards were purchased from Invitrogen in a pre-mixed preparation.

-NativeMark unstained protein standard (range 20-1236 kDa).

-Novex prestained protein standard (range 3.5-260 kDa).

2.1.5.4 Gel staining

-Acetic acid (glacial) 100%. (*VWR*).

-Gelcode Blue Stain Reagent (*Pierce*).

-Methanol, HPLC grade (*VWR*).

-SilverXpress silver staining kit.

2.1.5.5 Western blotting and transfer.

-CL-Xposure photosensitive film (*Pierce*)

-Nitrocellulose membrane. 0.45μm pore size (*Pierce*).

-Non-fat dried milk powder (*Marvel*).

-Immobilon-P, polyvinylidene fluoride (PVDF) membrane. 0.45μm pore size (*Millipore*).

-Superblock T-20 (*Pierce*).

-Tween-20 (*Sigma*).

-Whatman Chromatography paper.

-Western blotting substrate (Electrochemical detection kit- *Pierce*).

2.1.5.6 Glycerol gradient centrifugation

Reagents and proteins were purchased from Sigma unless otherwise stated.

-Glycerol, molecular biology grade.

-Catalase, from bovine liver. Lyophilized powder, reconstitiuted in 1X PBS (2,000-5,000 U/mg).

-L-Lactic Dehydrogenase (LDH), from *Lactobacillus leichmanii*. Lyophilized powder, reconstituted in PBS (150-300 U/mg).

-Ferritin, from human spleen (type V). In 0.15 M NaCl, 10 mM Tris, pH 8.0, contains 0.1% (w/v) sodium azide.

-Bovine Serum Albumin (BSA). Guaranteed purity ≥98%. Lyophilized powder, reconstituted in 1X PBS.

-Lambda phosphatase (*NEB*). Contained in 50 mM HEPES, 100 mM NaCl, 0.1 mM $MnCl_2$, 2 mM Dithiothreitol, 0.1 mM EGTA, 50% (w/v) Glycerol, 0.01% (w/v) Brij 35, pH 7.5 (400,000 U/ml).

2.2 METHODS

2.2.1 Cell culture

2.2.1.1 Isolation of human fibroblasts

Skin punch biopsies were performed by Dr. Daniel Healy on the forearm of two control patients and one individual each with G2019S, R1441G and Y1699C mutations in LRRK2 (see Table 2.1). Isolation of human fibroblasts was performed by Dr. Jan-Willem Taanman at the Royal Free Hospital, London.

2.2.1.2 Maintenance and passage of cells in culture

All cell culture was performed in a class II safety cabinet using aseptic techniques. Cell lines were cultured in DMEM supplemented with 10% FBS at 37°C in a 5% CO_2 humidified atmosphere. Media was replaced every 3-4 days and cells passaged when ~95% confluent. Cells were grown in flasks for maintenance and split into dishes to perform experiments. When cells reached ~90% confluency, passaging was performed. Media was removed by pipetting and cells washed once with DPBS to remove residual media. Tryple-Express was added and cells incubated at 37°C for 5-10 mins to facilitate detachment by the enzyme. After this time an equal amount of complete DMEM was added to quench enzyme activity and cell-containing media removed from flasks. Cells were pelleted at 1000 x g in a Hettich Rotina 35 benchtop centrifuge at RT for 3 mins and the supernatant removed. Complete DMEM was added and cells resuspended in an appropriate amount of media.

2.2.2 Molecular biology

2.2.2.1 RNA extraction

Cell pellets were obtained by trypsinisation of cells from one well of a 6 well plate for each condition. Pellets were washed twice in PBS, before RNA was extracted using the RNeasy Plus kit according to manufacturers instructions. Briefly, cells were lysed in lysis buffer (RNeasy kit) and cells homogenised by centrifugation through QIashredder columns. RNA was bound to the columns provided and contiminants removed by washing. RNA was eluted and integrity subsequently checked by analysis on an Agilent 6000 nanochip by Miss Daniah Trabzuni.

2.2.2.2 Reverse Transcriptase-PCR

1µg of RNA, ascertained by Nanodrop analysis, was used for each reaction. cDNA was made using Superscript III First Strand Synthesis kit (Invitrogen) using random hexamer primers. Primers were mixed with DNA and incubated at 65oC for 5 mins before cooling on ice and addition of the reaction mix containing dNTPs and the reverse-transcriptase (RT-PCR) enzyme. Cycling conditions are shown in Table 2.4.

Time	Temperature
5 mins	65°C
Cool on ice for 1 min	
10 mins	25°C
50 mins	50°C
5 mins	85°C
Leave at 4°C until needed	

Table 2.4. Cycling conditions used for RT-PCR.

2.2.2.3 Semi-quantitative PCR

Semi-quantitative PCR was performed using AccuPrime *Pfx* Supermix in Eppendorf Mastercycler gradient PCR machines. Primers used are detailed in Table 2.2 and were added at a final concentration of 200nM. 50ng of template cDNA extracted from cells was used for each reaction. Cycling conditions used are detailed in Table 2.5.

Time	Temperature	No of cycles
5 mins	95°C	X1
15 secs	95°C	X35
30 secs	60°C	
45 secs	68°C	
Leave at 4°C until needed		

Table 2.5. PCR cycling conditions.

PCR products were added to 6X DNA loading dye and run on a 0.8% agarose gel with ethidium bromide added at 1:25,000 to visualise DNA. Products were run at 120V for 40 mins and visualized using a UVP transilluminator. LRRK2 PCR products were normalized to GAPDH for each condition and quantified using ImageJ software downloaded from http://rsbweb.nih.gov/ij/.

2.2.2.4 Taqman quantitative-PCR

The levels of LRRK2 mRNA were quantified relative to the house-keeping gene β-actin, using the probes detailed in Table 2.3. The amount of cDNA used for experiments was optimised to ensure that the concentration of cDNA did not inhibit the PCR reaction (see Figure 5.3). 10ng of total cDNA was used for all experiments. Reaction mixtures of 20µl were made using cDNA, 2X Taqman Gene Expression Master Mix, β-actin and LRRK2 probes (20X concentration) in the same tube. PCR was performed in a Stratagene MX-3000P using the cycling conditions detailed in Table 2.6.

Time	Temperature	No of cycles
2 mins	50°C	X1
10 mins	95°C	X1
15 secs	95°C	X40
1 min	60°C	

Table 2.6. Cycling conditions used for Taqman quantitative-PCR.

2.2.2.5 Mutagenesis

Primers used for mutagenesis are detailed in Table 2.2. Mutagenesis was performed using the XL Quikchange mutagenesis kit. 125ng of primer was used with 20ng of plasmid template. Reaction mixtures were prepared according to manufacturers instructions and PCR was performed in an Eppendorf Mastercycler Gradient PCR machine, using the cycling conditions detailed in Table 2.7.

Time	Temperature	No of cycles
1 min	95°C	X1
50 secs	95°C	X18
50 secs	60°C	
15 mins	68°C	
7 mins	68°C	X1

Table 2.7. Cycling conditions for mutagenesis reaction.

PCR products were cooled on ice and transformed into XL10-Gold chemically competent cells according to manufacturer's instructions. Transformed *E-Coli* were plated on LB Agar supplemented with 100mM D-glucose and grown for 16 h at 37°C.

2.2.2.6 Plasmid purification

Clones were picked, grown in 15ml LB broth supplemented with 10% (v/v) 1M glucose and kanamycin 100mg/ml at 1:1000 (v/v), purified and sequenced. The successful clone containing the relevant mutation was grown in 600ml LB broth and purified using Qiagen HiSpeed maxiprep kit according to manufacturer's instructions. Plasmids were digested in EcoRI for 1 h at 37°C to ensure no rearrangements had occurred and run on a 1% agarose gel prepared in TAE at 120V for 30 mins, alongside a 1kb ladder to allow for identification of band sizes. The plasmid sequence was digested *in silico* to verify correct fragment sizes using the following website http://tools.neb.com/NEBcutter2/index.php.

2.2.3 Biochemical assays

2.2.3.1 Transfection

Hek293T cells were seeded and grown to ~80% confluency in 14cm^2 dishes in complete DMEM. Prior to transfection, DMEM was removed, cells washed with DPBS and serum-free DMEM added. DNA-Fugene HD complexes were made according to manifacturers at a ratio of 1:3 where 20µg plasmid DNA was used for each plate with 60µl Fugene HD. Complexed DNA was added drop-wise to cells and left overnight before media was removed and replaced with complete DMEM. Cells were allowed to grow for a further 24h before cells were harvested and protein extracted.

2.2.3.2 Protein extraction and protein estimation

Protein was extracted by scraping cells on ice into 1X lysis buffer supplemented with protease inhibitors. Cells were left to lyse on ice for 20 mins with occasional vortexing and insoluble material removed by centrifugation at 4^{o}C for 15 mins at 16,000g in a Beckman OptiMAX. Supernatents were removed and 10µl used in BCA assays and compared to a BSA standard curve to ascertain protein concentration. Reaction mixtures were prepared according to manufacturer's instructions.

2.2.3.3 Immunoprecipitation- Antibody

After extraction, lysates were pre-cleared by addition of 30µl agarose beads rotating at 4^{o}C for 1 h, before addition of 5µg anti-LRRK2 polyclonal antibody, which was left to bind at 4^{o}C overnight while rotating. Protein recognised by the antibody was immunoprecipitated by addition of 30µl protein G sepharose and incubation for 2 h rotating at 4^{o}C. Beads conjugated to immobilized protein, were collected by spinning for 15 seconds at 16,000g and the supernatent removed. Beads were washed 3 times in HiSalt wash buffer with vortexing, and twice in HiSalt wash buffer, rotating at 4^{o}C for 30 mins.

2.2.3.4 Immunoprecipitation- Agarose immobilized antibody

Myc-tagged proteins were extracted from whole cell lysates by incubating supernatants with anti-myc agarose overnight, rotating at 4^{o}C. Prior to incubation,

myc-agarose beads were blocked in 200ng/ml BSA at 4°C for 3 h with rotation. Unbound BSA was removed by washing twice using HiSalt buffer with vortexing and once with 1X lysis buffer. Beads containing bound LRRK2 were collected by spinning for 15 secs at 16,000 x g and the supernatant removed. Beads were washed 3 times in HiSalt wash buffer with vortexing, and twice in HiSalt wash buffer rotating at 4°C for 30 mins. An additional wash was performed in 1X kinase buffer when protein was required for kinase assays.

2.2.3.5 Affinity purification- glutathione-agarose

Affinity purification of recombinant GST-tagged proteins was performed using the cys-glu-gly tripeptide, glutathione conjugated to agarose beads. Beads were reconstituted by addition of PBS and vortexed. After incubation at 4°C for 20 mins, GST-agarose beads were washed twice in 0.9% NaCl solution to remove preservatives from the suspension solution. As described, beads were blocked using 10% BSA (w/v) at 4°C for 2h with rotation and unbound BSA removed by washing twice using HiSalt buffer with vortexing and once with 1X lysis buffer. After incubation overnight at 4°C rotating, beads were washed Beads were washed 3 times in HiSalt wash buffer with vortexing, and twice in HiSalt wash buffer rotating at 4°C for 30 mins. An additional wash was performed in 1X kinase buffer.

2.2.3.6 Sample preparation for ESI-QTOF mass spectrometry analysis

Bound protein was eluted in 4X LDS at 100°C for 20 mins. Samples were run on SDS-PAGE 4-12% gels and protein visualized by staining with Gelcode blue gel stain. When protein was required for analysis by mass spectometry, bands were excised with a scalpel. ESI-QTOF mass spectrometry was performed by Dr Wendy Heywood (UCL Institute of Child Health, Biological Mass spectrometry centre).

2.2.3.7 Kinase assays

All kinase assays using recombinant GST-tagged kinases, were performed using a kinase: substrate molar ratio of 1: 50 unless stated. Specifically, kinases were used at a concentration of 10nM for each assay and substrates used at 500nM. Assays were performed in 1X kinase buffer, with myelin basic protein (MBP) used as a generic substrate and specific substrates chosen as described. Reactions were

mixed on ice and the assay performed at 18°C. 1 µl of 32P γ-labelled ATP was added to catalyse each reaction and reactions mixed by pipetting prior to the removal of a time point. For assays performed over a time course, 10µl of reaction mixture was removed at each time point, including a 'zero' time point, where ATP was added to the mixture and an aliquot taken immediately. Each time point was added straight to 4X LDS loading buffer containing 10% (v/v) β-mercaptoethanol to stop the reaction. Proteins were denatured at 100°C for 10 mins.

For kinase assays with immunoprecipitated proteins, assays were performed at 37°C and shaken at 1000rpm in an Eppendorf Comfort thermomixer. The whole reaction mixture was added to 4X LDS and boiled for 20 mins at 100°C to elute immunoprecipitated proteins.

2.2.3.8 Kinase assays using modified forms of ATP

Immunoprecipitated proteins were washed once in kinase buffer and 25µg MBP added as a substrate in 1X kinase buffer. ATP and N^6-modified ATPs were added to the reaction at a final concentration of 1mM. Assays were performed for 3 h at 37°C shaking at 1000rpm in an Eppendorf Comfort thermomixer.

2.2.3.9 GTP Kinase assays

For guanine nucleotide assays, ΔN-LRRK2 at a total concentration of 10nM was used. Recombinant LRRK2 was preincubated with 10mM GDP, GTP or GTPβγOH in 1X kinase buffer in a total volume of 50µl for 60 mins at 37°C celcius, to compete away any nucleotide bound to the ROC domain upon purification. The mixture was cooled on ice for ten mins before addition of MBP. MBP was used at 50 times molar excess compared to LRRK2. Assays were conducted over a time course with time points taken at various intervals.

For guanine nucleotide assays, control reactions were incubated for 60 mins at 37°C celcius prior to assaying, to ensure that this incubation did not affect comparison between experimental groups.

2.2.3.10 Kinase assay radiography

Time-points were electrophoresed as described and transferred to PVDF. Radiolabelled proteins were visualised by exposing to CL-Xposure and developed using a Konica SRX-10 developer. Quantification of radioisptope incorporation, was performed by exposing membranes to a phosphorscreen and imaged using a Storm phosphorimager (*GE Healthcare*). Densitometry was performed using ImageJ.

2.2.3.11 Separation using glycerol gradients

Each sample was diluted to a total volume of 100μl in 1X glycerol buffer before centrifugation. 100ul of 9-35% glycerol diluted in 25 mM HEPES (pH 7.4), 0.5% Triton X-100 (v/v) and 1 mM DTT (Berger *et al.* 2010) was layered in 1.5ml Beckmann polycarbonate centrifuge tubes on dry ice to prevent mixing of the layers. Samples were loaded on top and centrifuged at 100,000 x g, for 8 h in a Beckmann swing bucket TLS-55 rotor. After centrifugation, 100ul fractions were removed by pipetting, for blotting and Coomassie staining.

2.2.3.12 Modified-ADP radiolabelling

γ-Phosphate ^{32}P labeled ATP was used as a γ-phosphate donor (see Figure 2.2). 100 U of nucleoside diphosphate kinase (NDPK) from baker's yeast was reconstituted in HBS to a concentration of 10 U/μl and mixed with 350 μCi of (γ-32P) ATP (Perkin Elmer) for 10 mins at room temperature for NDPK autophosphorylation to occur.

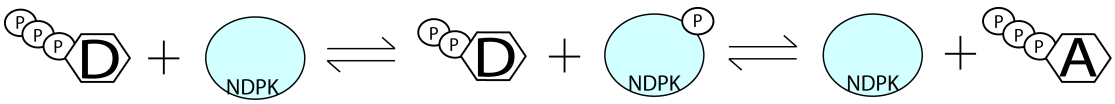

Figure 2.1. Transfer of a phosphate from a donor nucleoside (D) to an acceptor nucleoside (A) using NDPK to catalyse the reaction. 1) NDPK is incubated with a donor nucleoside triphosphate (e.g GTP). Donor is bound by NDPK. 2) NDPK hydrolyses γ-phosphate from donor and autophosphorylates. 3) Donor is removed and acceptor added. Acceptor nucleoside diphosphate is bound by NDPK and γ-phosphate added to create acceptor nucleoside triphosphate.

Unincorporated GTP and ADP were removed from the mixture with 2 spins through a G50 biospin column (GE healthcare) at 1100 x g for 2 mins each. ADP analogs (1ul of 0.1 mM) were added to phosphorylated NDK and incubated at RT for 10 mins. NDPK was denatured at 80^{o}C for 2 min and collected by centrifugation at 15,000g for 2 mins. γ-32P PE-ATP was resuspended in 60μl double-distilled H_2O and the amount of incorporated γ-32P assessed using TLC.

2.2.3.13 Thin Layer Chromatography

γ-32P ATP was spotted on the TLC plate as calibration guide alongside 1μl of labeled PE-ATP and left to dry for 5 mins. Plates were placed in a TLC chamber in 1cm of TLC Running buffer and left for 40 mins to run, after which they were removed, air-dried for 10 mins and exposed to film for 2 h. Film developing was performed using a Konica. SR-X10 developer.

2.2.4 Western blotting

2.2.4.1 BlueNative PAGE

For visualization of native protein complexes, both recombinant and whole cell lysate proteins were analysed using the NativePAGE non-denaturing gel system. N-dodecyl-D-maltoside (DDM) was added at a final concentration of 5% (w/v), along with Coomassie G-250 at a final concentration of 1.25% (w/v). Glycerol was added to a final concentration of 10% (v/v) to assist with loading). Samples were run along side an unstained native ladder to assess complex size. 4-16% or 3-12% Bis-Tris NativePAGE gels were assembled with dark blue cathode buffer and run at 120V until the dye front covered one third of the gel. At this point, the cathode buffer was exchanged light blue cathode buffer and the gel run for a further 4 h at 180v. Protein complexes were visualised by silver staining or western blotting and quantified using the NIH software ImageJ.

2.2.4.2 SDS-PAGE electrophoresis

Samples were loaded onto gradient 4-12% Bis-Tris gels unless otherwise stated. Novex pre-stained protein standard was also run alongside samples, in order to assess subsequent transfer and to calculate size of denatured proteins. All gels were run in 1X MES buffer at 180V and electrophoresis terminated when the dye front reached the bottom of the gel.

2.2.4.3 BlueNative gel transfer

For western blotting, native gels were incubated in BN transfer buffer overnight at room temperature. They were subsequently transferred to PVDF for 80 mins at 80V. After membranes had air-dried, they were incubated in 9% (v/v) acetic acid to fix proteins and then soaked in Ponceau S staining solution for 5 mins. Removal of staining solution allowed visualisation of the native standard, which was subsequently marked on the membrane. After a further wash in PBST to remove residual Ponceau, western blotting was performed.

2.2.4.4 SDS-PAGE transfer

Gels were transferred to PVDF in 1X transfer buffer at 80V for 80 mins. Following transfer, membranes were left at 10mins at RT to air-dry and western blotting was subsequently performed.

2.2.4.5 Western blotting

Membranes were incubated in primary antibody at the concentrations listed in Table 2.8 for 6 h at room temperature in Superblock. Membranes were then washed twice in PBST for ten mins before blocking for 15 mins in 15% (w/v) non-fat milk. After washing again for 10 mins at room temperature in PBST, membranes were then incubated in horseradish-peroxidase conjugated, secondary antibody diluted in Superblock for 2 h at room temperature.

Protein	Species	Company	Concentration
LRRK2	Goat polyclonal	Everest	1:1000
LRRK2	Rabbit polyclonal	Epitomics	1:1000
β-actin	Mouse Monoclonal (AC-40)	Sigma	1:5,000
α-synuclein	Mouse monoclonal (clone 42)	BD Transduction labs	1:1000
p-S129 α-synuclein	Rabbit	Abcam	1:500
Myc	Mouse monoclonal (9E10)	Sigma	1:2000
phosphoserine	Mouse monoclonal	Invitrogen	1:500
Anti-goat	IgG produced in rabbit	Sigma	1:10,000
Anti-mouse	IgG (Fab specific) produced in goat	Sigma	1:10,000
Rabbit	IgG produced in goat	Sigma	1:10,000

Table 2.8. Antibodies used for western blotting.

Probed membranes were washed five times for a total of 90 mins before antibody binding was visualised using an electrochemiluminescent system (ECL).

2.2.4.6 Electrochemiluminescent detection of antibodies

Substrate was mixed according to manufacturer's instructions and added to membranes for 30 secs. Excess substrate was removed by blotting with tissue paper and membranes were exposed to CL-Xposure photosensitive film for varying amounts of time. Films were developed using a Konica SRX-10 developer.

2.2.4.7 Silver Staining

Gels were fixed by incubation in fixing solution, for 20 mins. Subsequent staining was then performed according to manufacturer's instructions, using the SilverXpress staining kit.

2.2.4.8 Coomassie staining

Gels were washed twice in double distilled water before staining with Gelcode blue stain, for 2h. Gels were subsequently destained for around 2 h until bands could be visualised.

2.2.4.9 Dephosphorylation of recombinant protein

To remove phosphate groups from ΔN-LRRK2, 5μg of recombinant protein was incubated with 2,000 U of lambda phosphatase in the supplied buffer at 30^{o}C for 4 h.

2.2.4.10 Dot-blotting

5μg of ΔN-LRRK2 was dotted onto nitrocellulose membranes and allowed to dry. Dried membranes were incubated in PBST for 30 mins at room temperature and subsequently probed with anti-phosphoserine antibody for 2 h at room temperature (Table 2.8). Membranes were washed twice in PBST for ten mins at room temperature and then blocked again with 5% (w/v) non-fat milk dissolved in PBST for 10 mins. Blots were re-washed twice in PBST for 10 mins at room temperature and then incubated in anti-rabbit secondary antibody (Table 2.8) for 45 mins. Membranes were imaged using ECL.

2.2.4.11 LRRK2 pulldowns

SH-SY5Y cells were grown to confluency in 14cm^2 dishes as described. Cells were lysed on ice in cell lysis buffer containing protease inhibitor cocktail for 20 mins, before lysates were clarified by spinning at 4^{o}C for 20 mins at 16,000 x g in a Beckman 5412 centrifuge and the insoluble fraction discarded. Lysates were precleared by addition of 30μl agarose beads rotating at 4^{o}C for 1 h before addition of 5μg anti-LRRK2 (Everest) polyclonal antibody which was left to bind rotating at 4^{o}C overnight. Protein recognized by the antibody was immunoprecipitated by addition of 30μl protein G sepharose and left for 2 h rotating at 4^{o}C. Beads containing immobilized protein were collected by spinning for 15 secs at 14,000 x g and the supernatent removed. Beads were washed 5 times in PBS containing 300mM NaCl and 1% Triton-X100 and bound protein eluted in 4X LDS at 100^{o}C for 20 mins. Samples were run on SDS-PAGE 4-12% gels as described and protein visualized using Gelcode blue gel stain (Pierce). A band of around 280kDa was visible which was excised using a scalpel and subjected to tryptic digest and amino acid sequencing by ESI-QTOF mass spectrometry.

3. CHARACTERISATION OF LRRK2 FUNCTIONING

3.1 INTRODUCTION

Full length LRRK2 has been shown to dimerise in a number of studies (Greggio *et al.* 2008, Sen *et al.* 2009, Berger *et al.* 2010) and this dimerisation is thought to be important for GTPase and kinase function (Gasper *et al*. 2009, Greggio *et al.* 2008). As kinase function has been attributed to LRRK2 toxicity (Greggio *et al.* 2006, Smith *et al.* 2006) understanding how this activity is regulated is an important step towards elucidating the mechanisms by which familial mutations affect LRRK2 behaviour. Current opinion is that the active form of LRRK2 is likely to be dimeric (Sen *et al.* 2009, Berger *et al.* 2010), with monomeric forms showing lower kinase activity. We do not know however, under what circumstances LRRK2 does dimerise and how the transition from monomer to dimer is regulated.

In order to characterise the internal regulation mechanisms of LRRK2, recombinant ΔN-LRRK2 produced in Sf9 cells and made commercially available (Invitrogen) has been used to assess LRRK2 self-regulation in the absence of other interacting proteins. BN PAGE has been used in these experiments to evaluate changes that may be occurring to LRRK2 quaternary structure as a result of familial mutations. BN PAGE is frequently used to separate and identify protein complexes in their native state. Solubilisation of proteins in non-ionic detergents such as digitonin or n-dodecyl-beta-D-maltoside (*DDM*) and addition of Coomassie G-250 in order to give protein a negative charge, means that SDS and other denaturing agents can be omitted during sample preparation. As such, proteins are able to migrate in non-denatured, complex form (reviewed in Wittig *et al.* 2006). This system allowed the quaternary structure of LRRK2 to be assessed.

Phosphorylation of residues within a kinase, either through autophosphorylation, or phosphorylation by another kinase is a widely used mechanism to activate, and regulate complex formation and enzymatic activity. Mitogen activated kinases such as ERK and MEK are activated by phosphorylation (Boulton *et al.* 1991), whereas phosphorylation of mTOR is deactivated by phosphorylation (Brunn *et al.* 1996). The tight regulation of this process, through associated phosphatases allows the process to be highly controlled. Many kinases, such as the insulin receptor are

commonly phosphorylated in response to ligand binding. Proteins containing domains such as SH2 and PTB, which recognize p-Tyrosine residues, mediate complex formation and facilitate interaction (reviewed in (Roque *et al.* 2005). These domains are found in a number of proteins including SMAD and Polo-Box domain containing proteins, and the 14-3-3 family of proteins, which have recently been shown to interact with LRRK2 (Dzamko *et al*. 2010, Nichols *et al.* 2010, Li X. *et al*. 2011). LRRK2 is known to be highly basally phosphorylated (Table 1.3) and as such, phosphorylation is a likely mechanism to regulate complex formation and enzymatic activity. To assess the role of phosphorylation in dimer formation, ΔN-LRRK2 was dephosphorylated and quaternary structure analysed using BN PAGE. To assess the enzymatic activity of dephosphorylated forms of LRRK2, ΔN-LRRK2 was separated using a glycerol gradient system and *in vitro* kinase assays performed to assess the kinase activity of high and low molecular weight species.

GTP binding has been shown to stimulate kinase activity of LRRK2 and GTPase-dead artificial mutants do not display kinase activity (Smith *et al.* 2006). What is unclear however, is if the ablation of kinase activity is caused by structural changes due to an unoccupied GTP binding pocket, or because LRRK2 cannot maintain kinase activity without GTP binding. Similarly, the role of interacting proteins in GTP binding and cycling is also still unclear. LRRK2 has been shown to interact with the GEF ARHGEF7 (Haebig *et al.* 2010), which stimulates GTPase activity *in vitro*, however LRRK2 is able to hydrolyse and cycle GTP without a GEF present (Guo *et al.* 2007). To assess the ability of the ROC domain to dimerise, quaternary structure has been assessed using a recombinant fragment expressed in *E Coli* (Deng *et al.* 2007). The kinase activity of ΔN-LRRK2 in the presence of different guanine nucleotides was analysed using MBP as a substrate.

3.1.1 Hypotheses

Experiments were designed to address the following hypotheses.

1) LRRK2 ROC domain is able to form dimers.
2) LRRK2 kinase activity is affected by guanine nucleotide binding.
3) LRRK2 dimer formation is mediated by autophosphorylation of residues within LRRK2.
4) Monomeric LRRK2 displays decreased kinase activity compared to dimeric LRRK2.

3.1.2 Aims

These hypotheses will be tested through fulfillment of the following aims.

1) To assess the propensity of ROC domain dimer formation using recombinant fragments of the GTPase domain.
2) To assess the impact of guanine nucleotides on recombinant ΔN-LRRK2 kinase activity using the generic substrate MBP.
3) To assess the effect of phosphorylation on dimer formation *in vitro* using dephosphorylated ΔN-LRRK2.
4) To perform kinase assays using immobilised LRRK2 in monomeric and dimeric form.

3.2 RESULTS

3.2.1 LRRK2 ROC domain exists predominantly as a dimer

GST-ROC domain with an N-terminal 6X histidine-tag and a TEV protease cleavage site (amino acids 1333–1516) was expressed and purified from *E.Coli* (gift of Dr. Junpeng Deng, Oklahoma state University, California. For protocol see Deng *et al.* 2008). As shown in Figure 3.1a, the ROC domain is around 25 kDa when analysed by SDS-PAGE. Dimeric forms of this domain can also be seen at ~ 50 kDa. Analysis by BN PAGE (Figure 3.1b) confirms that the ROC domain is dimeric, as the majority of this protein runs at ~50 kDa. There is a fraction of this protein forming higher order structures of around 100 kDa, likely corresponding to tetramers. Denaturation of the ROC domain by heating at 100°C for 30 mins (Figure 3.1b) shows that the purified ROC domain is present in monomeric form and a dimeric form that is heat-resistant and SDS-insoluble (Figure 3.1a).

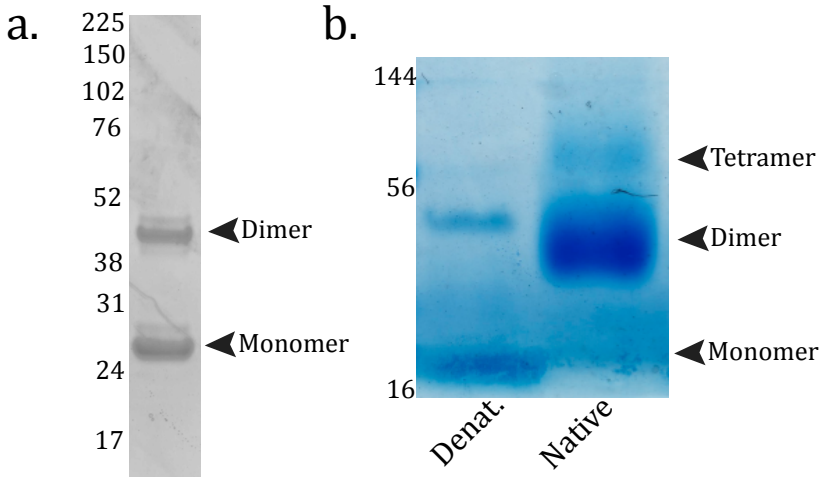

Figure 3.1a. Purified ROC domain run on SDS-Page. ROC domain protein was denatured and separated on SDS-Page. Molecular weight markers are shown on the left (kDa). ROC domain is shown as monomeric (~26 kDa) and dimeric (~52 kDa) species. **3.1b. BlueNative-PAGE analysis of LRRK2 ROC domain.** Denat.-ROC domain was denatured for 30 mins at 100°C before electrophoresis. Native-ROC domain was separated under non-denaturing conditions. Images are representative of three experiments.

3.2.2 Guanine nucleotide incubation decreases kinase activity

GTP binding studies have shown that full length LRRK2 has low affinity for GTP (Li X. *et al.* 2007). The classification of LRRK2 as a GAD is based in part on this low affinity for GTP (Gasper *et al.* 2009). In order to ensure that nucleotide bound to ΔN-LRRK2 was replaced with the experimental forms of guanine nucleotide, a vast molar excess of GTP (10mM) was used for each experiment. Some kinases, such as protein kinase C, are known to utilise the second messenger cyclic-GMP (cGMP), which activates kinase activity by disinhibiting the kinase domain (Francis *et al.* 1999). cGMP has also been shown to play a role in the activation of the bacterial ROCO protein GbpC in an activation cascade which involves cGMP activation of a GEF domain, leading to GDP/ GTP cycling and kinase domain activation (Van Egmond *et al.* 2008). To examine a role for cGMP in LRRK2 signalling, this form of guanosine was also used for these experiments, along with GDP, GTP and the non-hydrolysable GTPβγOH.

Preincubation of ΔN-LRRK2 with guanine nucleotides was shown to significantly alter kinase activity (Figure 3.2, $p=0.0043$, one-way ANOVA). GDP and GTPβγOH significantly lowered kinase activity compared to the control condition, in which ΔN-LRRK2 was incubated without nucleotide ($p<0.05$ vs control for each, one-way ANOVA followed by Bonferroni post-test). Similarly, despite the fact that GTP has been shown to stimulate kinase activity in full length LRRK2 (Ito *et al.* 2007), there was a significant decrease in MBP phosphorylation in these assays ($p<0.05$). Densitometry to quantify MBP phosphorylation by LRRK2 preincubated with cGMP, again showed a significant decrease in kinase activity compared to the control condition ($p<0.05$).

As the role of ROC-COR regulation of the kinase domain has been well documented, it is unlikely that the disruption of kinase activity with all forms of guanine nucleotide is representative of LRRK2 functioning *in vivo* and more likely attributed to the conditions used in these experiments. As such, it was decided that

ΔN-LRRK2 is not suitable for further investigation regarding the impact of guanine nucleotides on LRRK2.

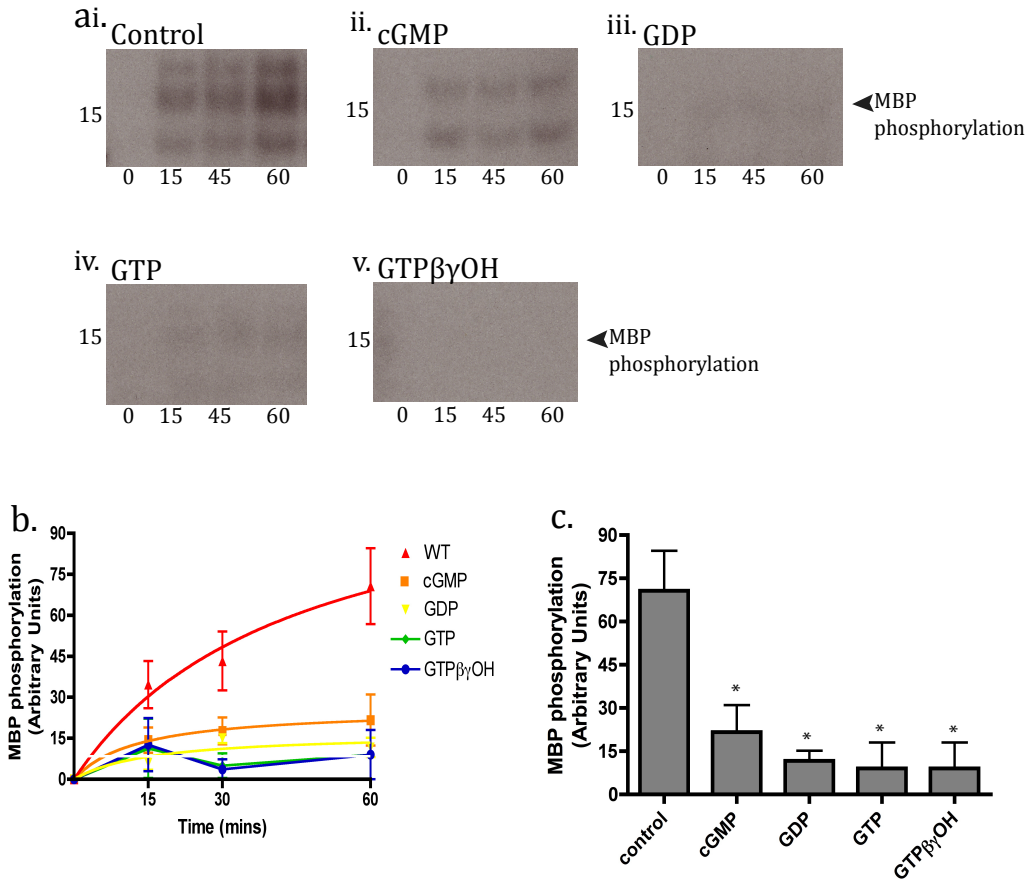

Figure 3.2a. Radiography showing LRRK2 phosphorylation of MBP in the presence of various guanine nucleotides. i-Control- wild type ΔN-LRRK2, ii- wild type incubated in 10mM cyclic guanosine monophosphate (cGMP), iii- wild type incubated in 10mM guanosine diphosphate (GDP), iv- wild type incubated in 10mM cyclic-guanosine monophosphate (cGMP), v- wild type incubated in 10mM GTPβγOH (a non-hydrolysable form of GTP). Time points are indicated below (mins). Molecular weight markers are shown on the right (kDa). Images are representative of three experiments. **3.2b. Quantification of MBP phosphorylation by ΔN-LRRK2 when incubated with guanine nucleotides.** Radiometric images were quantified using densitometry and results displayed as the mean of phosphorylation intensity (measured in arbitrary units) ± s.e.m. (n=3). **3.2c. MBP phosphorylation by ΔN-LRRK2 at 60 mins.** Values for MBP phosphorylation at 60 mins are displayed as mean ± s.e.m. *p<0.05 vs control, one-way ANOVA followed by Bonferroni post-test (n=3).

3.2.3 Dephosphorylation disrupts LRRK2 dimer formation.

KD mutations in full length and truncated LRRK2 overexpressed in cells have been shown to disrupt dimer formation, suggesting that kinase activity of LRRK2 is important for complex formation. Similarly, LRRK2 has been shown to be highly phosphorylated (Table 1.3). To assess if phosphorylation of LRRK2 could be controlling complex formation of LRRK2, recombinant ΔN-LRRK2 was dephosphorylated and the quaternary structure of the protein assessed.

Dot-blot analysis of basal LRRK2 phosphorylation (Figure 3.3a) shows that WT and KD forms are all phosphorylated. As shown by other groups, D1994A KD LRRK2 shows lower levels of phosphorylation than the WT forms, which is thought to be due to autophosphorylation (Kamikawaji *et al.* 2009). These results suggest that, although autophosphorylation may not occur in this protein, there are low levels of basal phosphorylation at serine residues, presumably due to post-translational modification by endogenous Sf9 kinases. Dephosphorylation of WT ΔN-LRRK2 using lambda phosphatase and subsequent analysis using a pan-phosphoserine (p-Serine) antibody, shows that the level of serine phosphorylation is markedly reduced and that this phosphatase is efficient in stripping phosphates from ΔN-LRRK2. To assess the impact of this dephosphorylation on WT ΔN-LRRK2 complex formation, protein was run on BN PAGE and visualised by western blotting (Figure 3.3b).

As shown in Figure 3.3, dephosphorylation of WT ΔN-LRRK2, results in a shift in the dimeric species to a lower, seemingly monomeric species. Poor resolution of protein when subjected to western blotting after BN electrophoresis and the inhibition of transfer by Coomassie G-250 (Eubel *et al.* 2005) however, meant that western blotting results were not optimally reproducible. As this was the case, another technique was sought to reliably separate various LRRK2 species and investigate the effects of dephosphorylation on LRRK2 complex formation. Due to the success of glycerol gradients in separating low and high molecular weight species from LRRK2 in cell models (Berger *et al.* 2010), it was decided to use a similar system for recombinant LRRK2 in these experiments. This system was

optimized for separation of lower molecular weight species (Figure 3.4a) and used for subsequent experiments.

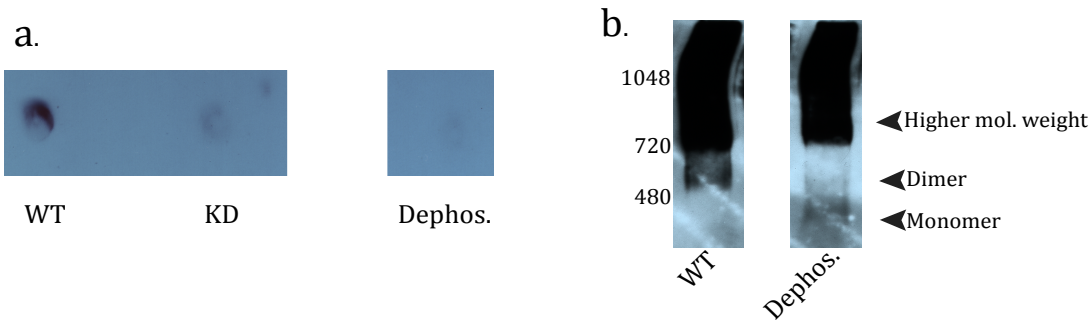

Figure 3.3a. Dot-blot analysis of basal ΔN-LRRK2 phosphorylation. WT- wild type, KD-D1994A kinase dead LRRK2, Dephos- Dephosphorylated WT LRRK2, previously incubated with lambda phosphatase to remove phosphate groups. Equal amounts of LRRK2 were spotted for each condition and a p-Ser antibody used to assess phosphorylation levels. Images are representative of three separate experiments**. 3.3b. BlueNative PAGE analysis of ΔN-LRRK2 complex formation when subjected to dephosphorylation.** Higher mol. weight- Higher molecular weight ΔN-LRRK2 present in complexes larger than 720 kDa. Dephosphorylated WT ΔN-LRRK2 was run under non-denaturing conditions and subjected to western blotting using anti-LRRK2 (Everest). Image is representative of at least three experiments.

As shown in Figure 3.4, centrifugation and subsequent analysis of the protein contained in different percent glycerol fractions, showed that centrifugation for 8 h results in good separation of the protein standards. As such, 8 h spins were used for each subsequent experiment. WT, KD and G2019S ΔN-LRRK2 were dephosphorylated and subjected to centrifugation through the glycerol gradient system (Figure 3.4b). Electrophoresis and subsequent Coomassie staining of each glycerol fraction, showed that untreated ΔN-LRRK2 appears mostly as higher molecular weight species, of above 440kDa. When WT protein was treated with

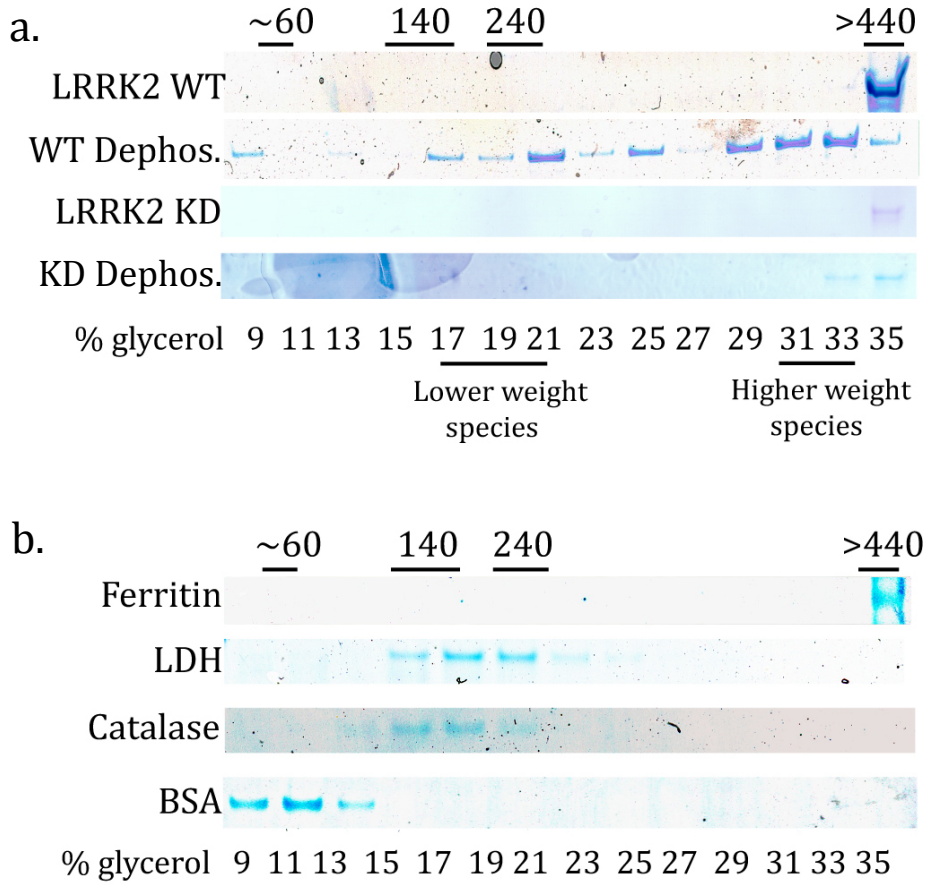

Figure 3.4a. Glycerol gradient analysis of ΔN-LRRK2. Dephos- ΔN-LRRK2 dephosphorylated using lambda phosphatase. WT- wild type ΔN-LRRK2, KD- D1994A kinase dead. ΔN-LRRK2 in WT and KD forms was subjected to centrifugation through glycerol gradients to assess complex size. Gradients were removed by pipetting and an aliquot of each gradient (indicated below) separated by SDS-PAGE. Protein was visualised by Coomassie staining. Molecular weight markers are indicated above (kDa). Images shown are representative of at least three separate experiments. **3.4b. Calibration of glycerol gradient spin system.** BSA- Bovine serum albumin. LDH- L-Lactic dehydrogenase. Proteins of known molecular weights in native form were subjected to centrifugation through glycerol gradients to calibrate optimum separation times. BSA-67 kDa, LDH-242 kDA, Catalase-140 kDa, Ferritin-440 kDa. Images shown have been centrifuged for 8 h and are representative of at least three separate experiments. Molecular weight markers are shown above (kDa).

phosphatase and subjected to centrifugation, these higher weight complexes are disrupted. LRRK2 was contained instead in fractions corresponding to a lower weight and possibly monomeric species (~200kDa) and a higher weight, presumably dimeric species (lower than 440 but higher than 260kDa) (Figure 3.4a). Phosphatase treatment of the kinase dead form of ΔN-LRRK2 was shown to have little effect on the overall quaternary structure of this protein, supporting dot-blot data (Figure 3.3a) showing that D1994A is minimally phosphorylated.

3.2.4 Low molecular weight LRRK2 has decreased kinase activity

Studies looking at the localisation and kinase activity of membrane bound LRRK2 in comparison to membrane bound LRRK2, have shown that LRRK2 is more likely to be monomeric when in the cytosol. Importantly, cytosolic LRRK2 has been shown to display lower kinase activity than membrane bound LRRK2 (Berger *et al.* 2010). This could be due to the presence of interactors or a membrane associated conformation of LRRK2, which promotes kinase activity. To investigate whether low molecular weight (likely monomeric) LRRK2 possesses intrinsically lower kinase activity than higher molecular weight LRRK2 (likely to be dimeric), ΔN-LRRK2 was dephosphorylated and separated by size using glycerol gradient centrifugation and the kinase activity of the two groups assessed. Protein from fractions 5-8 (17-23% glycerol) were pooled and designated as lower molecular weight, and protein from fractions 13 and 14 (33-35%) pooled and designated higher molecular weight LRRK2. To ensure that quaternary structure was preserved and that the addition of ATP was not able to promote the reoccurrence of complex formation, glutathione-agarose beads were used to precipitate and immobilize LRRK2 from both of these fractions.

Incubation of protein from these two fractions with MBP in the presence of ATP, showed that the activity of lower weight LRRK2 was significantly reduced compared to higher molecular weight LRRK2 (Figure 3.5. $p=0.0024$, unpaired t-test). This supports the idea that monomeric LRRK2 is likely to display lower kinase activity than dimeric LRRK2 and that dimerisation is required for LRRK2

kinase activity. These results also suggest that LRRK2 kinase activity is likely to require phosphorylation at certain residues.

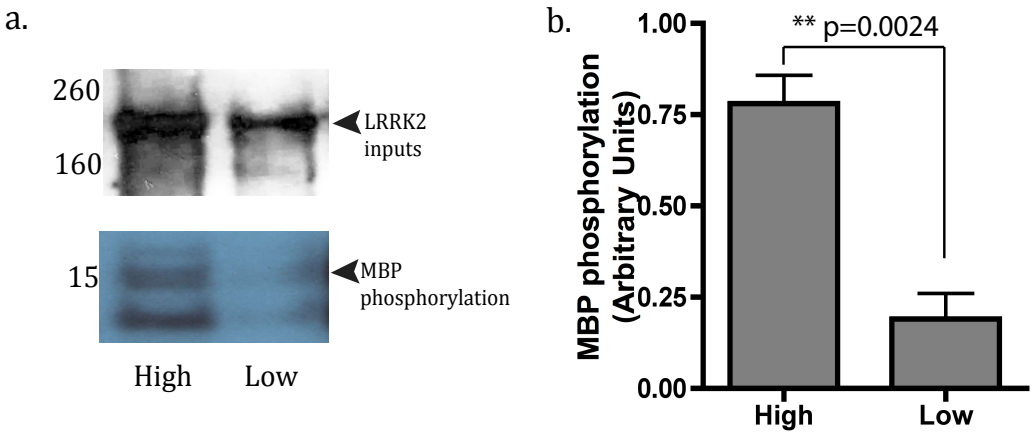

Figure 3.5a. MBP phosphorylation by low and high molecular weight LRRK2. Autoradiography of MBP phosphorylation from ΔN-LRRK2 precipitated from low and high molecular weight fractions, separated by glycerol gradient centrifugation**.** LRRK2 inputs are shown above (western blotting). Molecular weight markers are shown on the keft (kDa). Images are respresentative of at least three separate experiments. **3.5b. Quantification of high and low molecular weight kinase activity towards MBP.** Kinase activity from protein contained in high and low molecular weight fractions was quantified using densitometry and corrected for protein abundance (n= 3). ** p=0.0024, unpaired t-test. Values shown are expressed as mean ± s.e.m and are representative of at least three separate experiments.

3. 3 DISCUSSION

LRRK2 is a large protein containing many protein-protein interaction domains and two enzymatic domains (Marin, 2006). To regulate these domains, there are many layers of regulation controlling LRRK2, however the exact details of this functioning are yet to be conclusively characterised. These experiments aimed to better understand regulatory processes that are intrinsic to LRRK2, and to look at the behavior of this protein when in isolation, in order to contribute to building up a mechanism of LRRK2 regulation, that can be used to understand how LRRK2 may be contributing to AD PD. To do this, recombinant fragments of LRRK2 were used, as this minimised the effects that interacting proteins could be having on LRRK2 regulation. These experiments were successful in their aims to assess the propensity of the ROC domain to form dimers and in assessing the effect of phosphorylation on ΔN-LRRK2 dimer formation. Dephosphorylation of recombinant LRRK2 separated higher molecular weight forms into lower molecular weight forms and the kinase activity of these different forms was assessed. Characterisation of LRRK2 kinase activity when pre-treated with guanine nucleotides was unsuccessful (Figure 3.2), likely due to competition for the ATP binding pocket between the mM concentrations of GTP and the low concentration of radiolabelled ATP. Use of GTP as a phosphate donor instead of ATP has been well described for numerous kinases (Diaz-Nido *et al.* 1988) and as such phosphorylation of MBP could have been occuring using the non-radioactive guanine nucleotides instead of the radiolabelled ATP, which would account for the lack of MBP radiolabelling. In this case, modification of the experimental design used for these experiments may prove successful in the future.

The solved crystal structure of the ROC domain has shown that this single-domain fragment is dimeric (Deng *et al.* 2008). In these experiments, BN analysis supports data that this domain is able to form dimeric species (Figure 3.1a). Denaturing the ROC domain fragment by boiling and adding SDS (Figure 3.1a, b) shows that a proportion of the dimer species observed, are likely to have occurred as a result of the purification process, or represent an aggregation of this domain, as the dimers are not disrupted by these denaturation methods. As this ROC-domain containing

fragment of LRRK2 was purified from *E-Coli*, and SDS-PAGE separation showed that there were no other bands visible, this protein is unlikely to be contaminated by other proteins. In this case, the dimerisation seen by BN PAGE analysis is probably mediated by high intermolecular affinity of the ROC domain with itself. GTPase assays using the ROC 1333-1516 protein have shown robust GTPase activity (Deng J. *et al.* 2008), which is likely to require dimerisation (Gasper *et al.* 2009). It is unclear however, if the SDS-insoluble dimers are also active. The complex mechanisms proposed for LRRK2 GTPase function (Gasper *et al.* 2009) suggest that these forms of the protein are less likely to be active.

Analysis of quaternary structure when LRRK2 is dephosphorylated, showed that removal of phosphate groups disrupts dimeric and higher order complex formation of ΔN-LRRK2 (Figure 3.4a). The decreased levels of basal phosphorylation seen in KD compared to WT protein (Figure 3.3a) support other studies in suggesting that this phosphorylation is likely to be autophosphorylation (Kamikawaji *et al.* 2009), although phosphorylation may be occurring through kinase-dependent interaction with other kinases. The finding that dephosphorylation of LRRK2 disrupts higher molecular weight complexes is important, in that it provides a possible mechanism for regulation of dimerisation. Importantly, dephosphorylation of D1994A does not disrupt dimer formation, supporting the idea that LRRK2 kinase-dependent phosphorylation of LRRK2 regulates complex formation. It is important to consider these results in the context of a GST-tagged protein, as GST is well known to dimerise (Singh *et al.* 1987). In this case, dimerisation of ΔN-LRRK2, in particular the kinase dead form of the protein may mediated by the GST-tag.

Centrifugation of dephosphorylated ΔN-LRRK2 through glycerol gradients, allowed immunoprecipitation of different sized LRRK2 species, and it was shown that lower molecular weight LRRK2 displays lower kinase activity than higher molecular weight LRRK2 (Figure 3.5a). These results are supportive of data published by other groups using full length LRRK2 (Sen *et al*. 2009, Berger *et al.* 2010) and therefore suggest that ΔN-LRRK2 is a good model for LRRK2 kinase function. These results also suggest that the N-terminus is not necessary for

dimerisation or kinase activity, as the protein in truncated to residue 970 (Anand *et al.* 2009). The disruption of dimerisation by dephosphorylation, supports the idea that this mechanism is important for kinase activity and so in turn, that autophosphorylation is important for kinase activity. These results suggest that there are key residues, which need to be autophosphorylated in order to facilitate enzymatic activity. Taken together, these results support a model of LRRK2 regulation in which enzymatic activity and quaternary structure are closely linked.

3.3.1 Future directions

The results of these experiments take steps towards understanding how full-length LRRK2 may be self-regulating. As such, future experiments can build upon these findings. In particular, dephosphorylation of recombinant LRRK2 and subsequent separation using glycerol gradients allows different species of LRRK2 to be separated and characterised. In this study, kinase activity of monomeric and dimeric forms of LRRK2 were assessed, however the technique allows for analysis of GTPase activity and assessment of GTP binding in these LRRK2 species.

Identification of the residues controlling dimerisation is an important goal in understanding LRRK2 regulation. Identification of these residues could provide a marker for LRRK2 activation in cell culture and allow the role of LRRK2 in signal transduction to be better understood. There have been many attempts to map the phosphosites of LRRK2, with much success as detailed in Table 1.3. As such, there are a number of possible candidates for the residues, which could be promoting LRRK2 dimerisation. Of these, S971, S973, S975, S976 and S979 in the N-terminus are contained in the ΔN-LRRK2 fusion protein (they appear after the truncation) and are good candidates for regulatory amino acids, as they are not contained in the enzymatic domains. In this case it is likely that they have an alternate function such as mediation of quaternary structure. Systematic mutagenesis of candidate residues to alanine or glycine, followed by analysis of quaternary structure, should allow important residues for dimer regulation to be identified. Once discovered, the effect of mutating these residues in overexpressed protein can be assessed in terms of enzymatic activity and quaternary structure. Generation of phospho-

antibodies could provide a readout of LRRK2 activation in cell models and contribute to the understanding of LRRK2 functioning *in vivo*.

4. THE EFFECT OF MUTATIONS ON LRRK2 STRUCTURE AND FUNCTION

4. 1 INTRODUCTION

Mutations in LRRK2 have been shown to cause autosomal dominant PD. The majority of these mutations are situated in the ROC, COR and kinase domains of LRRK2, suggesting that they are likely to affect the enzymatic outputs of this protein. Indeed *in vitro* analysis of the most common mutations has shown that G2019S consistently increases kinase activity (reviewed in Greggio *et al.* 2009), and Y1699C and R1441C seem to be decreasing GTP hydrolysis (Lewis *et al.* 2007, Daniels *et al.* 2011). The relationship between enzymatic activity and quaternary structure has been shown in LRRK2 with artificially induced kinase and GTPase dead mutations. These proteins overexpressed in cells have been shown to display an inability to form dimers and instead adopt higher molecular weight structures (> 1MDa), which possibly consist of aggregated LRRK2 (Greggio *et al.* 2008). In mutation carriers, LRRK2 has also been shown to aggregate *in vivo*, with LRRK2 shown in some LBs and other intracellular inclusions in the brainstem (Alegre-Abarrategui *et al.* 2008). In this case, it would seem likely that LRRK2 complex formation could be affected by familial mutations. LRRK2 has been shown to form robust interactions with HSP90 (Hurtado-Lorenzo *et al.* 2008) and 14-3-3 and for 14-3-3, this interaction has been shown to be affected by familial mutations (Dzamko *et al.* 2010, Nichols *et al.* 2010, Li X. *et al.* 2011). If the main function of LRRK2 is to serve as a scaffold that is regulated by enzymatic activity, it would seem likely that complex formation is affected by the presence of familial mutations and that these mutations change the propensity of the protein to form dimers. In turn, mutations may alter the affinity of LRRK2 for its interacting partners and therefore affect the size of the complexes that contain LRRK2.

To assess the impact of familial mutations on the ability of LRRK2 to form complexes, WT and mutated forms of ΔN-LRRK2 were analysed using BN electrophoresis and the difference between monomeric and dimeric LRRK2 assessed for each of these mutants. These results were compared to BN analysis of LRRK2 extracted from fibroblasts donated by patients carrying LRRK2 mutations, in order to understand the role of interacting proteins in this process and to assess any changes in complex formation that may be occurring. The kinase activity of

ΔN-LRRK2 in WT and mutated forms was assessed using MBP and autophosphorylation, to understand how familial mutations are affecting the enzymatic activity of LRRK2 *in vitro* and the possible role they may be having in altering the behaviour of LRRK2, which leads to the pathogenesis of AD forms of PD.

4.1.1 Hypotheses

Experiments were designed to address the following hypotheses.

1) ΔN-LRRK2 is able to form dimers.
2) Familial mutations in LRRK2 alter the propensity of this protein to form dimers and complexes. It is hypothesized that ΔN-LRRK2 carrying familial mutations are more likely for form dimeric as opposed to monomeric species.
3) LRRK2 forms complexes with other protein *in vivo*.
4) The ability of LRRK2 to form complexes *in vivo* is affected by familial mutations.

4.1.2 Aims

These hypotheses will be tested through fulfillment of the following aims.

1) To examine LRRK2 dimer formation in WT and mutated forms using recombinant ΔN-LRRK2 and endogenous LRRK2 from PD patient fibroblasts carrying LRRK2 mutations.
2) To assess any differences in binding partners of WT and mutated LRRK2.
3) To determine the effect of familial mutations on the kinase activity of ΔN-LRRK2.

4.2 RESULTS

4.2.1 Assessment of endogenous LRRK2 complex formation

4.2.1.1 Mutant ΔN-LRRK2 forms monomeric and dimeric species

Analysis of recombinant ΔN-LRRK2, shows that both WT and mutant forms of the are present in dimeric and monomeric form (Figure 4.1b). The kinase-dead (D1994A) form of ΔN-LRRK2 is also dimeric, which contradicts data from analysis of full length LRRK2, both in endogenous and overexpressed form (Greggio *et al.* 2008, Sen *et al.* 2009, Berger *et al.* 2010). Similarly, there is a high proportion of monomeric species in these experiments across mutant and wild type forms, which has been shown to be less abundant when LRRK2 from cells has been analysed (Greggio *et al.* 2008, Sen *et al.* 2009). Plotting densitometry values along the path of LRRK2 migration (Figure 4.1c) to analyse the size distribution of this protein, confirmed that there are two peaks at around 200 and 400 kDa, with some protein corresponding to higher molecular weights (over 400 kDa). Interestingly, despite equal loading of protein, the I2020T and R1441C mutants consistently showed lower band intensity. As purity for all mutations is similar as >80% (Invitrogen), this raises the possibility that the solubility of these forms of LRRK2 could be affected by the mutations, as BN analysis is dependent on protein solubility to facilitate migration.

To assess if mutations are affecting the preference of protein to be in a monomeric or dimeric conformation, the ratio of dimer: monomer for each mutation was assessed. Average values for each peak, were generated by measuring densitometry values for a fixed area and ratios calculated. It was shown that there is no significant difference in the means of these ratios ($p=0.0876$). This suggests that point mutations are not affecting the preferred quaternary structure of Δ-LRRK2.

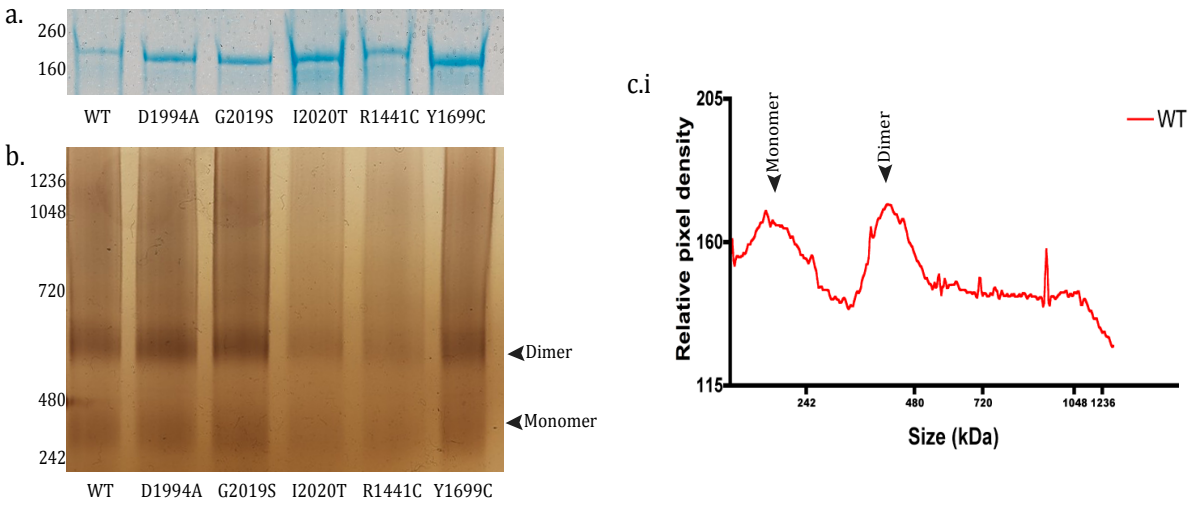

Figure 4.1a. Coomassie stain of ΔN-LRRK2 protein. Equal amounts of protein were analysed for each mutant. LRRK2 is present as a band of ~200kDa. Molecular weight markers are indicated on the left (kDa). **4.1b. Silver stain of ΔN-LRRK2 analysed under non-denaturing conditions.** Equal amounts of each protein were analysed under BlueNative conditions and gels subsequently silver-stained to visualize complex formation. Image is representative of three experiments. **4.1c.i Quantified distribution of WT ΔN-LRRK2 quaternary structure.** Gels were analysed according to staining intensity for a cross section of each gel. The two peaks are likely to correspond to dimeric and monomeric WT LRRK2 as indicated. Distributions are representative of three experiments.

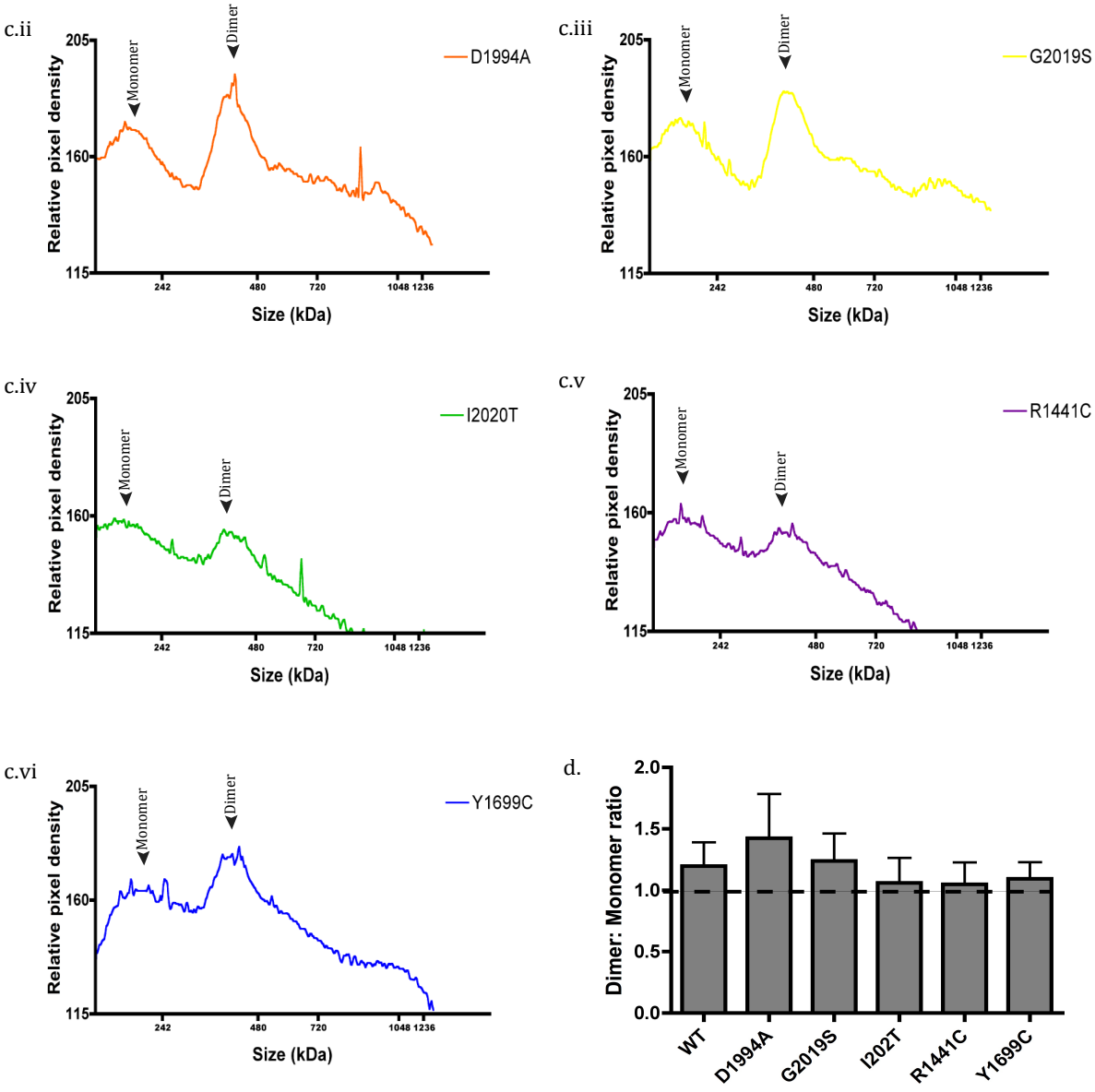

Figure 4.1c (continued). ii-D1994A kinase dead iii-G2019S iv-I2020T v-R1441C vi-Y1699C. **4.1d. Ratio of monomer: dimer formation for LRRK2 WT and mutated forms.** Band intensities were calculated using densitometry and values of dimer: monomer expressed as a proportion. Values are represented as mean ± s.e.m (n=3). Values >1 represent a preference for dimer formation and values <1 suggest a higher propensity for monomeric structure. There is no difference in the mean monomer: dimer ratio for each condition (one way ANOVA, p=0.0876).

4.1.2.2 Familial mutations do not affect LRRK2 quaternary structure *ex vivo*

To assess the impact of familial mutations on LRRK2 *in vivo*, that is endogenous LRRK2 in its native complexed state, protein was extracted from fibroblasts, which are heterozygous for the mutations R1441G, Y1699C and G2019S. This protein was used in BN PAGE to assess any changes to complex formation. Recently, a rabbit polyclonal raised against the C-terminal peptide CELAEKMRRTSV, has been used successfully for immunohistochemistry on human brain tissue and shown to recognize endogenous LRRK2 (Alegre-Abarrategui *et al.* 2009). This antibody has since been made commercially available and was therefore used for western blotting of protein extracted from fibroblasts with R1441G, Y1699C and G2019S mutations, and those from unaffected siblings used as controls (see Table 2.1).

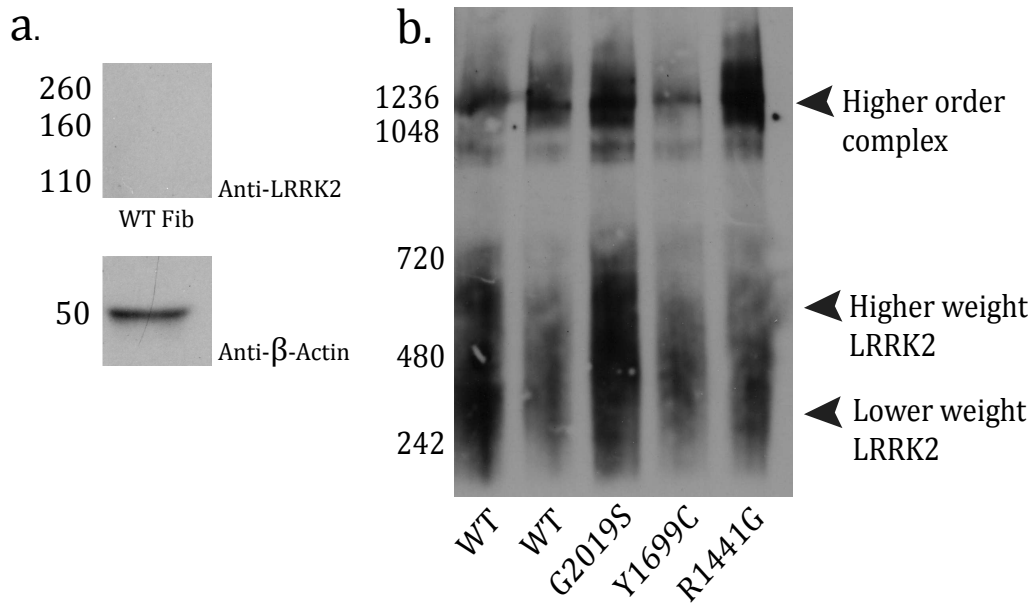

Figure 4.2a. SDS-PAGE analysis of LRRK2 levels in human fibroblasts. WT Fib –Wild Type human fibroblast lysate. Whole cell lysate was separated using SDS-PAGE and probed for LRRK2 (upper panel) and β-actin (lower panel). Molecular weight markers are shown on the left (kDa). **b. Blue Native analysis of LRRK2 extracted from human fibroblasts.** Equal amounts of whole cell lysate was run for each condition. The expected migration of lower and higher weight LRRK2 and higher order complex forms of LRRK2 are shown. Image is representative of three separate experiments.

Western blotting showed that LRRK2 is expressed at low levels in fibroblasts (Figure 4.2a). Analysis using BN-PAGE detected the presence of LRRK2 at around 600kDa, which is the expected size for a dimer and also lower molecular weight immunoreactivity around 260kDa, which corresponds to a monomeric LRRK2 species (Figure 4.2). The resolution of these species is poor, likely due to the limitations of western-blotting blue native protein caused by the interference of coomassie with the transfer process (Eubel *et al.* 2005), however this data would appear to show that endogenous LRRK2 extracted from patients expressing WT and mutated forms of the kinase is present in two main forms; lower molecular weight forms corresponding to monomeric and dimeric LRRK2 and a higher weight complex at around 1.2 MDa. These protein complexes are not affected by the presence of familial mutations, suggesting that familial point mutations do not disrupt binding of LRRK2 to interacting partners, or of dimer formation, as discussed.

4.1.2.3 ΔN-LRRK2 displays kinase activity that is affected by familial mutations

The recombinant ΔN-LRRK2 GST-fusion protein, has been shown to exhibit autophosphorylation activity and kinase activity towards the LRRKtide, a peptide derived in sequence from the ERM protein moesin (Jaleel *et al.* 2007). Similarly, characterisation of this protein has shown robust autophosphorylation and kinase activity towards MBP when in WT and G2019S form (Anand *et al.* 2009). The availablity of a recombinant form of LRRK2, means that the intrinsic kinase activity of the protein can be characterized, both in wild type (WT) and mutant form, as the G2019S, I2020T, R1441C and Y1699C substitutions are also commercially available. A kinase dead LRRK2 mutant containing a D1994A substitution (West *et al.* 2007), was also used in these experiments to control for background kinase activity from co-purified kinases.

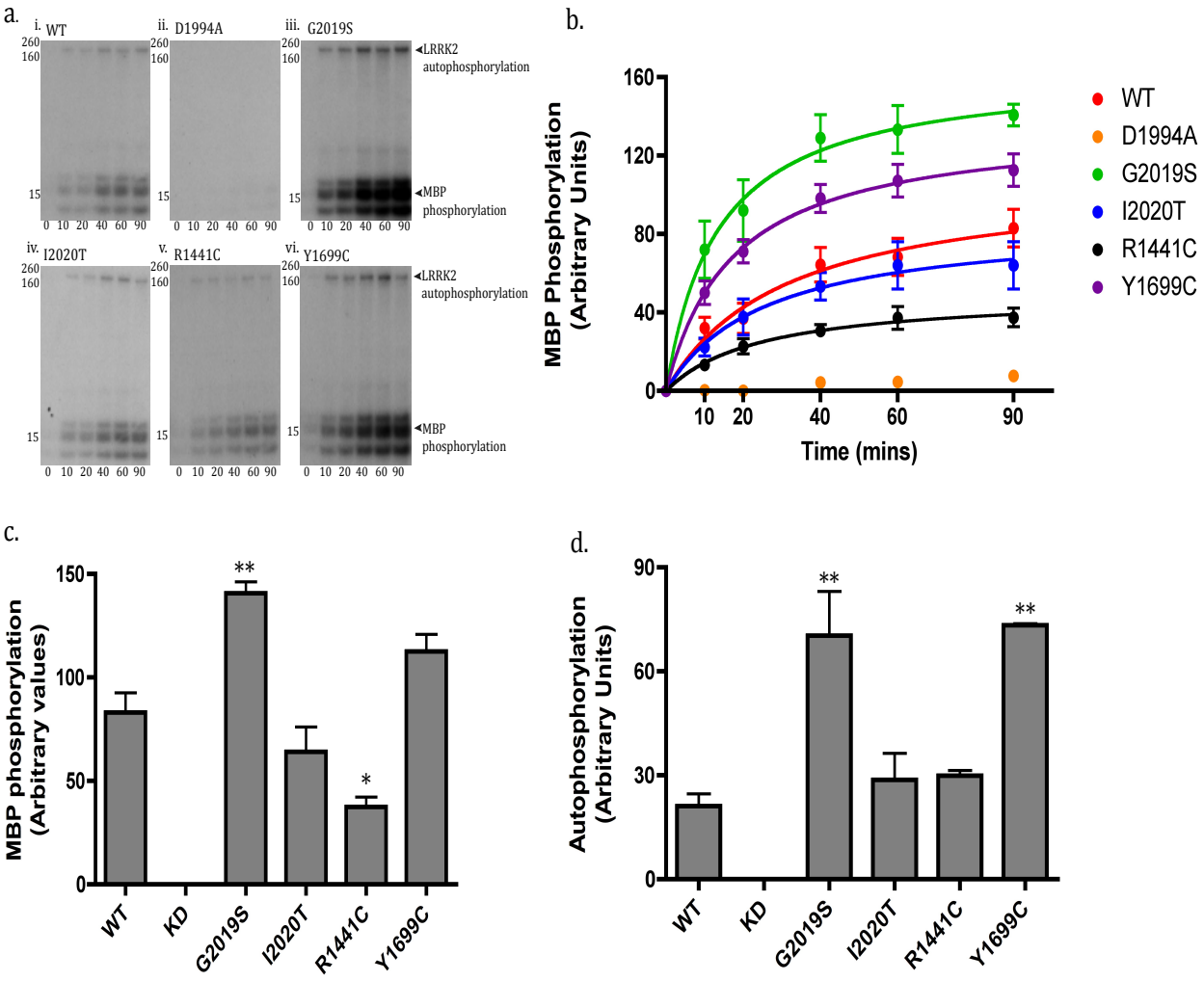

Figure 4.3a. ΔN-LRRK2 phosphorylation of MBP assessed by radiography. i-wild type. ii-kinase dead. iii. G2019S. iv-I2020T. v-R1441C. vi-Y1699C. Reaction mixtures were incubated for 90 mins, with time points taken as indicated. MBP consists of multiple isoforms with an average molecular weight of ~18kDa. Molecular weight markers are shown on the left (kDa). Images are representative of three experiments. **4.3b. Quantification of MBP phosphorylation by ΔN-LRRK2.** Radiometric images were quantified using densitometry and are shown here as mean values ± s.e.m (n=3). **4.3c. MBP phosphorylation by LRRK2 at 90 mins.** Final time points were taken and are displayed here as mean ± s.e.m * $p<0.05$, ** $p<0.01$, (vs WT, One-way ANOVA with Bonferroni post-test compared to WT). **4.3d. Autophosphorylation of ΔN-LRRK2.** Autophosphorylation from MBP phosphorylation assays was quantified at the 90 mins time point using densitometry and is shown here as mean ± s.e.m (n=3).

Quantification of MBP phosphorylation levels by ΔN-LRRK2, showed that all forms of the protein displayed phosphorylation of MBP, apart from the artificial mutant D1994A. This lack of phosphorylation in this condition suggests there are low levels of co-purified kinases with the ΔN-LRRK2 protein (Figure 4.3aii, b). Statistical analysis of this increase showed it to be significant compared to WT ($p<0.01$). The I2020T substitution appeared to decrease kinase activity towards MBP when compared to WT, however this difference was not significant ($p>0.05$). Similarly Y1699C ΔN-LRRK2 showed a trend towards increased MBP phosphorylation compared to WT, but this difference was also non-significant ($p>0.05$). R1441C was shown to have significantly decreased kinase activity compared to WT ($p<0.05$).

4.1.2.4 The effect of familial mutations on autophosphorylation

As well as pseudosubstrate phosphorylation, catalytically active forms of LRRK2 exhibited robust autophosphorylation. As expected, kinase dead D1994A did not display autokinase activity. In order to compare activity between LRRK2 mutations, autophosphorylation was quantified using densitometry. Similar to MBP phosphorylation (Figure 4.3c), G2019S autophosphorylation activity was significantly increased compared to WT ($p<0.01$, One-way ANOVA with Bonferroni post-test). Interestingly, Y1699C also showed a significantly increased autophosphorylation compared to WT ΔN-LRRK2 ($p<0.01$). I2020T and R1441C both displayed a trend towards reduced autophosphorylation compared to WT, however, this difference was not significant ($p>0.05$ for both).

4.3 DISCUSSION

These experiments were successful in their aims to investigate the effects of familial mutations on LRRK2 quaternary structure and kinase activity. The results obtained suggest that these amino acid substitutions are more likely to be affecting the enzymatic outputs of this protein, than the ability to form complexes. BN analysis shows that ΔN-LRRK2 has the propensity to dimerise and that the ratio of monomeric: dimeric species is unchanged in the presence of point mutations (Figure 4.1d). In protein extracted from fibroblasts, there was also no apparent change in complex size for mutant LRRK2 compared to WT (Figure 4.2b). Due to the limitations of BN analysis, differences in terms of monomer: dimer ratios could not be investigated in these experiments. Characterisation of the kinase activity of ΔN-LRRK2 showed that this protein is kinase active when in WT and mutant forms, with the D1994A substitution reducing kinase activity to a negligible level (Figure 4.3). G2019S was shown to increase the kinase activity of ΔN-LRRK2 and R1441C significantly reduced the kinase activity of this protein. Autophosphorylation was increased in both the G2019S and Y1699C conditions, with no autophosphorylation shown in assays with D1994A (Figure 4.3d).

The absence of the N-terminal of ΔN-LRRK2, shows that this region of the protein not is required for dimerisation or kinase activity, suggesting instead a regulatory role (Greggio *et al.* 2009), or function in mediating the cellular localization of LRRK2. It is perhaps unsurprising that point mutations do not result in a complete disruption of dimerisation, given that this would translate to a loss of function. The data published regarding the kinase activity of G2019S (West *et al.* 2005) have shown that this mutation increases the kinase activity of LRRK2, more likely resulting in a gain of function. Similarly, functioning of the ROC domain is thought to be dependent on dimerisation (Gasper *et al.* 2009) and although R1441C and Y1699C have been shown to decrease GTP hydrolysis (Lewis *et al.* 2007, Daniels *et al.* 2011), dimerisation is likely to be necessary for GTPase activity to occur at all. In this case it is likely that changes in the conformation of LRRK2 mutants are occurring at a local level, as suggested by structural investigation into the R1441C mutation (Deng J. *et al.* 2008, Li Y. *et al.* 2009). To fully understand these changes, a

crystal structure of full length LRRK2 and therefore knowledge about the overall topology of LRRK2 is needed.

If dimeric LRRK2 is the active form of this protein, with monomeric LRRK2 the inactive form, it would seem plausible that familial mutations could increase the proportion of dimeric species. Similarly, if autophosphorylation mediates dimer formation and autophosphorylation is increased in G2019S and Y1699C ΔN-LRRK2 (Figure 4.1) then it would be logical to assume that these mutants display a higher proportion of dimeric species. This was shown not to be the case *in vitro* for these experiments and monomer: dimer ratio was shown to be unchanged for all mutations, including the artificial kinase-dead D1994A mutation (Figure 4.1d). Importantly, the dimeric species seen in the D1994A mutant, are in stark contrast with results from other groups using full length forms of LRRK2, which have shown that kinase dead LRRK2 is unable to dimerise (Greggio *et al.* 2008, Berger *et al.* 2010) and (Sen *et al.* 2009). The most likely explanation for this is the GST-tag fused to the N-terminus of the ΔN-LRRK2 protein. GST has been shown to dimerise (Hayes *et al.* 1982), and a GST tag can be used *in vitro* to promote dimerisation in the absence of chaperone proteins or oligomerisation domains (Baer *et al.* 2001). In this case, it would seem likely that the GST tag is affecting the ability of ΔN-LRRK2 to dimerise. Similarly, GST tags are often used to improve the solubility of proteins fused to them (reviewed in Esposito *et al.* 2006). As such, the abundance of monomeric species seen in these experiments could be due to an improved solubility afforded by the tag, which is not seen in overexpressed LRRK2 from cells.

Silver staining of BN gels showed that the staining intensity for I2020T and R1441C was about half that of the other mutants (Figure 4.1c iv, v), suggesting perhaps that these mutants are less soluble than WT. Indeed this has been previously suggested for the R1441C mutation (Li Y. *et al.* 2009). The guaranteed purity of this protein is >80% (Invitrogen) suggesting that this is not due to differing concentrations of LRRK2 (if this were the case, staining intensity would be at most ~20% less). This raises the possibility that decreased solubility of some mutations and therefore lower levels of LRRK2 protein occur in patients with PD.

As such, further investigation is needed to ascertain this mechanism could be a potential factor in the pathogenesis of PD in patients carrying familial mutations.

The results of studies looking at the kinase activity of LRRK2 carrying familial mutations are in agreement with those from existing studies, which show differential ability of ΔN-LRRK2 to phosphorylate a target protein depending on the mutation that is carried (Anand *et al.* 2009). The ablation of kinase activity in the D1994A mutant, emphasizes the importance of this reside for functional enzyme activity. The lack of background kinase activity with this mutant also shows that minimal co-purification of other kinases has occurred and that the kinase activity displayed in likely attributed to the ΔN-LRRK2 protein. In the Wyeth study, which originally characterized ΔN-LRRK2, the G2019S mutant displayed significantly increased autophosphorylation activity compared to WT, findings which were replicated here. Similarly, phosphorylation of the LRRKtide by G2019S was also increased compared to WT, which was replicated in these experiments using MBP as a substrate (Figure 4.3a). Interestingly, Anand *et al* (2009) showed that the G2019S mutation lowers affinity for ATP in this mutant, whilst increasing kinase activity by keeping the protein in an 'on' conformation, which could explain the increased activity in these experiments. For the other mutations, assessing kinase activity using ^{32}P incorporation into the LRRK2tide showed no differences but specific activity of R1441C was higher and I2020T was lower. In these experiments R1441C exhibited lower MBP phosphorylation than WT, with no difference in the activity of I2020T. The reduced levels of soluble protein for R1441C and I2020T (Figure 4.3a) suggests that the actual levels of kinase activity for these mutants may be higher.

The differences in results between this study, and the experiments done by the Wyeth group, are likely attributed to differences in the techniques used. Anand *et al* used the LRRK2tide as a substrate for their kinase assays, for which LRRK2 has a higher affinity than MBP (Jaleel *et al.* 2007). This may affect autophosphorylation, as autokinase activity of LRRK2 can differ depending on the substrate being used. The different techniques used in the Wyeth paper and these experiments (FRET vs autoradiography followed by densitometry respectively) could account for some of

the differences in results. Indeed, within experiments, different techniques gave different results for the activity of R1441C and I2020T in the results published by Anand *et al*. Differences between these mutants and WT were not identified using ^{32}P incorporation into the LRRK2tide to assess kinase activity, but only when FRET was used to look the activities of individual mutants. A review of the kinase results from different groups (Greggio *et al.* 2009) also has shown that, apart from G2019S, data from other mutants is variable depending on technique used to analyse kinase activity. When compared to results from other groups, the data contained in these experiments also support this idea.

4.3.1 Future directions.

BN analysis of LRRK2 extracted from cells shows that this protein is present in a high molecular weight complex of around 1.2 MDa. The next important step in understanding LRRK2 functioning, for these experiments is to identify the components of this complex using immunoprecipitation. It has been suggested that LRRK2 may function in a number of signaling cascades including ERK, mTOR and JNK. Activation of these pathways using the appropriate ligands or metabolic stimuli, should allow for analysis of any changes to this complex and possible identification of any new binding partners.

The use of generic substrates to characterise LRRK2 kinase activity perhaps tells us little about PD pathogenesis, as we cannot be sure that these results will translate to a cellular context in which LRRK2 is heavily regulated and undoubtedly behaves differently than *in vitro*. As the exact details of this regulation are unknown, it could turn out that instead of hyperactivating a downstream component, familial mutations in LRRK2 over-repress interacting proteins, which results in reduced signaling. In this case, identifying LRRK2 kinase substrates is crucial to assess the effect of familial mutations *in vivo* and to identify therapeutic targets. An interesting question regarding regulation of LRRK2, is the effect that 14-3-3 may be having on LRRK2 kinase activity. This could be investigated by using recombinant 14-3-3 added to kinase assays, or co-immunoprecipitation of overexpressed LRRK2 and 14-3-3. In this way, the effect of familial mutations on

LRRK2 kinase activity could also be assessed to characterise the role that changes in LRRK2 kinase activity are playing in PD pathogenesis.

5. IDENTIFICATION OF NOVEL LRRK2 INTERACTING PROTEINS AND KINASE SUBSTRATES

5.1 INTRODUCTION

Although LRRK2 is classified as a kinase, the large number of protein-protein interaction domains it contains, suggests that a major function of the protein is to serve as a scaffold. LRRK2 has been shown to associate with Hsp90 *in vivo* (Hurtado-Lorenzo *et al.* 2008) and 14-3-3 has been shown to bind to phosphorylated residues in the N-terminus of LRRK2 (Dzamko *et al.* 2010, Nichols *et al.* 2010, Li X. *et al.* 2011). The phosphorylation of S910 and S930 residues in LRRK2 has been attributed to an exogenous kinase, therefore LRRK2 must be interacting with another kinase. Similarly, this must also mean that there is a phosphatase linked to LRRK2 that is yet to be identified.

Many kinase substrates for LRRK2 have been suggested, however there is little consensus on a single target. There are many kinases with a large number of substrates, Cdk1 is known to have more than 200 phosphorylation targets (Ubersax *et al.* 2003). In this case it is possible that LRRK2 also phosphorylates a high number of substrates. Despite this, no single kinase substrate has been confirmed by more than one group. Conversely, many groups believe that LRRK2 is not a genuine kinase and uses kinase activity to instead regulate its own activity (reviewed in Greggio *et al.* 2009). In order to understand the role of LRRK2 physiological functioning, and in turn understand how mutations in this protein can contribute to Parkinson's disease, it is important that these issues are clarified by identifying the binding partners and enzymatic targets of LRRK2.

The transient nature of phosphorylation events makes identification of kinase substrates extremely difficult and many interactions are easily missed, even when cross linking by photoamino acids or disulphide linkers are used. Similarly ATP and organic phosphate are ubiquitous in cells and are used by all kinases, so tagging substrates, for example with ^{32}P is non-specific for the kinase of interest. Using a technique coined 'chemical genetics' (Shah *et al.* 1997), Kevan Shokat's lab first addressed the issue of kinase substrate tagging, through a combination of mutagenesis to change the structure of the ATP binding pocket, and addition

chemistry to generate substituted forms of ATP, which do not occur naturally (Figure 5.1).

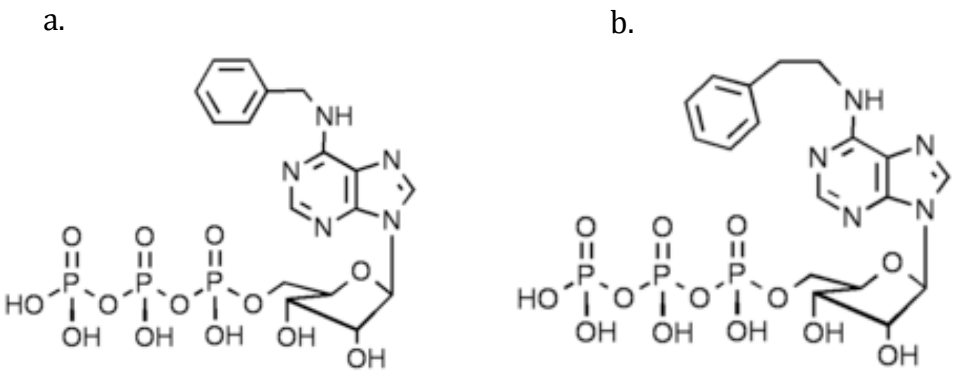

Figure 5.1. N^6-modified ATPs commonly used to identify kinase substrates. a- N^6 (2-Benzyl)-ATP. **b-**N^6(2-Phenethyl)-ATP .

Using the tyrosine kinase v-Src, the ATP pocket mutations V323A/ I338A, were engineered into the overexpressed kinase and allowed v-Src to accept the ATP analog N^6-(cyclopentyl)-ATP preferentially to normal ATP. By incubating v-Src with whole cell lysates, Shokat and colleagues were able to identifiably tag its substrates using ^{32}P γ-labelled forms of the N^6-modified nucleotide. The group have since refined this method and identified a single residue, termed the 'gatekeeper' which controls orientation of the γ-phosphate and therefore entry of ATP to the ATP binding pocket (Liu *et al.* 1998). LRRK2 kinase substrates have yet to be convincingly shown *in vivo,* however serine/threonine kinases are best documented in terms of gatekeeper identification and mutation, and as such, LRRK2 is a good candidate for modification using this approach.

Immunoprecipitation is the most commonly used method for identifying interacting proteins. Tagged forms of overexpressed LRRK2 were successfully utilised to identify 14-3-3 as LRRK2 interactors (Dzamko *et al.* 2010, Nichols *et al.* 2010, Li X. *et al.* 2011), however this technique also commonly causes false positive results due to the spatial constraints of overexpressing a single protein in vast numbers in a single cell. In successful immunoprecipitation of endogenous protein complexes remains to be the gold standard in identifying protein-protein

interactions. The success of this technique depends on having a highly specific antibody that can recognise its target protein in native form. For many areas of research, including the LRRK2 field it is the lack of specific antibodies that forms a bottleneck in the identification of proteins interacting with a gene product of interest. Recently, a rabbit polyclonal raised against the C-terminal peptide CELAEKMRRTSV, has been used successfully for immunohistochemistry on human brain tissue and shown to recognize endogenous LRRK2 (Alegre-Abarrategui *et al.* 2009). As such, this antibody is a possible candidate for use in endogenous LRRK2 precipitation. Since publication, this antibody has been made commercially available (Everest Biotechnologies) and was used in these experiments to immunoprecipitate endogenous LRRK2 from SH-SY5Y cells, in an attempt to identify LRRK2 interacting proteins.

5.1.1 Hypotheses

Experiments were designed to address the following hypotheses.

1) LRRK2 forms part of a complex *in vivo*.
2) LRRK2 is a functional kinase and phosphorylates other proteins as a member of a signal transduction cascade.

5.1.2 Aims

These hypotheses will be tested through fulfillment of the following aims.

1) To assess levels of LRRK2 expression in laboratory cell types and subsequently evaluate LRRK2 anti-bodies for immunoprecipitation.
2) To identify and modify the LRRK2 gatekeeper residue
3) To generate a modified form of LRRK2 which accepts an N^6-modifed form of ATP.
4) To use gatekeeper modified LRRK2 and its corresponding ATP analogue to identify and validate LRRK2 kinase substrates.

5.2 RESULTS

5.2.1 Identification of LRRK2 complex components.

In order to identify the components of the 1.2MDa complex observed from BN analysis (Figure 4.2b), the expression levels of LRRK2 in quickly dividing cell lines (as opposed to the primary fibroblast lines, which grow extremely slowly) was assessed using PCR based techniques, with the ultimate aim of using the Everest anti-body to immunoprecipitate endogenous LRRK2. RNA was extracted from Hek293T, HT1080i, SH-SY5Y and 1321N1 cells. To establish the quality of the RNA, 1μl of total RNA was analysed using an Aglient 2000 chip to calculate RNA integrity (RIN, Schroeder *et al.* 2006).

5.2.2.1. LRRK2 expression assessed by Semi-Quantitive PCR

Analysis showed that the RNA was of good quality, as all samples had RIN numbers close to, or over 9 and are therefore suitable for reverse transcription and downstream analysis by PCR. Total cDNA from cell lines was generated and PCR performed. The level of LRRK2 was normalised to that of a GAPDH PCR product from the same cDNA, in order to control for differences in the efficiency of each RT-PCR reaction. All PCR reactions were performed in triplicate.

Quantification of LRRK2 PCR products from each cell type showed that there was a similar level of LRRK2 mRNA in each sample (Figure 5.2d). There was a trend for higher levels of LRRK2 expression in Hek293T cells, but this difference was shown to be non-significant (One-way ANOVA p=0.1133).

a.

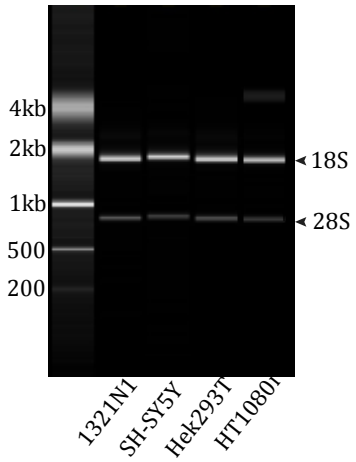

b.

	RNA Integrity Number
1321N1	9.50
SH-SY5Y	8.80
Hek293T	9.50
HT1080i	9.00

c.

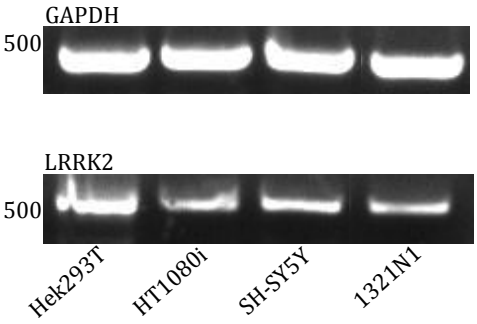

d.

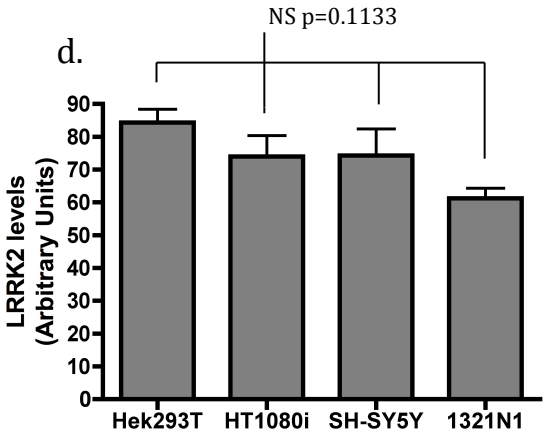

Figure 5.2a. Electrophoresis of RNA extracted from human cell lines. RNA was run on an Agilent 2000 chip to verify RNA integrity and the resulting agarose gel images shown here. 1µl of RNA from each extraction was used per assay. Base pair markers are shown on the left. **Table 5.1b. Data obtained from Agilent 2000 chip analysis of RNA.** High RIN numbers for each sample, show that RNA degraded very little since being extracted**. Figure 5.2c. Semi-quantitative PCR of LRRK2 and GAPDH.** Total RNA was extracted from various cell lines and cDNA generated. PCR products for LRRK2 and GAPDH were amplified. **5.2d. Quantification of LRRK2 amplification products.** PCR reactions were performed in triplicate and the relative levels of LRRK2 amplification products calculated. LRRK2 PCR products were normalized to GAPDH, n=3. A one-way ANOVA was performed and the differences between each group shown to be non-significant p=0.1133.

5.2.2.2 Taqman PCR to assess the levels of LRRK2 in various laboratory lines.

To analyse the expression levels of LRRK2 using a more sensitive technique, it was decided that Taqman quantitative PCR (qPCR) would be used (Bonetta, 2005). The use of ready-calibrated probes in this system, means that generation of a standard curve and calculation of absolute amounts of cDNA is not necessary. Instead, the levels of amplification relative to a control, are calculated using a threshold value, referred to as C_T. The cycle number at which the fluorescence levels intersect the threshold is used to calculate the fold gene change between samples, providing that they were amplified in the same run, as PCR efficiencies are known to vary between experiments (Rebrikov *et al.* 2006). Fold change is calculated using the equation detailed in Equation 5.1.

$$\text{Fold change} = 2^{-\Delta\Delta CT}$$

$$2^{-\Delta\Delta C_T} = [(C_T \text{ gene of interest} - C_T \text{ internal control})\text{Sample A} - (C_T \text{ gene of interest} - C_T \text{ internal control})\text{Sample B}]$$

Equation 5.1. Fold change calculation using the 2-ΔΔCT method.

5.2.2.3. Optimisation of Realtime conditions for amplification of LRRK2

To show that the concentration of cDNA used does not inhibit the PCR reaction, cDNA from Hek293T cells was used at 10, 25 and 50ng and the efficiency of amplification assessed. Each sample was run in triplicate and C_T values generated are as shown below (Table 5.2)

LRRK2 C_T values	10ng	25ng	50ng
A	32.05	31.13	31.19
B	31.98	30.98	31.16
C	32.50	31.31	31.96
β-Actin C_T values	**10ng**	**25ng**	**50ng**
A	21.23	18.93	20.08
B	20.99	18.72	19.56
C	21.36	18.75	19.51

Table 5.2. Taqman PCR C_T values for LRRK2 and β-actin. A, B and C represent individual replicates for each condition.

From these values it is immediately apparent that LRRK2 has quite low expression in Hek293T cells, as the C_T value for LRRK2 is high. Cycle numbers of 36 or over are considered to be obsolete as the assays lack sensitivity over this value (Lindecrona *et al.* 2002). The fold change between conditions was calculated using the equation for $2^{-\Delta\Delta CT}$ and it was demonstrated that 10ng is the optimal concentration for these experiments as this concentration provided the highest amplification of LRRK2 (Figure 5.3). 25ng cDNA was shown to reduce LRRK2 amplification by ~1.4 times and 50ng showed a decrease of around two thirds.

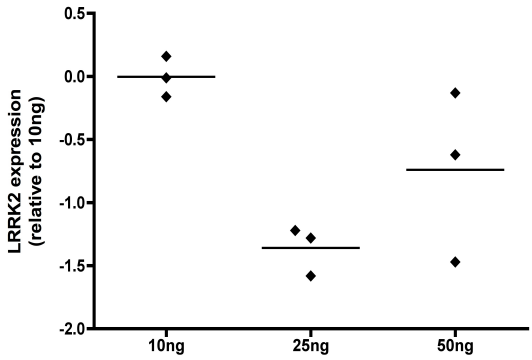

Figure 5.3. Fold change in gene expression for LRRK2 when different concentrations of cDNA are used. cDNA was generated from Hek293T and LRRK2 and β-actin amplified using the Taqman gene expression system. Varying amounts of total cDNA were used and each PCR was performed in triplicate, with results normalized to β-actin expression.

Examining the amplification plots for the β-actin probe, shows that the final fluorescence levels are similar for the 10ng and 25ng conditions, but are reduced in the 50ng condition, suggesting that PCR kinetics are affected by increased amounts of cDNA template for this probe (Figure 5.4).

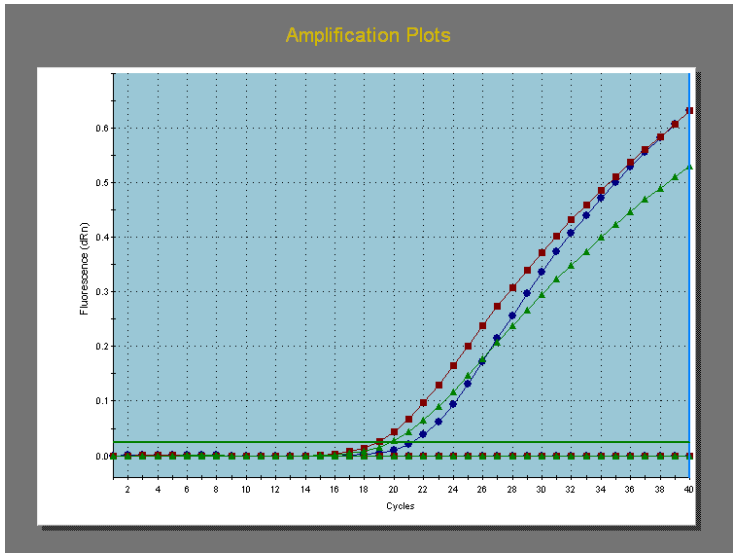

Figure 5.4. Amplification plots for β-actin from Hek293T cDNA. cDNA was generated from Hek293T, cells and the PCR for each condition done in triplicate. Replicates are shown as averages of C_T values (n=3). Green-50ng, Red- 25ng, Blue 10ng.

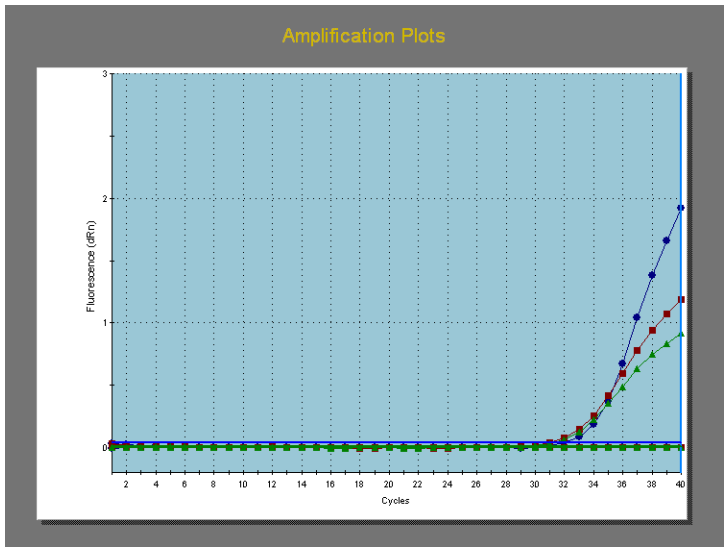

Figure 5.5. Amplification plots for LRRK2 from Hek293T cDNA. cDNA was generated from Hek293T, cells and the PCR for each condition done in triplicate. Replicates are shown as averages of C_T values (n=3). Green-50ng, Red- 25ng, Blue 10ng.

Amplification plots for LRRK2 also support the C_T calculations that higher amounts of cDNA are inhibiting the amplification reaction (Figure 5.5). Final fluorescence values at 40 cycles are lower as the amount of template increases. To ensure optimal amplification of LRRK2, it was decided that 10ng of template would be used for subsequent assays.

5.2.2.4 Taqman analysis of LRRK2 expression in various cell types.

RNA from SH-SY5Y, 1321N1, HT1080i and Hek293T cell lines was reverse transcribed in triplicate and the resulting cDNA used in Taqman assays to assess the relative levels of LRRK2 from each. The LRRK2 C_T values generated were corrected to corresponding β-actin C_T values and the $2^{-\Delta\Delta CT}$ equation used to calculate relative levels of LRRK2 in each line (Figure 5.1). LRRK2 values were normalised to β-actin measurements, generated in the same PCR reaction for each sample. Taqman assays were performed twice on separate occasions, and the results compared to ensure accuracy.

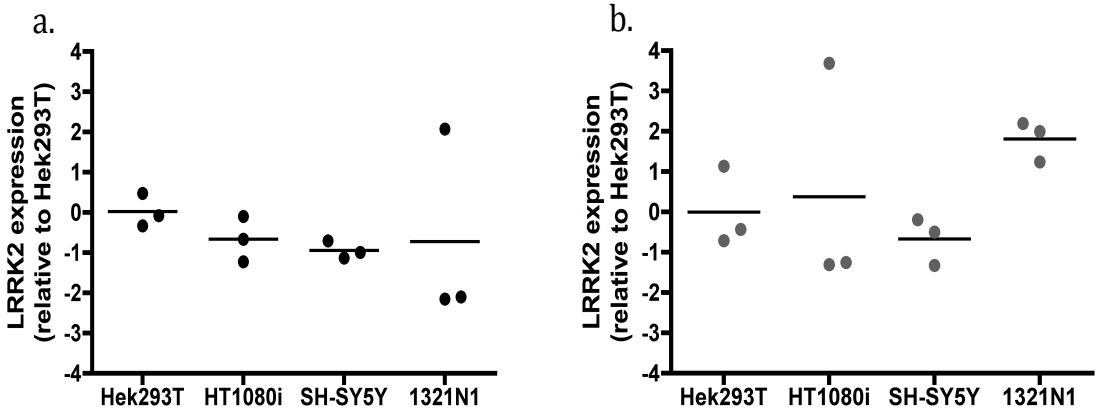

Figure 5.6a. LRRK2 expression in various laboratory cell types. Results were normalized to β-actin expression. Each PCR was done in duplicate and three cDNA samples from each cell line were used. n=3 for each cell line, PCRs were conducted in duplicate and the average fold-change for each plotted. **5.6b. Repeat of LRRK2 expression assay.** As 5.6a.

Taqman analysis of LRRK2 expression in various cell types showed that there was no difference in expression between the lines used (Figure 5.6a, One-way ANOVA p=0.4373. Figure 5.6b, p=0.3267). These results and the results of a repeated experiment (Figure 5.6a and b) showed that the results obtained were highly variable. C_T values for these assays were in the region of 35 for both experiments, accounting for the variability of the results. These values also show that LRRK2 expression in the cell types chosen is extremely low.

5.2.3 Immunoprecipitation of LRRK2 from SH-SY5Y cells

Analysis of LRRK2 mRNA expression by PCR and qPCR showed that there was no difference in expression between the cell types used. As such, it was decided that immunoprecipitation would be performed using protein extracted from SH-SY5Y cells. They are the most neuronal-like cell type of the cells used and successful immunoprecipitation from this cell line would therefore be most relevant to PD. LRRK2 was therefore immunoprecipitated from SH-SY5Y cells and the analysed by SDS-PAGE. Western blotting confirmed that LRRK2 expression levels in these cells is low (Figure 5.7a). Immunoprecipitation resulted in a single band of around 260kDa being extracted (Figure 5.7b).

The excised band was sent for peptide sequencing using Nanoflow HPLC-linked ESI-QTOF mass spectrometry. Mass spectrometry was kindly performed by Dr Wendy Heywood (Biological Mass Spectrometry centre, UCL Institute of Child Health, London). A total of 16 peptides were generated and sequenced, which were mapped with high confidence to the microtubule associated protein 1B (MAP1B) protein. These peptides represent an 8.6% coverage of the protein. The ESI-QTOF system used has a detection threshold for proteins in the femtomolar range, suggesting that if LRRK2 was present in these samples, it was at levels lower than the detection threshold.

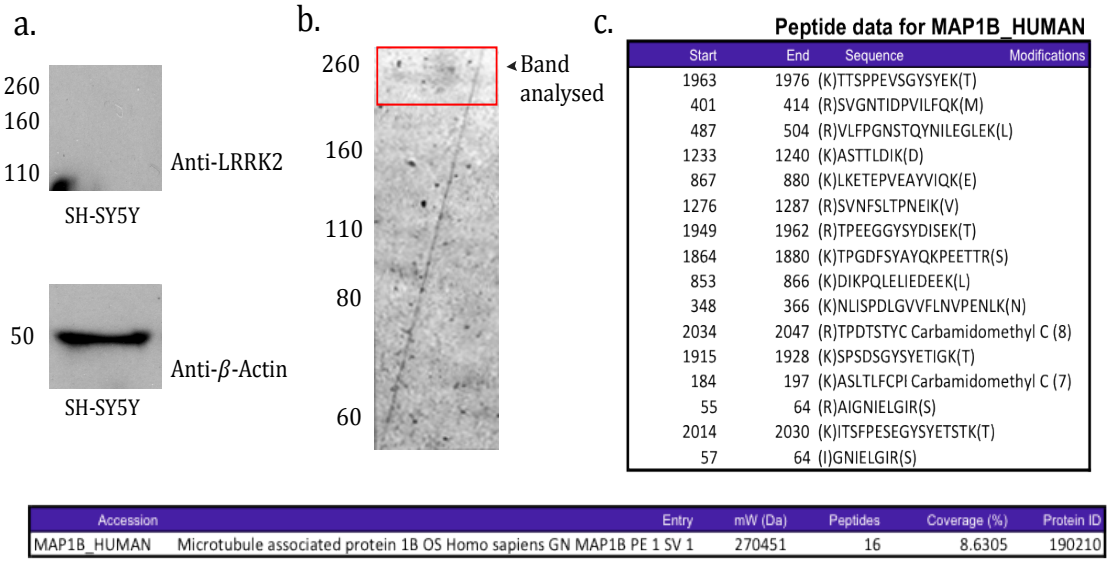

Peptide data for MAP1B_HUMAN

Start	End	Sequence	Modifications
1963	1976	(K)TTSPPEVSGYSYEK(T)	
401	414	(R)SVGNTIDPVILFQK(M)	
487	504	(R)VLFPGNSTQYNILEGLEK(L)	
1233	1240	(K)ASTTLDIK(D)	
867	880	(K)LKETEPVEAYVIQK(E)	
1276	1287	(R)SVNFSLTPNEIK(V)	
1949	1962	(R)TPEEGGYSYDISEK(T)	
1864	1880	(K)TPGDFSYAYQKPEETTR(S)	
853	866	(K)DIKPQLELIEDEEK(L)	
348	366	(K)NLISPDLGVVFLNVPENLK(N)	
2034	2047	(R)TPDTSTYC Carbamidomethyl C (8)	
1915	1928	(K)SPSDSGYSYETIGK(T)	
184	197	(K)ASLTLFCPI Carbamidomethyl C (7)	
55	64	(R)AIGNIELGIR(S)	
2014	2030	(K)ITSFPESEGYSYETSTK(T)	
57	64	(I)GNIELGIR(S)	

Accession	Entry	mW (Da)	Peptides	Coverage (%)	Protein ID
MAP1B_HUMAN	Microtubule associated protein 1B OS Homo sapiens GN MAP1B PE 1 SV 1	270451	16	8.6305	190210

Figure 5.7a. Western blot analysis of endogenous LRRK2 levels in SH-SY5Y cells. SH-SY5Y lysates were separated by SDS-PAGE and probed for LRRK2 (upper panel) and β-actin (lower panel). Molecular weight markers are indicated on the left (kDa). **b. Immunoprecipitated protein sent for analysis by mass spectrometry**. A single faint band of around 270kDa was seen when immunoprecipitation was performed on SH-SY5Y cells using the anti-LRRK2 goat polyclonal (Everest). Eluted protein was run on SDS-PAGE and the resulting band visualised by coomassie staining. This band was cut out and sent for analysis by Nanoflow HPLC-linked ESI-QTOF mass spectrometry. Molecular weight markers are indicated on the left (kDa). **Table 5.3c. Peptide map of protein immunoprecipitated from SH-SY5Y cells.** Peptides generated for sequencing using MALDI-TOF spectometry are shown. These peptides were found to map to microtubule associated protein 1B (MAP1B) protein with an 8.6% coverage of the protein.

5.2.3 Modification of the LRRK2 gatekeeper residue

5.2.3.1 Identification of the gatekeeper residue

Mutation of the gatekeeper residue in many serine/threonine kinases has allowed successful identification of kinase substrates for these proteins (Shah *et al.* 1997). To identify the gatekeeper residue in LRRK2, sequence alignment was performed using a number of kinases successfully modified using the Shokat method.

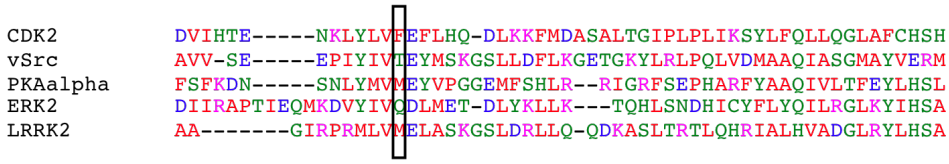

Figure 5.8. Sequence alignment of LRRK2 with other kinases successfully engineered to accept a modified form of ATP. Sequence alignment shows that the corresponding residue of LRRK2 is methionine, in position 1947.

According to the original experiments, the gatekeeper residue must be a hydrophobic residue in subdomain V. Sequence alignment of LRRK2 with subdomain V of other kinases, shows that a methionine in position 1947 is likely to be the gatekeeper residue. There can be high confidence in this result, as methionine is the most commonly found gatekeeper residue (Zhang *et al.* 2005).

5.2.3.2 M1947A can be successfully expressed in HEK293T

Site-directed mutagenesis was performed using full length N-terminally myc-tagged LRRK2 in WT and KD forms, to change the methionine at position 1947 to an alanine. Overexpression of this protein in Hek293T cells and subsequent western blotting and Coomassie staining, showed that the M1947A artificial mutant can be expressed and immunoprecipitated from Hek293T cells (Figure 5.9). KD LRRK2 showed consistently lower expression and precipitation than WT LRRK2 in these experiments. This has also been reported by other groups, perhaps due to the reduced stability of this protein (Greggio *et al.* 2006).

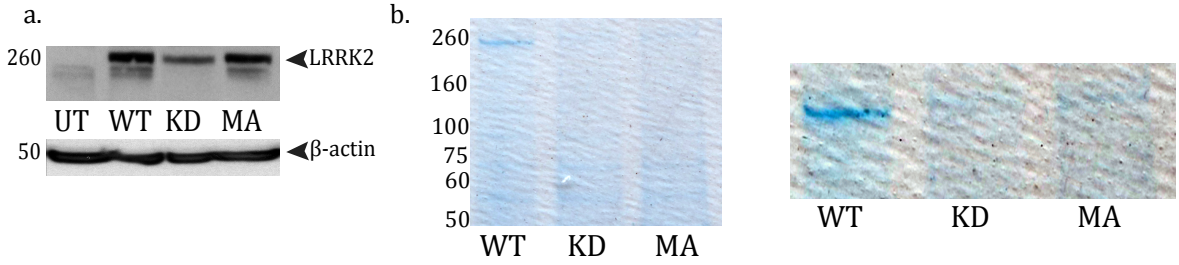

Figure 5.9a. Expression of M1947A in Hek293T cells. UT-Mock transfected Hek293T cells. WT-Wild type N-myc-LRRK2, KD- Triple mutant K1906M/D1994A/D2017A kinase dead N-myc-LRRK2. MA-M1947A N-myc-LRRK2. LRRK2 was overexpressed in Hek293T cells and western blotting performed to assess expression (LRRK2 visualised using anti-myc antibody). Molecular weight markers are shown on the left (kDa). Images are representative of at least three experiments. **5.9b. Coomassie staining of immunoprecipitated LRRK2.** Myc-LRRK2 was overexpressed and immunoprecipitated from Hek293T cells. Gels were coomassie stained to assess levels of LRRK2 immunoprecipitation. Images are representative of at least three experiments.

5.2.3.3 Radiolabelling of N^6-modified ADP

To tag and differentiate substrates phosphorylated using N^6-Modified ATPs, N^6-modified ADPs were radiolabelled using the phosphotransferase nucleoside diphosphate kinase (NDPK, see Figure 2.2). NDPK is an enzyme found in a number of species, including humans, which catalyses the removal of a γ-phosphate from ATP, to be repositioned on a nucleoside diphosphate other than ADP, eg GDP. It has been used successfully to radiolabel N^6-modified ATPs (Habelhah *et al.* 2001). NDPK was used in these experiments to remove the ^{32}P γ-phosphate from ^{32}P labeled GTP and add it to N^6-phenylethyl-ATP to generate radiolabelled ATP analogues. GTP was used as a donor to minimise background levels of kinase activity from co-purified kinases.

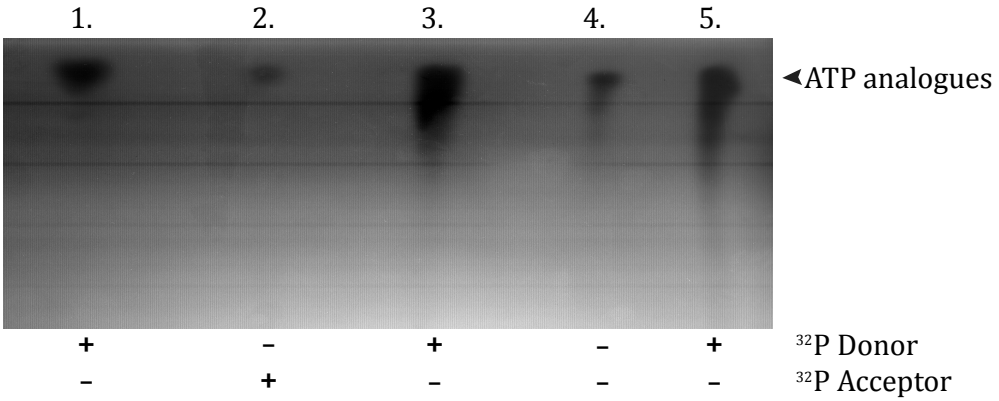

Figure 5.10. TLC analysis of 32P labeled ATP analogs. NDPK was used to label PE-ADP with a ^{32}P γ-phosphate. Radioactive nucleotides were subsequently analysed by TLC. *Lane 1*- 0.25ul 32P-labelled GTP. Efficiency of reaction can be estimated by comparing to this reaction. *Lane 2*- 1µl of radiolabelled PE-ATP. *Lane 3*- Flowthrough from radiolabelling reaction. Consists of unused GTP. *Lane 4*- Radiolabelling control reaction performed without PE-ADP. Radioactivity is due to ^{32}P-labelled GTP from the donation reaction that has not been removed and has carried over. *Lane 5*- Unused GTP from the control reaction.

TLC plate analysis of ^{32}P transfer from ATP to PE-ADP, showed that transfer is occurring, however the efficiency is poor as there is a low amount of radiolabelled PE-ATP (Figure 5.10, *Lane 2*.). In the control reaction completed without PE-ADP as the acceptor, it is apparent that carry over of ^{32}P-labeled GTP from the donation reaction is occurring. This suggests that, the radiation shown from labeling of PE-ATP, also consists of residual GTP. For optimal efficiency of this technique, there cannot be radiolabelled GTP present, otherwise false-positives may occur from WT kinases utilising this nucleotide as a phosphate donor. In order to address this issue, it was decided that subsequent experiments would be performed using cold N^6-modified ATPs and phosphorylation visualised using pan-p-Serine antibodies.

5.2.3.4 M1947A mutants are unable to utilize normal ATP.

Shokat and colleagues have successfully engineered kinases to accept ATP carrying benzyl and phenethyl moieties (Figure 5.1) at the N^6 position, and as such it was decided that these ATPs would be good candidates for experimentation. Kinase assays using immunoprecipitated LRRK2 showed that the M1947A mutant is unable to utilise ATP (Figure 5.11a).

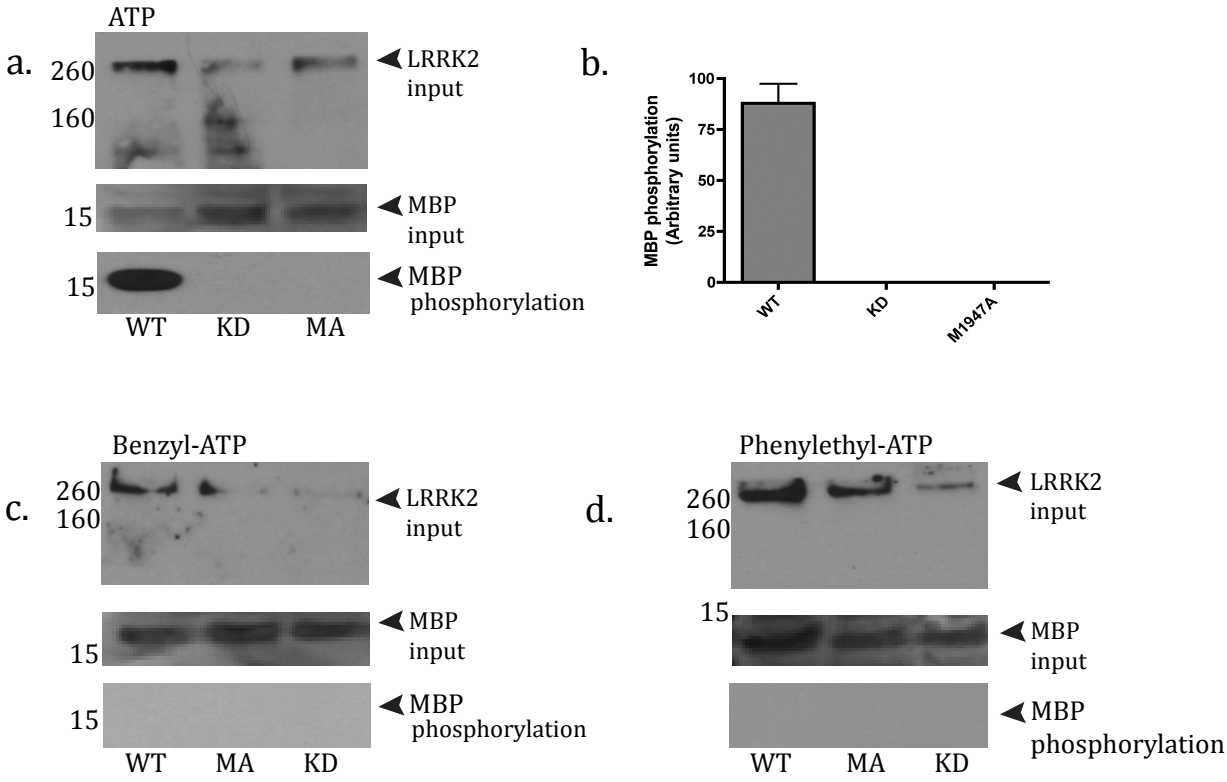

Figure 5.11a. LRRK2 phosphorylation of MBP using ATP analogues. WT- wild type LRRK2, KD- triple mutant kinase dead LRRK2, MA-M1947A LRRK2. Results shown are representative of three experiments. Phosphorylation of MBP was visualised using western blotting and pan-p-Ser antibodies. LRRK2 inputs were visualised using anti-myc antibodies. MBP inputs are taken from ponceau stains of PVDF membranes. Molecular weight markers are shown on the left (kDa). Results shown are representative of three experiments. **5.11b. Quantification of MBP phosphorylation using non-modified ATP.** Bar chart shows mean values ± s.e.m (n=3). **5.11c. Autoradiography of kinase assays using modified forms of ATP.** Results are representative of three experiments and show western blot analysis of MBP p-Ser residues. **5.11d.** As 5.11c.

Most WT kinases are unable to use N^6-modified forms of ATP (Shah *et al.* 1997). As confirmed in Figure 5.11a, WT LRRK2 is unable to use these modified forms of ATP. Changing the amino acid in the gatekeeper position lowers the affinity of a kinase to normal ATP so that it preferentially accepts the modified form, however, there is also no MBP phosphorylation from the M1947A mutant when incubated with unmodified ATP (Figure 5.11a). Looking at the ability of M1947A LRRK2 to use PE-ATP or Ben-ATP analogs, shows that this mutant is also unable to use these forms of ATP (Figure 5.11 b,c).

5.2.3.5 Quaternary structure of M1947A LRRK2

As LRRK2 kinase activity is required for dimer formation, to identify if the M1947A is affecting overall kinase activity of the protein, or to see if changes to the current protocol such as trying different ATP analogues were likely to be successful, BN western blots were performed (Figure 5.12). As shown, N-myc-LRRK2 is present in mostly higher order complexes, with some protein shown to be present at around monomeric and dimeric size. The triple kinase mutant shows a different pattern of electrophoresis, with higher order complexes seemingly disrupted and more protein present at lower weight fractions.

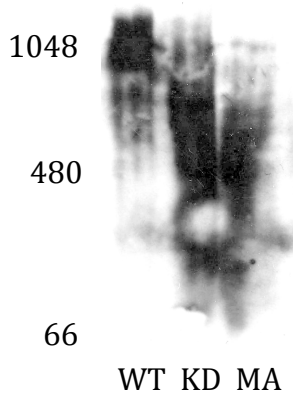

Figure 5.12. BlueNative analysis of N-Myc-LRRK2 overexpressed in Hek293T cells. WT-Wild type, full length N-terminally tagged Myc-LRRK2, KD- kinase dead N-Myc-LRRK2. MA-M1947A N-myc-LRRK2. Whole cell lysate from Hek293T cells was transfected with N-myc-LRRK2 was run out on BlueNative PAGE and analysed using western blotting. Image is representative of at least three separate experiments. Molecular weight markers are shown on the left (kDa).

The M1947A mutant shows a similar electrophoretic pattern to the KD, in that higher order complexes are disrupted and there is more protein present in lower weight fractions. This suggests that the M1947A substitution is affecting LRRK2 in a similar manner to the kinase dead mutations. In this case it is unlikely that trying other forms of ATP, would be beneficial. Interestingly, the disruption of complex formation in the overexpressed kinase-dead mutants represents a shift from higher order complexes, to seemingly dimeric species. This suggests that in this protein, it is interaction with other proteins that is being disrupted and not the ability to dimerise. It has been reported that some kinases are 'intolerant' to gatekeeper residue mutation and require additional 'rescue' mutations, which restore kinase function (Zhang *et al.* 2005). In this case, it would seem that LRRK2 is intolerant to the M1947A mutation and requires further modification for this technique to be successful.

5.3 DISCUSSION

As a large protein with multiple protein interaction domains, complex formation is likely to play an important part in LRRK2 functioning. The aim of this study was to identify LRRK2 interacting proteins and kinase substrates, in order to better understand how LRRK2 acts in a cellular context and how it may be causing neuronal death in familial forms of PD. Because of technical issues associated with these techniques however, these aims were not successful. Analysis of LRRK2 expression in commonly used cell lines emphasised the difficulties faced in addressing these aims, as LRRK2 expression is extremely low, making purification of this protein more difficult. Attempts to immunoprecipitate endogenous LRRK2 were unsuccessful, most likely due to the low expression levels of LRRK2 in the cell types used. This low expression of LRRK2 suggests that nonspecific binding of abundant proteins, such as MAPs was more likely to occur during immunoprecipitation. This may explain why MAP1A was immunoprecipitated from SH-SY5Y cells using an antibody specific to LRRK2 (Table 5.3b).

Attempts to identify LRRK2 kinase substrates through engineering a gatekeeper pocket mutation into the ATP binding pocket of LRRK2 also proved to be unsuccessful, as mutation of M1947 to an alanine disrupted kinase activity of LRRK2 (Figure 5.11a). Ablation of kinase activity was shown to disrupt complex formation of the M1947A mutant, however this protein is still able to dimerise (Figure 5.12). This is contrary to the findings of many other groups (Greggio *et al.* 2008, Sen *et al.* 2009, Berger *et al.* 2010) and perhaps suggests a more complex mechanism of dimer formation in which LRRK2 is able to adopt active and inactive dimer conformations, which differ according to the other proteins complexed. These forms may have differing stabilities. The difference in results compared to those from other studies (Greggio *et al.* 2008, Sen *et al.* 2009, Berger *et al.* 2010) is perhaps due to different conditions used. In the experiments described here, a high concentration of detergent was used (5% DDM, w/v) to maximise the solubility of LRRK2. This may affect the species that were able to migrate when BN electrophoresis was performed.

5.3.1 Future directions

Success of the gatekeeper technique for identification of kinase substrates is intimately linked to the structure of the ATP pocket for each kinase. For kinases with determined crystal structures, the chance of success can be more easily estimated, however for kinases such as LRRK2, which are without a crystal structure, the success of engineering a pocket mutation can only be determined by trial and error. The 'second site suppressor strategy' allows rescue of kinases, which are rendered inactive when the first mutation is engineered (Zhang *et al.* 2005). To rescue intolerant kinases, mutation of residues around a hotspot in the β-sheet in the N-terminal subdomain has been shown to revive kinase activity and allow identification of kinase substrates for previously unmodifiable kinases. In this case, sequence alignment of LRRK2 with other kinases successfully modified using the second site suppressor strategy, could allow for identification of potential rescue mutations and allow kinase substrates for LRRK2 to be characterised.

These experiments have shown that LRRK2 expression is low in many of the laboratory cell types that are commonly used. In depth analysis of LRRK2 expression in pre and post-natal mice has also reported low levels of LRRK2 mRNA (Biskup *et al.* 2007). An explanation for this could be that LRRK2 expression levels are repressed at a transcriptional level and perhaps induced in response to some sort of stimulus. In order to assess factors regulating the expression of LRRK2, Analysis of expression levels in response to stimuli, could be performed by examining potential changes in LRRK2 expression, when cells are subjected to stressors such as H_2O_2. Similarly, examining possible changes in LRRK2 expression in response to MAP kinase cascade activation, would allow the role of LRRK2 in these cascades to be better understood. Addition of mitogens to cells in culture and subsequent analysis of changes to gene expression, could provide information regarding the potential role of LRRK2 in these cascades.

Although the immunoprecipitation of LRRK2 using the Everest antibody was unsuccessful in these experiments, modifying the techniques used may allow for successful purification of this protein in the future for example using size exclusion

to enrich the concentration of LRRK2 before immunoprecipitation. The Everest antibody has previously been used for immunohistochemistry (Alegre-Abarrategui *et al.* 2009) and western blotting. These techniques all involve denaturing proteins before identification and therefore it is possible that this antibody is useful for pulling down denatured LRRK2. Chemical and photo-crosslinkers allow interactions to endure treatment by SDS and other denaturing chemicals and therefore, this antibody could be used in combination with crosslinkers in attempt to identify LRRK2 complex components. Alternative methods to pull down LRRK2 such as immobilising ΔN-LRRK2 on GST-beads before incubation with whole cell lysate, or immunoprecipitation of 14-3-3 and screening for LRRK2 containing complexes, could also be used to identify the cellular context that LRRK2 functions within *in vivo*. This could contribute further to our understanding of how LRRK2 is contributing to the pathogenesis of PD, by identifying potential signaling pathways that are perturbed in this disease.

6. INVESTIGATION OF PUTATIVE LRRK2 KINASE SUBSTRATES *IN VITRO*

6.1 INTRODUCTION

The kinase domain of LRRK2 shares a high degree of homology to those contained in RIP kinase family members (Meylan *et al.* 2005). These proteins are functional kinases *in vivo* with functions centred around regulation of apoptotic and pro-survival signaling (Declercq *et al.* 2009). Identification of kinase substrates for LRRK2 has provided many possible candidates, and there is consensus that LRRK2 targets serine and threonine residues for phosphorylation (Pungaliya *et al.* 2010, Anand *et al.* 2009). Despite the many substrates reported, a single kinase substrate is yet to be confirmed by more than one group. In these experiments, a number of putative LRRK2 kinase substrates have been assessed *in vitro*. α-Syn was chosen because of the important role it plays in PD pathogenesis. Y2H studies from a collaborating group have identified TUBB5 and the DVLs as potential interactors of the ROC domain (Sancho and Harvey. Unpublished, Sancho *et al.* 2009). GTPase experiments with these proteins have proved to be technically challenging and as such, these protein have instead been assessed here, as possible kinase substrates of LRRK2.

The prevalence of α-syn pathology in LRRK2 familial PD, and the strong overlap between idiopathic and PARK8-linked PD, has led to the suggestion that there may be some sort of interaction between LRRK2 and α-syn, either directly, or in a common pathway (Singleton, 2005). Other groups have shown that LRRK2 and α-syn can be co–immunoprecipitated from post-mortem brain tissue from individuals with dementia with Lewy bodies and (Qing *et al.* 2009a) and LRRK2 has been shown to directly phosphorylate α-syn at S129 (Qing *et al.* 2009b). The efficiency of this phosphorylation was not explored in depth however, and as such, it is unclear whether this phosphorylation is likely to be physiological. In order to address these issues, LRRK2 phosphorylation of α-syn has been assessed here using *in vitro* kinase assays. The β and γ varients of synuclein were also used, to assess if LRRK2 is also able to phosphorylate these peptides and if so, to determine if there is a preference for any one varient. α, β and γ-synuclein are 140, 134 and 127 amino acids long respectively, with β and γ-syn showing considerable

sequence homology to α-syn. Each form of synuclein contains a hydrophobic region in the middle section and a conserved region of KTKEGV N-terminal repeats (Pandey *et al.* 2006). γ-synuclein has been shown to share a 55.9 and 54.3% similarity, with the α- and β-synucleins respectively (Lavedan *et al.* 1998). As such it is likely that if LRRK2 is able to phosphorylate α-syn, these members of the synuclein family could also be kinase substrates.

To characterise the nature of the LRRK2-DVL interaction identified by Y2H, by examining the DVL family as phosphorylation targets for LRRK2, recombinant DVL2 and DVL3 have been used in kinase assays with WT and mutant recombinant LRRK2 protein. Similarly, the β-tubulin isoform TUBB5 was also assessed as a kinase substrate by performing *in vitro* kinase assays with LRRK2, to assess phosphorylation of this isoform. For each experiment, a positive control was used to model physiological phosphorylation of each substrate under *in vitro* conditions. CK1 has been shown to phosphorylate DVLs in response to Wnt activation of the frizzled receptor (Korr *et al.* 2006). CK1 has also been shown to phosphorylate α-syn *in vitro* and *in vivo* (Okochi *et al.* 2000) and so this protein was used in kinase assays as a positive control for α-synuclein, DVL2 and DVL3. DVL1 is not currently available commercially so was not used for these experiments. GRK2 has been shown to phosphorylate β-tubulin *in vitro* and in cells (Yoshida *et al.* 2003) and was therefore used as a positive control for TUBB5 kinase assays. To ensure that recombinant proteins used in these assays are not co-purified with other kinases, kinase dead D1994A ΔN-LRRK2 was used as a negative control for each experiment. To try and account for the likelihood of false positive results, the RIP kinase, RIPK5 was included in kinase assays. RIPK5 is involved in apoptosis signalling (Zha *et al.* 2004) and has not been shown to interact with, or be involved in signalling pathways with the synuclein family, DVL2 or 3, or TUBB5 to date. As such, it is a good candidate for inclusion as a non-specific kinase in these experiments.

Many kinases require cofactors such as cAMP, or interaction with other proteins in order to function properly. Similarly, all kinases have different kinetics and

substrate affinities. In order to take the differences in basal kinase activity into account, efficiency values were calculated for each condition, by taking into account the levels of autophosphorylation and MBP phosphorylation for each kinase. These calculations were made on the assumption that a kinase should be able to phosphorylate its own substrate more efficiently than a non-specific substrate. As such, substrate phosphorylation was divided by both of these values and the ratio used as an indicator of substrate affinity; a value above one indicates a higher affinity for the substrate compared to autophosphorylation or MBP. A value below one suggests that substrate affinity is poor and that autophosphorylation or MBP phosphorylation is more efficient. In this case, it can be argued that substrate phosphorylation is more likely to be occurring due to assay conditions rather than a physiological interaction. For each assay LRRK2 was used in WT and G2019S form.

6.1.1 Hypotheses

Experiments were designed to address the following hypotheses.

1) LRRK2 is a functional kinase and is able to phosphorylate other proteins *in vitro.*
2) α-synuclein is unlikely to be a physiological interactor of LRRK2.
3) LRRK2 is able to phosphorylate the TUBB5 isoform of β-tubulin.
4) LRRK2 is able to phosphorylate DVL isoforms 2 and 3.

6.1.2 Aims

These hypotheses were investigated by fulfilling the following aims.

1) To compare phosphorylation of α, β and γ-synuclein family members by LRRK2.
2) To assess the efficiency of α-synuclein phosphorylation by LRRK2 *in vitro.*
3) To assess LRRK2 phosphorylation of β-tubulin *in vitro* for possible future experiments.
4) To assess the ability of LRRK2 to phosphorylate DVL2 and DVL3 *in vitro.*

6.2 RESULTS

6.2.1 Assessment of α-synuclein phosphorylation by LRRK2

6.2.1.1 Synuclein family phosphorylation by LRRK2

To look at the specificity of kinase activity towards α, as opposed to β or γ-synuclein (β-syn, γ-syn), kinase assays were performed using these forms of synuclein. Phosphorylation of each substrate was quantified at 90 mins. Radiography and subsequent quantification of synuclein phosphorylation showed that there are undetectable levels of phosphorylation by co-purified kinases in these assays and as such, phosphorylation values obtained and are instead likely attributed to the kinase being investigated (Figure 6.1a). CK1 was shown to phosphorylate all forms of synuclein, with RIPK5 and ΔN-LRRK2 phosphorylation of these varients occurring at low levels. Quantification of phosphorylation and comparison between groups showed that CK1 phosphorylation was significantly higher than the non-specific activity of RIPK5 ($p<0.001$, one way ANOVA followed by Bonferroni post-test, Figure 6.1b). RIPK5 phosphorylation of α-syn was not significantly higher than background ($p>0.05$, Figure 6.1b). This was also the case for LRRK2 ($p>0.05$). Phosphorylation for all synuclein varients was shown to be the same for each kinase (Figure 6.1c). These results show that WT LRRK2 is unable to phosphorylate α-syn *in vitro*. LRRK2 does not show preferential phosphorylation of β or γ-syn compared to α-syn *in vitro* ($p>0.05$).

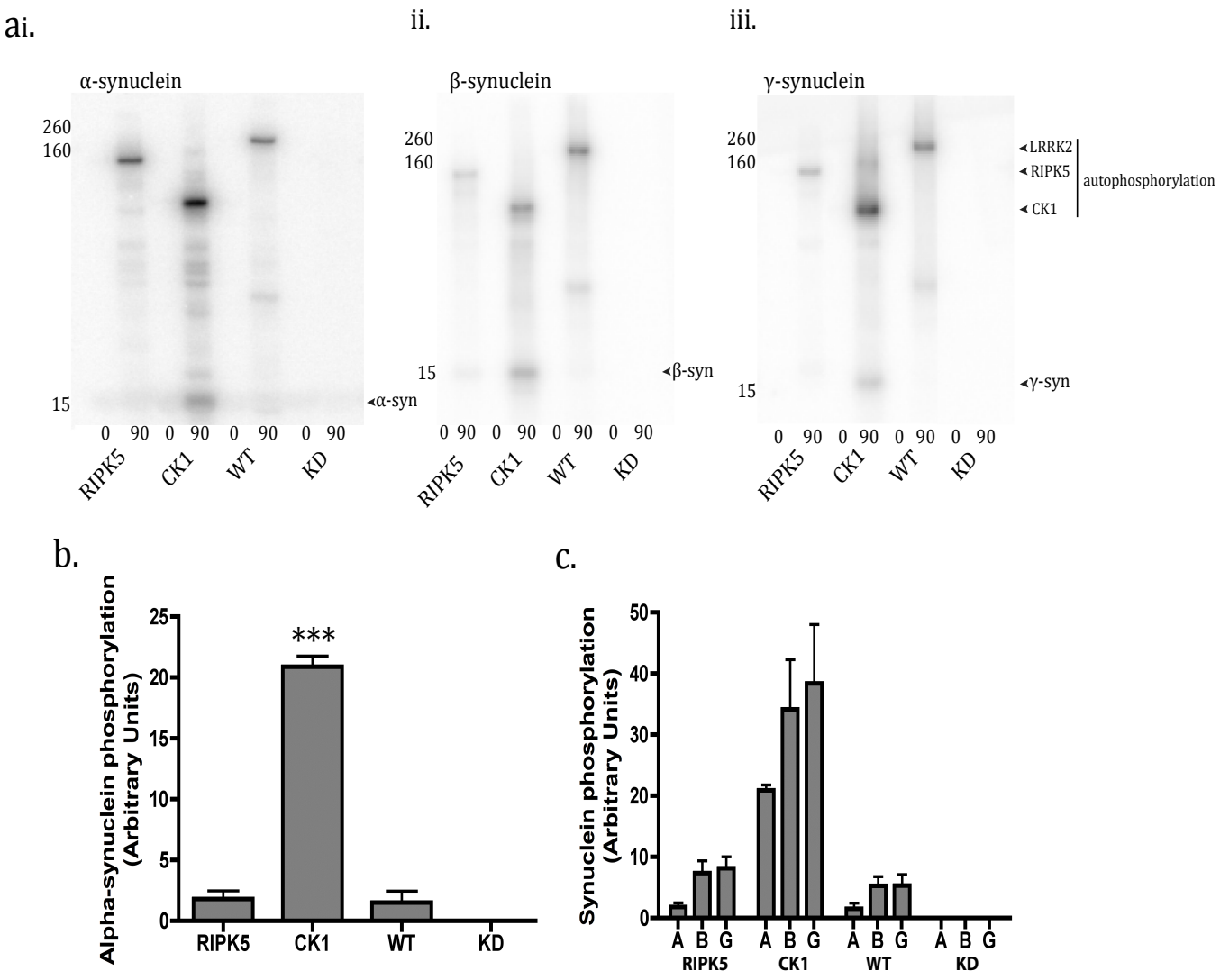

Figure 6.1a. Autoradiography of Synuclein phosphorylation. RIPK5- Receptor interacting protein kinase 5, 132.7 kDa. CK1- Casein kinase 1, 78.9 kDa. WT- Wild type ΔN-LRRK2, 204.9 kDa. KD-D1944A ΔN-LRRK2, 204.9 kDa. i-α-synuclein, 16 kDa. ii-β-synuclein, 14 kDa. iii-γ-synuclein, 17 kDa. Time points were taken at 0 and 90 mins as indicated below. Molecular weight markers are indicated on the left (kDa). Images are representative of at least three experiments. **6.1b. Quantification of α-synuclein phosphorylation by various kinases.** The 90 mins time point for each condition (taken from 6.1ai), was quantified and displayed as a bar chart showing the mean and s.e.m of phosphorylation values (N=3). *** $p<0.001$, CK1 vs RIPK5, one-way ANOVA between all groups with a Bonferroni post-test. **6.1c. Comparison of synuclein phosphorylation by various kinases.** There was no difference between α, β and γ-synuclein for each kinase ($p>0.05$).

6.2.1.2 Impact of familial mutations on α-synuclein phosphorylation by LRRK2

It has been shown in numerous studies that the G2019S mutation causes increased kinase activity *in vitro* (reviewed in Greggio *et al.* 2009). To assess if LRRK2 phosphorylation of α-syn is affected by familial mutations, kinase assays were performed using mutant forms of ΔN-LRRK2. Quantification of phosphorylation, showed that mutant forms of LRRK2 displayed little or no phosphorylation of α-syn. These results were not significantly higher than in the negative control condition for each mutant (p.0.05 vs KD), with the exception of G2019S, which displayed higher phosphorylation of α-syn than the KD condition ($p<0.05$). These results suggest that G2019S ΔN-LRRK2 is the only form of LRRK2 able to phosphorylate α-syn *in vitro*.

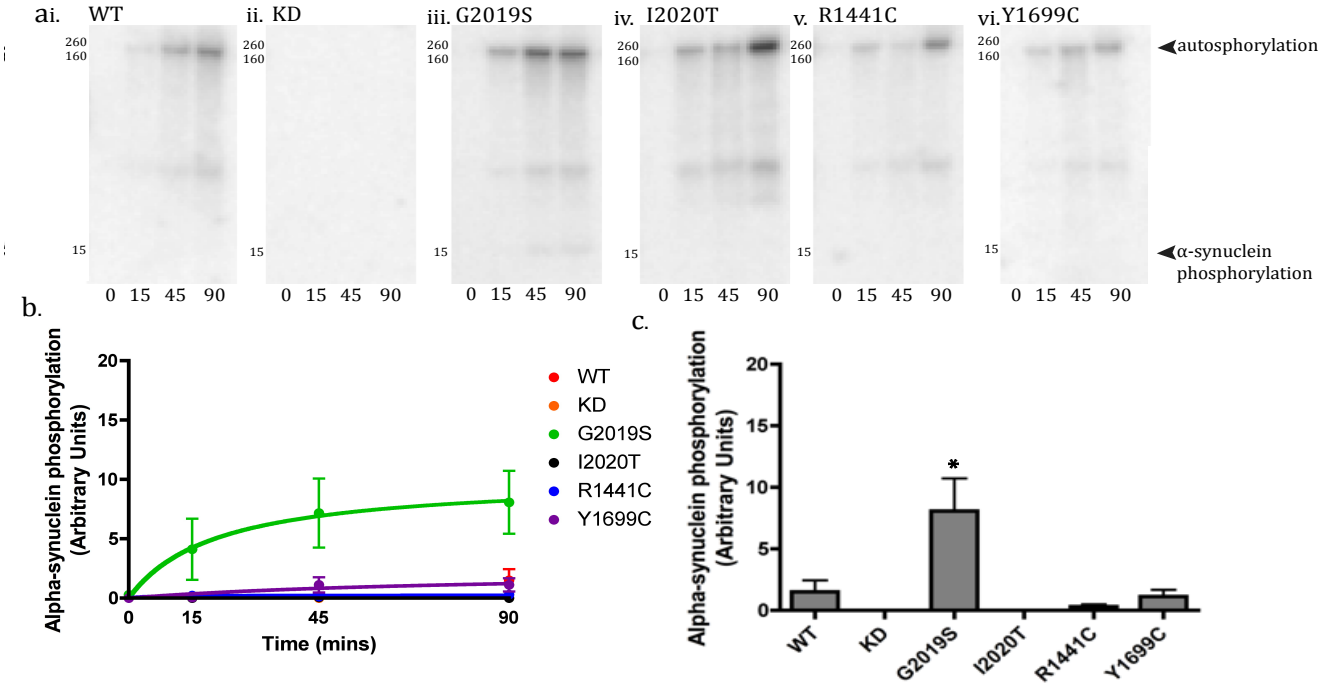

Figure 6.2a. α-synuclein phosphorylation by mutant ΔN-LRRK2. i-WT. ii-KD (D1994A). iii-G2019S. iv-I2020T. v-R1441C. vi-Y1699C. ΔN-LRRK2 was incubated with alpha-synuclein for 90 mins and time points taken as shown underneath. Images are representative of three experiments. Molecular weigh markers are shown on the left (kDa). **6.2b. Quantification of α-synuclein phosphorylation**. Kinase assays were transferred to phosphor screen and phosphorylation quantified using densitometry. Values shown are mean ± s.e.m over time (n=3). **6.2c. Quantification of α-syn phosphorylation at 90 mins.** The values for phosphorylation at 90 mins were taken and plotted as means ± s.e.m on a bar chart (n=3). * $p<0.05$ vs KD, one way ANOVA with Bonferroni post-test.

6.2.1.3 Assessment α-syn phosphorylation efficiency

To look at α-syn phosphorylation in relation to the level of kinase activity towards a non-physiological substrate, α-syn phosphorylation was compared to phosphorylation of MBP. Figure 6.3a shows the radiographic images of these experiments. Quantification of MBP phosphorylation by densitometry and expression of MBP as a ratio to α-syn phosphorylation, shows that the positive control, CK1 displays a preference for α-syn phosphorylation over MBP phosphorylation, as the ratio of α-syn: MBP phosphorylation is greater than one (Figure 6.3b). For both RIPK5, and G2019S LRRK2, these values are less than one, showing that MBP phosphorylation is preferential to α-syn phosphorylation for these kinases.

Calculation of an efficiency value for α-syn phosphorylation, which considers autophosphorylation, shows that this value is below 1 for all kinases (Figure 6.3c). This suggests that α-syn phosphorylation is less efficient than autophosphorylation for all kinases. Interestingly, this is also the case with the positive control CK1.

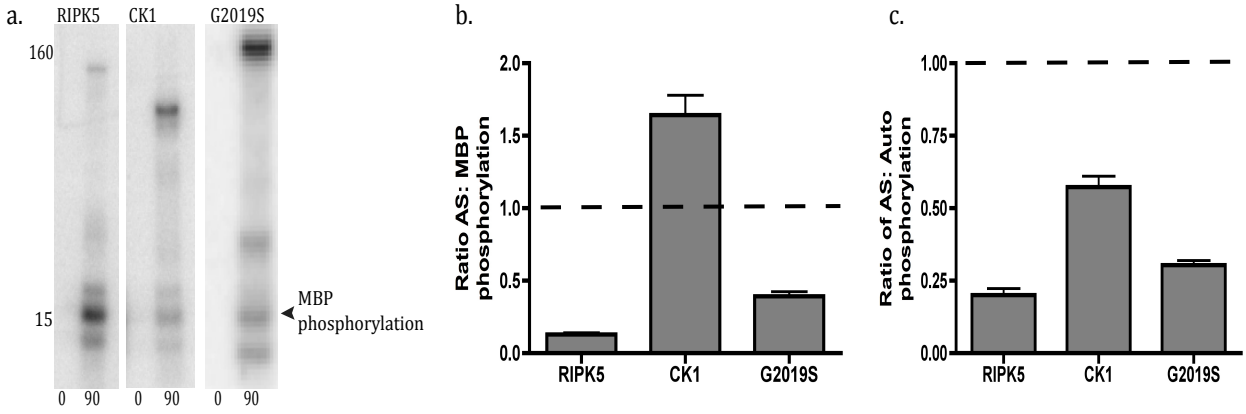

Figure 6.3a. Phosphorylation of MBP shown by radiography. Phosphorylation of MBP at 0 and 90 mins is shown . Time points are indicated below. MBP is a mixture of different isoforms with an average molecular weight of 18 kDa. Molecular weight markers shown on the left (kDa). Images are representative of three experiments. **6.3b. Ratio of α-synuclein: MBP phosphorylation at 90 mins**. The values for α-syn phosphorylation at 90 mins were divided by values for MBP phosphorylation at 90 mins for each kinase and are displayed as mean ± s.e.m (n=3). **6.3c. Ratio of α-synuclein: autophosphorylation at 90 mins**. The values for α-syn phosphorylation at 90 mins were divided by the values for autophosphorylation in each assay and are displayed as mean ± s.e.m (n=3).

6.2.1.4 S129 phosphorylation of α-synuclein

α-Syn phosphorylation at S129 has been shown to be important in PD pathogenesis (Smith *et al.* 2005). It has been shown that CK1 can phosphorylate α-syn at this residue (Okochi *et al.* 2000). As G2019S LRRK2 is able to phosphorylate α-syn *in vitro*, the ability of this mutant for of LRRK2 to phosphorylate S129 and perhaps provide a link between LRRK2 and pathogenic changes to α-syn, was assessed using phosphospecific antibodies. Kinase assays were performed and analysed using western blotting with a p-S129 antibody (Table 2.8).

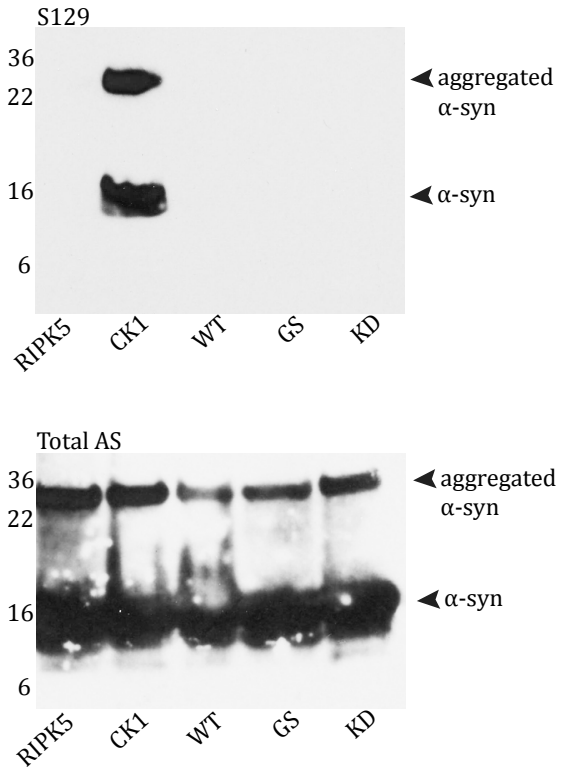

Figure 6.4. S129 phosphorylation of α-synuclein by RIPK5, CK1 and LRRK2. WT- Wild type, GS- G2019S, KD-D1994A, kinase dead LRRK2. Higher weight species at ~28 kDa are likely to be SDS-insoluble dimers of α-syn that have formed due to protein incubation at 37°C. Images shown are representative of three assays. Equal amounts of protein were loaded for each condition.

Western blotting showed that the positive control CK1, was able to phosphorylate α-syn at S129. SDS-insoluble dimers that formed during the kinase assay were also phosphorylated at this residue. As expected, no immunoreactivity at this residue was shown in the RIPK5 condition, however none of the LRRK2 forms used in these assays were able to phosphorylate α-syn at S129 either (Figure 6.4), suggesting that S129 is an unlikely kinase target for G2019S LRRK2

.

6.2.2 Assessment of TUBB5 phosphorylation

6.2.2.1 TUBB5 by LRRK2

Y2H experiments by collaborators have identified TUBB5 as a potential binding partner of the ROC domain (Sancho and Harvey, unpublished results). Interaction and phosphorylation of β-tubulin by LRRK2 has been shown by other groups (Gillardon 2009a, b), and as such phosphorylation of the TUBB5 isoform by LRRK2 was assessed in these experiments.

Incubation of TUBB5 with ΔN-LRRK2 in the presence of 32P γ-labelled ATP, showed that LRRK2 is able to phosphorylate this isoform of β-tubulin *in vitro* (Figure 6.5a). Phosphorylation of TUBB5 was also seen in the negative control, suggesting low-level contamination of the purified substrate with other kinases. When values were corrected for background phosphorylation, statistical analysis showed that all active kinases, including the non-specific kinase RIPK5, were able to phosphorylate TUBB5 at a level significantly higher than in the KD condition ($p=0.0001$, One-way ANOVA). Interestingly, quantification and analysis of TUBB5 phosphorylation for the positive control GRK2 and RIPK5, showed that there was no difference in TUBB5 phosphorylation between these conditions ($p>0.05$, one-way ANOVA, followed by Bonferroni post-test). LRRK2 phosphorylation of TUBB5 on the other hand was significantly higher than in the GRK2 condition for both WT and G2019S ($p<0.05$ for each). Interestingly, there was no difference in absolute phosphorylation by G2019S compared to WT ($p>0.05$), despite the fact that higher activity of G2019S has been commonly reported (reviewed in Greggio *et al.* 2009).

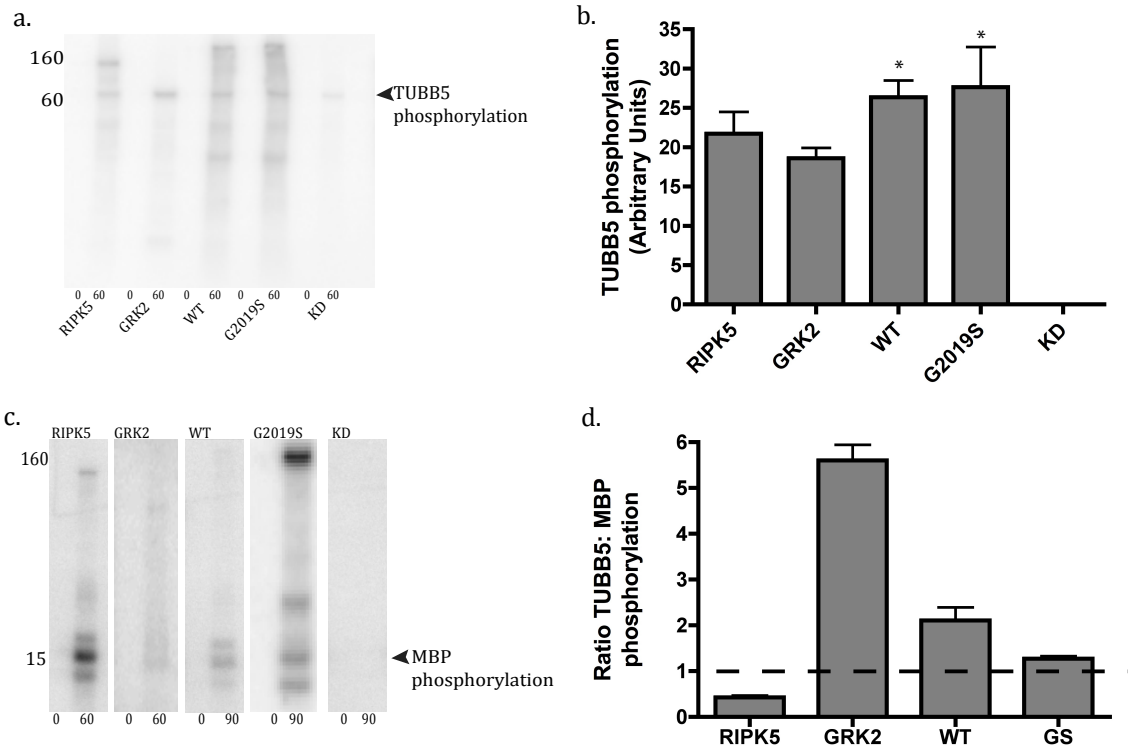

Figure 6.5a. Autoradiography of TUBB5 phosphorylation. RIPK5- Receptor interacting protein kinase 5, 132.7 kDa. GRK2- G-protein coupled receptor kinase 2, 82.3 kDa. WT- Wild type ΔN-LRRK2, 204.9 kDa. KD-D1944A ΔN-LRRK2, 204.9 kDa. TUBB5 has a molecular weight of 74.9 kDa. Time points were taken at 0 and 90 mins as indicated below. Molecular weight markers are indicated on the left (kDa). Images are representative of three experiments. **6.5b. Quantification of TUBB5 phosphorylation.** Densitometry was used to quantify phosphorylation of TUBB5 by each of the kinases used in this assay. Values obtained for the KD condition were subtracted and TUBB5 phosphorylation shown as values above background. Bar charts show mean ± s.e.m for each condition (n=3). * $p<0.05$ vs RIPK5. One-way ANOVA followed by Bonferroni post-test. **6.5c. Phosphorylation of MBP shown by radiography.** Phosphorylation of MBP at 0 and 90 mins is shown. Time points are indicated below. MBP is a mixture of different isoforms with an average molecular weight of 18 kDa. Molecular weight markers are shown on the left (kDa), images are representative of three experiments. **6.5d. Ratio of TUBB5 phosphorylation: MBP phosphorylation for various kinases.** Phosphorylation values for TUBB5 were divided by MBP phosphorylation values for each kinase. Values show mean ± s.e.m for each condition (n=3).

6.2.2.2 Assessment of the efficiency of TUBB5 phosphorylation

Results obtained from these experiments showed that GRK2 did not display quantifiable autophosphorylation, despite the fact that GRK2 is known to autophosphorylate (Sarnago *et al.* 1999). As such, the efficiency of TUBB5 phosphorylation was instead assessed, by comparing to phosphate incorporation into MBP (Figure 6.5d). Comparison of TUBB5 with MBP phosphorylation for the positive control GRK2, showed that phosphorylation of the physiological substrate *in vitro* was more efficient than of MBP by more than five times, as might be expected (Figure 6.5d). Wild type ΔN-LRRK2 showed around two-fold higher phosphorylation of TUBB5 than MBP, suggesting that TUBB5 phosphorylation is higher in efficiency than MBP phosphorylation. G2019S ΔN-LRRK2 phosphorylation of TUBB5 was shown to be higher than MBP by around 1.3 times, a value that suggests a lower efficiency when compared to WT. Non-specific phosphorylation of TUBB5 by RIPK5 showed preferential phosphorylation of MBP when values were compared, with β-tubulin phosphorylated at around half the efficiency of the pseudosubstrate. Taken together, these results suggest that TUBB5 is a good candidate for interaction with LRRK2 and as such are good targets for further investigation.

6.2.3 Assessment of DVL phosphorylation by LRRK2

6.2.3.1 LRRK2 phosphorylation of DVL3 is higher than DVL2

Y2H studies have shown that the DVL proteins may interact with the ROC domain of LRRK2, and that this interaction is perturbed by familial mutants of LRRK2 (Sancho *et al.* 2009). To investigate these proteins as potential kinase substrates for LRRK2, *in vitro* kinase assays were performed using DVL2 and DVL3 as substrates.

In vitro kinase assays using DVL2 as a substrate, showed that all active kinases investigated, displayed low-level phosphorylation of DVL2 (Figure 6.6a). The negative control KD ΔN-LRRK2, showed no DVL2 phosphorylation, suggesting that there are undetectable levels of phosphorylation by co-purified kinases in these experiments. Analysis of DVL2 phosphorylation by CK1 at 90 mins, showed that phosphorylation of the positive control is higher than background as would be expected ($p<0.05$ vs KD, one-way ANOVA followed by Bonferroni post-test), but no higher than the non-specific phosphorylation showed in the RIPK5 condition ($p>0.05$ vs RIPK5). Phosphorylation of

DVL2 by WT and G2019S LRRK2 were shown to be no higher than background ($p>0.05$ vs KD), although RIPK5 showed significantly higher phosphorylation of DVL2 than in the KD condition ($p<0.05$ vs KD). These results suggest that LRRK2 in WT and G2019S forms are unable to phosphorylate DVL2 *in vitro*.

Quantification of DVL3 phosphorylation at 90 mins (Figure 6.6f) showed that there is robust phosphorylation of DVL3 by all active kinases ($p>0.05$ vs KD for all conditions, one-way ANOVA followed by Bonferroni post-test). Again, there was no quantifiable phosphorylation displayed in the KD condition. CK1 phosphorylation of DVL3 was higher than background ($p<0.001$ vs KD, one-way ANOVA followed by Bonferroni post-test), but not higher than the non-specific phosphorylation displayed by RIPK5 ($p>0.05$). LRRK2 phosphorylation for both WT and G2019S forms was shown to be higher than background ($p<0.001$ vs KD) but was again, no higher than in the RIPK5 condition ($p>0.05$). There was no difference between WT ΔN-LRRK2 and G2019S phosphorylation of DVL3 ($p>0.05$). This shows that, although LRRK2 phosphorylation of DVL3 occurred at seemingly high levels, DVL3 is also highly phosphorylated by RIPK5 meaning that this phosphorylation is less likely to be physiological.

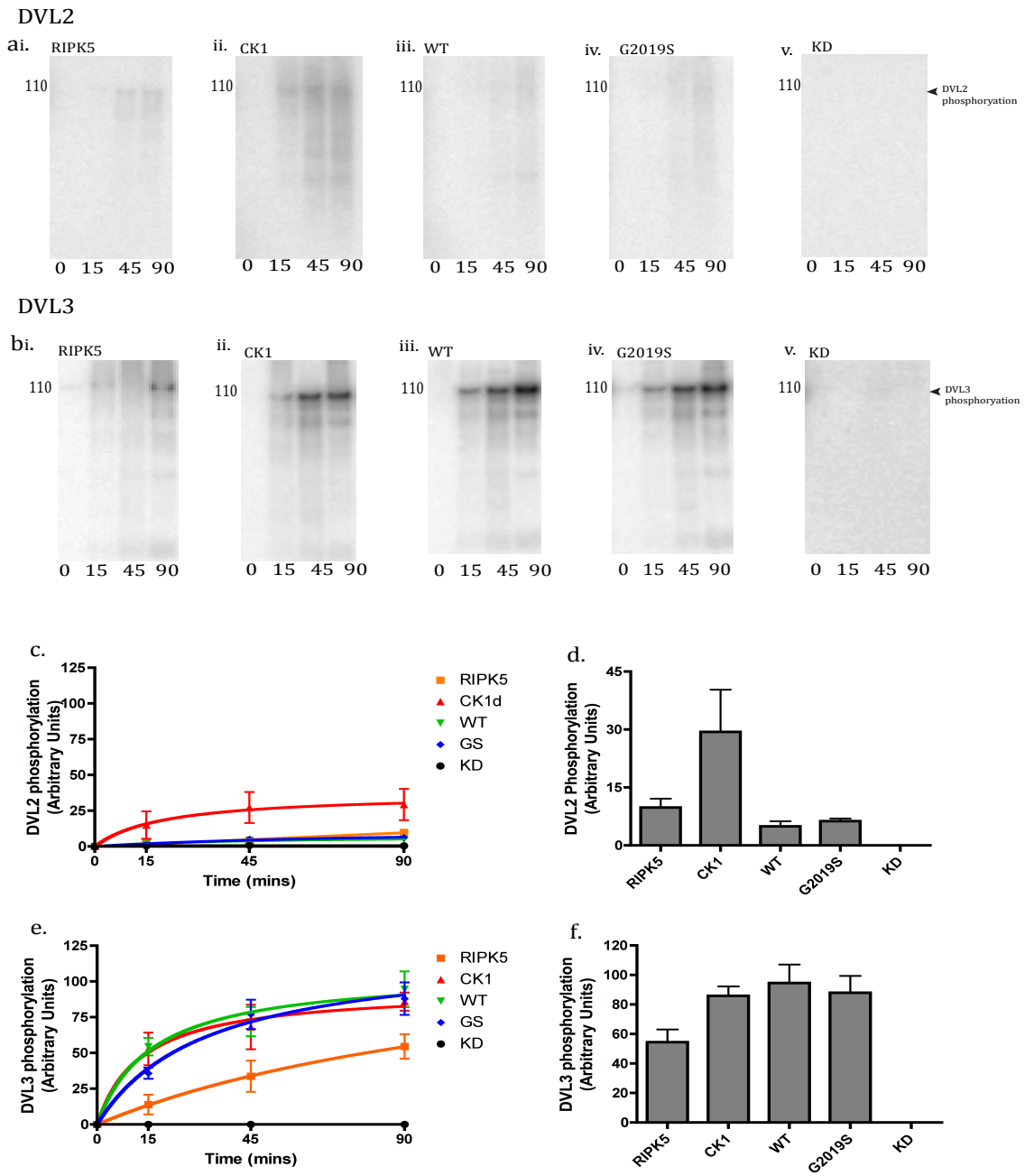

Figure 6.6a. Autoradiography of DVL2 phosphorylation. RIPK5- Receptor interacting protein kinase 5, 132.7 kDa. CK1- Casein kinase 1, 78.9 kDa. WT- Wild type ΔN-LRRK2, 204.9 kDa. KD-D1944A ΔN-LRRK2, 204.9 kDa. DVL2 has a molecular weight of 105.9 kDa. Time points were taken as indicated below (mins). Molecular weight markers are indicated on the left (kDa). Images are representative of three experiments. **6.6b. Quantification of DVL2 phosphorylation.** Densitometry was used to quantify phosphorylation of DVL2 at 90 mins for each kinase. Bar charts show mean ± s.e.m for each condition (n=3). **6.6c. Autoradiography of DVL3 phosphorylation.** As Figure 6.6a. DVL3 has a molecular weight of 104.7 kDa. **6.6d Quantification of DVL2 phosphorylation.** As Figure 6.6b.

6.2.3.2. Comparison of DVL3 phosphorylation to MBP phosphorylation

Autophosphorylation occurred at low levels for all kinases in these experiments. For LRRK2, autophosphorylation occurred at low, but visible levels. For RIPK5 and CK1 however, no autophosphorylation was detectable (Figure 6.6a and b). Analysis of DVL2 phosphorylation, showed that values were no higher than background for each kinase except the positive control ($p>0.05$ vs KD for each condition). As such, substrate phosphorylation in these experiments was not analysed further. DVL3 phosphorylation was shown to be higher than background for all active kinases assayed, therefore the levels of DVL3 phosphorylation were compared to MBP, in order to assess the efficiency of phosphorylation for each kinase (Figure 6.7).

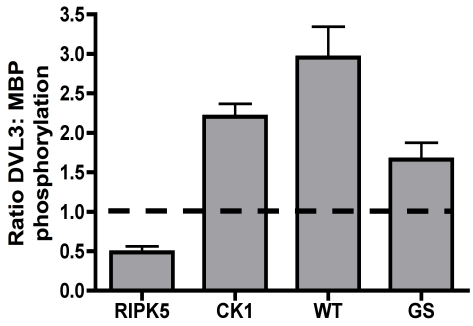

Figure 6.7. Ratio of MBP: DVL3 phosphorylation for enzymatically active kinases. Phosphorylation values for DVL3 were divided by MBP phosphorylation values for each kinase. Values show mean ± s.e.m for each condition (n=3).

Comparison of CK1 phosphorylation of DVL3, shows that MBP was phosphorylated at around three times lower levels than substrate phosphorylation (Figure 6.7). WT LRRK2 phosphorylation of DVL3 is around 3 times higher than MBP phosphorylation, with the G2019S mutant showing MBP phosphorylation of MBP at around half the efficiency of DVL3. Non-specific phosphorylation of DVL3 by RIPK5 shows an efficiency ratio less than one, despite the robust phosphorylation of DVL3 displayed (Figure 6.6 c, d). These results suggest that MBP is phosphorylated at around twice the level of DVL3. As such DVL3 may be a good candidate for further investigation as a LRRK2 kinase substrate.

6.3 DISCUSSION

LRRK2 is known to be toxic when overexpressed in cells, and it has been shown that this toxicity is mediated by kinase function (Greggio *et al.* 2006, Smith *et al.* 2006). As a putative kinase, identifying the kinase substrates of LRRK2 is vital in order to understand how mutations in LRRK2 cause AD PD. In these experiments, proposed interactors of LRRK2 were used in kinase assays to assess the likelihood of being physiological kinase substrates. Using ΔN-LRRK2 allowed highly controlled kinase assays to be performed, in which the concentration of LRRK2 and the molar excess of each substrate could be carefully manipulated. This system allowed the aims to be successfully achieved and the synuclein family, DVLs and TUBB5 were assessed as kinase substrates. From the results of all *in vitro* kinase assays described here, it would seem that DVL3 is the best candidate for interaction with LRRK2, as phosphorylation of this protein was shown to occur at levels three times higher than the generic substrate MBP. Other substrates assayed did not show the same level of preference when compared to LRRK2.

6.3.1 Synuclein phosphorylation

Examination of α-syn as a potential kinase substrate, showed that WT LRRK2 is unable to phosphorylate α-syn *in vitro* (Figure 6.1a, b). β and γ-syn were not preferable as kinase substrates (Figure 6.1c). The presence of the G2019S hyperactivating mutation, induced phosphorylation of α-syn that was statistically significant, however comparison of this phosphorylation to autophosphorylation, showed that autophosphorylation is more efficient in this system. Similarly, G2019S kinase activity towards the generic substrate MBP was also higher than towards α-syn. It could be hypothesised that G2019S induces abnormal phosphorylation of α-syn, which does not occur in the WT form. This would provide a possible mechanism for LRRK2 mutations and PD pathogenesis, however the lack of phosphorylation at S129 makes this seem less likely. The G2019S substitution is unlikely to cause structural changes on a scale that could induce differential substrate recognition, especially as these functions are likely mediated by the protein-protein interaction domains and not by the kinase

domain, From the data shown in this study, it can be concluded that α-syn is unlikely to be a LRRK2 kinase substrate *in vitro* and also, that LRRK2 does not phosphorylate the S129 residue under these conditions. As such, it would seem less likely that α-syn is a kinase substrate for LRRK2 *in vivo* also.

Other groups have shown an interaction between α-syn and LRRK2 *in vitro* (Qing *et al.* 2009a, b), however these experiments utilised whole cell lysate containing overexpressed LRRK2, instead of purified LRRK2. The phosphorylation of α-syn at S129 in these experiments could be a response to the overexpression of LRRK2, and not necessarily caused by LRRK2 itself. Combining the results of the two studies, it seems more likely that if LRRK2 and α-syn do share a common signalling function, this may be due to a common signalling pathway, rather than a direct interaction. Indeed α-syn and the 14-3-3 proteins have been shown to display a high degree of homology and it has been shown that α-syn can bind to 14-3-3 (Ostrerova *et al.* 1999). If this is the case, the recently discovered interaction between LRRK2 and 14-3-3 could provide a functional link between these two proteins (Dzamko *et al.* 2010, Nichols *et al.* 2010, Li X. *et al*. 2011).

6.3.2.TUBB5

Initial analysis of TUBB5 phosphorylation by LRRK2 shows that the GST-fusion protein is able to phosphorylate TUBB5 *in vitro,* with a higher affinity for this β-tubulin isoform than the psuedosubstrate MBP. Surprisingly, phosphorylation of TUBB5 by G2019S ΔN-LRRK2 in these experiments was shown to occur at the same level as WT. When compared to MBP phosphorylation, the affinity of G2019S ΔN-LRRK2 was lower than the WT condition (~2 times compared to ~1.3 times), however the ratio still showed a preference for TUBB5 over MBP.

Previous studies investigating putative substrates of LRRK2 have shown that G2019S displays consistently higher kinase activity compared to compared to WT (West *et al.* 2005, Anand *et al.* 2009, Pungaliya *et al.* 2010). Similarly, *in vitro* kinase assays performed by other groups have shown that the ΔN-LRRK2 protein can phosphorylate β-tubulin *in vitro* and that G2019S increases tubulin

phosphorylation by ~3 fold (Gillardon, 2009a, b). In this study, β-tubulin isoforms were purified from bovine brain and were perhaps more likely to have interacting proteins present which could have affected the outcome of these assays. The results from the experiments detailed here raise interesting questions regarding the role of the G2019S mutation, because they suggest that the effect of this mutation on kinase activity may be more nuanced than a mere blanket increase. Instead it could be hypothesised that G2019S does not increase kinase activity *per se*, but perhaps effects some sort of intra-molecular regulation, such as delaying the 'off' mechanism for kinase activity. When a robust cellular readout for LRRK2 function has been identified, these questions can be answered more fully.

Initial analysis of the results obtained, suggest that TUBB5 is a good candidate for LRRK2 interaction. As with the positive control, WT and G2019S ΔN-LRRK2 phosphorylation of the structural protein was shown to be more efficient than MBP, suggesting that it is less likely that the interaction is solely due to the *in vitro* conditions used. As such, interaction of LRRK2 and TUBB5 would be good candidate for further investigation in cellular models, as the tubulins provide a direct link to the tau pathology that is seen in the brains of some LRRK2 mutation carriers.

6.3.3 DVLs

In the present study, LRRK2 was demonstrated to phosphorylate DVL3 at levels with no significant differece from those displayed by the positive control (Figure 6.6e). LRRK2 was shown to phosphorylate DVL3 at a higher level than MBP, suggesting that LRRK2 has a higher affinity for DVL3 *in vitro* (Figure 6.7). As with TUBB5, the absolute phosphorylation values for DVL3 are similar for WT and G2019S. As the presence of familial mutations has been shown to decrease the strength of any proposed interaction between LRRK2 and DVLs (Sancho *et al.* 2009), it would be expected that phosphorylation of a DVL2 or 3 would be lower in G2019S than WT. For DVL3, when kinase activity towards MBP was taken into account, G2019S actually showed a decreased affinity for DVL compared to WT.

The functional implications of LRRK2 involvement in Wnt signalling, suggest that if LRRK2 is a member of this pathway, it is likely to play an important role in development. If so, if LRRK2 and DVL3 do interact in vivo, why do mutations in LRRK2 cause PD and not developmental disorders? Further experimentation in cell models will allow this interaction to be explored in more detail.

6.3.4 The role of interacting proteins

Phosphorylation of a substrate is often dependent on cellular context and interactions with other proteins. As all kinase assays described in this thesis were performed *in vitro*, there are numerous factors that were not present. As such, it cannot be concluded that LRRK2 does not phosphorylate α-syn (Figures 6.1, 6,2) or DVL2 (Figure 6.6a, c, d) *in vivo*. The lack of cellular context in these assays is exacerbated by the fact that LRRK2 is missing a region of around 100kDa, which could be crucial for mediating protein-protein interaction. In terms of α-syn it means that there could still be possibility that LRRK2 and α-syn are physiological interactors, however more investigation is needed to elucidate the role LRRK2 kinase activity is playing in α-syn signalling and pathogenesis. The fact that GRK2 displayed the lowest phosphorylation of TUBB5, emphasises the importance to interacting proteins for kinase to function optimally. GRK2 has been shown to require numerous cofactors to function including phosphorylation at certain residues and G-protein interactions, (Pitcher *et al.* 1998). The lack of these factors *in vitro* likely offers some explanation for the low kinase activity seen by GRK2 in these experiments.

6.3.5 Future directions

The experiments using RIPK5 that are detailed here, have shown that non-specific phosphorylation of a substrate *in vitro* is able to occur at robust levels (Figure 6.1, 6.5, 6.6). In this case, results from *in vitro* experiments must be interpreted cautiously and interpreted in the context of functional data obtained from cell culture or animal studies. For TUBB5, and DVL3, this means comparison to functional studies using known outputs of Wnt activation such a β-catenin

degradation and tubulin function, such as cytoskeletal dynamics. Mass spectrometric analysis of phosphorylation sites generated by LRRK2 *in vitro*, could provide possible functional readouts of LRRK2 involvement in these cascades. Generation of phosphospecific antibodies against residues phosphorylated by LRRK2 and mutation of these phosphorylation sites in overexpressed mutants, should allow further examination of potential LRRK2 involvement in these pathways.

Although WT ΔN-LRRK2 was unable to phosphorylate α-syn, the G2019S mutant was able to phosphorylate the peptide at low levels (Figure 6.2c). It has been shown that G2019S is unlikely to phosphorylate α-syn at S129 *in vitro*, however there is a possibility that the S87 residue (Okochi *et al.* 2000) may be a target instead. To determine this, and to identify other possible phosphorylation sites, mass spectrometry of α-syn phosphorylated by G2019S could also be performed.

7. GENERAL DISCUSSION

7.1 EVALUATION OF METHODS

The experiments in this thesis were designed to ask questions about the most basic level of LRRK2 functioning and as such, focused mainly on LRRK2 dimer formation and the effects of familial mutations on LRRK2 structure and kinase function. These questions were asked, with the long-term aim of being able to build on this knowledge and contribute to a holistic knowledge of LRRK2 functioning, in order to understand the contribution of this protein to PD pathogenesis. In order to achieve these aims, experiments were largely performed using *in vitro* conditions, to isolate elements of functioning that are intrinsic to LRRK2. This meant that results could be interpreted without the influence of LRRK2 interacting proteins. These conditions meant that each experiment could be carefully controlled and was optimally reproducible, as results could be corrected for the amount of protein used. When investigating the role of familial mutations on dimer formation (Figures 4.1, 4.2) and kinase activity (Figure 4.3), this element of control was crucial in order to interpret results properly, as the most important factor in each experiment was to delineate LRRK2 functioning from the functioning, or influence of any other protein. Using other methods, such as immunoprecipitation of tagged proteins would not allow such accurate quantification of protein or guarantee of purity. Experiments using phosphatase to look at the importance of phosphorylation on the dimerisation of LRRK2 (Figures 3.3b, 3.4), were also able to be performed by virtue of their *in vitro* conditions, as this meant that the results could not be confounded by the presence of other proteins or kinases.

7.1.1 Use of recombinant protein

Technically, LRRK2 is challenging to examine experimentally, because of the high levels of toxicity caused when the protein is overexpressed in cells. The large size of LRRK2, means that plasmid production and manipulation can be difficult and as yet, full length recombinant LRRK2 is unavailable. Currently, the most successful system for purifying the largest possible fragment of LRRK2, remains to be producing an N-terminally truncated GST-fusion protein spanning residues 970-

2527 in Sf9 cells, which has been shown to produce a relatively clean and enzymatically active protein (Jaleel *et al.* 2007). The GST tag is likely beneficial with regard to the solubility of ΔN-LRRK2. This 25 kDa protein, which replaces ~100kDa of the N-terminal region of LRRK2, has been shown dimerise however (Hayes *et al.* 1982) and so the presence of the tag could be affecting the structure and functioning of this protein. More generally, performing experiments using recombinant protein *in vitro*, means that *in vitro* characterisation of protein behaviour will not necessarily translate to a physiological setting. For LRRK2 and the experiments described in this thesis, this means that the changes in kinase activity seen with the introduction of familial mutations to ΔN-LRRK2, must be compared to results from experiments using techniques such as cell or animal models, in order to assess the value of this data. As MBP is not a physiological kinase substrate of LRRK2, the increase in kinase activity seen for G2019S and decreased displayed by R1441C (Figure 4.3) must be interpreted with caution, as behaviour towards a genuine substrate, which will interact with different electrostatic bonding, may be dissimilar.

7.1.2 Use of *in vitro* assay conditions

An important observation from the *in vitro* kinase assays performed in this thesis, was that for all proteins apart from α-syn, RIPK5 was able to demonstrate robust phosphorylation of each putative LRRK2 substrate, despite this kinase having no documented links to any of these proteins (Figures 6.5, 6.6). This emphasises how easily false-positive results are obtained under *in vitro* conditions and highlights the importance of using additional controls to analyse *in vitro* kinase assay data. Comparison of putative substrate phosphorylation, to phosphorylation of MBP, provided an accurate benchmark for non-specific kinase activity and for each condition it was shown that the negative control had a higher affinity for MBP than the putative substrate (Figures 6.3, 6.5d, 6.7). Similarly, for each positive control, apart from CK1 in the DVL2 condition, phosphorylation of the physiological substrate was higher than MBP phosphorylation, supporting the idea that a generic substrate is less likely to be phosphorylated than a physiological one.

Quantification of kinase autophosphorylation in these experiments, showed that the efficiency of autophosphorylation is highly variable and does not necessarily depend on the affinity of a kinase to a substrate. Autophosphorylation in experiments with DVL2 (Figure 6.6a, b) was negligible for all kinases, despite low phosphorylation of DVL2. Conversely, autophosphorylation in the DVL3 condition was also negligible, whereas substrate phosphorylation in this case was extremely efficient. In this case, the 50 times molar excess of substrate used for these assays could be inducing interactions between the substrate and kinase which are affecting the ability to autophosphorylate. This would suggest that some proteins are more 'sticky' than others, which could be affecting autophosphorylation due to conformational constraints induced by protein-protein interactions.

In vitro analysis of LRRK2 substrate phosphorylation in this thesis (Chapter 6), highlighted issues with the assumptions usually made about phosphorylation. *In vitro* kinase assays are often based upon the assumption that higher levels of phosphorylation mean that a reaction is more likely to be physiological. GRK2 phosphorylation of TUBB5 *in vitro* however, shows that this is not always the case, as GRK2 showed the lowest phosphorylation of TUBB5 (Figure 6.5b). GRK2 phosphorylation of MBP was also low, likely due to the numerous co-factors required by GRK2 *in vivo* (Pitcher *et al.* 1998) that were not present *in vitro*. These results emphasise the importance of scaffold proteins and other environmental factors such as lipid or cytoskeletal association. The fact that this cellular context is missing from *in vitro* assays, means that we can only be truly sure of the validity of results obtained *in vitro*, when we fully understand functioning *in vivo*. Signal transduction by kinases *in vivo,* is largely dependent on phosphorylation of a target residue in a manner that is highly controlled. Phosphorylation of Akt is an example of this, as stimulation of cells with insulin or EGF results in a peak of activity that lasts for only ten mins before phosphates are removed by PP2A (Ugi *et al.* 2004). Transduction of a signal therefore, may require phosphorylation of a small number of proteins to ensure that over-amplification does not occur. In this case, perhaps it is more important to look at the accuracy of phosphorylation *in vitro* rather than total levels of phosphorylation, as it could be argued that false-positive phosphorylation *in vitro* is less likely to occur at a residue that has important

downstream effects. Instead perhaps, kinase assays should focus on the phosphorylation of individual residues when they are known, rather than looking at the cumulative effect of numerous residues, the majority of which are likely to be non-specific.

7.1.2 Evaluation of other techniques used in this thesis

7.1.2.1 Analysis of quaternary structure

BN analysis has been widely used to analyse the complex formation of proteins since the technique was devised in the early 1990's (Schagger *et al.* 1991). By allowing proteins to migrate in their complexed forms, the technique can be used to characterise the quaternary structure of target proteins and analyse changes in these complexes in response to different stimuli. The rate of migration using BN PAGE, is affected by the total area of a protein and how compact it is; proteins with a more tightly packed structure appear smaller than those with a more relaxed conformation that occupies a larger volume. Similarly, the use of detergent is also a factor when comparing protein migration, as the loosening of electrostatic bonds by detergents affect the overall shape of the protein and thus its migration pattern. This means that changes to the conformation of a protein can be viewed as an electrophoretic shift (Wittig *et al.* 2006), however estimation of size using this technique is less precise and the poor resolution of complexes means that minor changes to protein conformation are not detectable using this technique. For comparison of ΔN-LRRK2 in WT and mutated form, this means that minor changes to quaternary structure may be occurring, however BN electrophoresis is unable to detect these changes. In this case, analysis of the protein using other techniques such as analytical ultracentrifugation may allow for more accurate analysis of mutated LRRK2.

The presence of Coomassie in BN PAGE analysis, to facilitate migration by induction of a negative charge allows visualisation of abundant protein, however the dye also affects the efficiency and reproducibility of transfer when western blotting is performed, this reducing the downstream applications that this technique can be used for. In the experiments described here, these constraints

meant that use of BN analysis to determine the quaternary structure of dephosphorylated ΔN-LRRK2 was impractical (Figure 3.3b) and BN PAGE was discontinued in favour of glycerol gradient centrifugation (Figure 3.4). This technique was utilised to successfully analyse changes to ΔN-LRRK2 quaternary structure, when phosphate groups were removed.

7.1.2.2 Glycerol gradient centrifugation

Glycerol gradient centrifugation has been used successfully by other groups to separate LRRK2 according to size and examine the enzymatic properties of different sized complexes (Berger *et al.* 2010). Analysis of LRRK2 from different fractions showed that although this technique is also lacking in resolution, separation of low and higher weight ΔN-LRRK2 (thought to be monomeric and dimeric species) was highly reproducible and allowed the kinase activity of these species to be examined. As such, although complexes over 440 kDa were unable to be separated, the gradients used allowed lower molecular weight LRRK2 to be analysed, providing results that are in agreement with those from full length and endogenous LRRK2 (Berger *et al.* 2010, Sen *et al.* 2009). Future studies using size-exclusion gel-filtration, as used previously by a number of groups (Greggio *et al.* 2008, Jorgensen *et al.* 2009, Sen *et al.* 2009) could be used alongside glycerol gradient centrifugation to analyse the complex size of LRRK2.

7.1.2.3 ATP pocket modification for identification of kinase substrates

Modification of the ATP pocket and subsequent overexpression of modified kinases in cells, is associated with a reduction of false-positive results when identifying kinase substrates (Shah *et al.* 1997). Other approaches, such as whole proteome screens using protein arrays or denatured proteins, are less likely to yield genuine results, as phosphorylation that occurs is independent of cellular context. In this case, necessary cofactors and other proteins needed to mediate phosphorylation are absent and the chance of both false-positive and false-negative results are also increased. By overexpressing 'gatekeeper' modified kinases and performing kinase assays *in situ* in cells, the technique is more likely to yield genuine results. The use of protein overexpression in these experiments increases the likelihood of false-positive results, however the ATP modification

technique has been well documented to yield physiologically relevant results (Specht *et al.* 2002) and the risk of false-positive results can be minimised by using the correct controls and validating results in other models. Advances in gene technology mean that point mutations can now be engineered into the genome of cells or animals without the need for overexpression (Urnov *et al.* 2005) and as such, ATP pocket mutations can be produced in place of WT, however these approaches are expensive and therefore less commonly used. In this case, 'gatekeeper' modification of a kinase and overexpression in cell models remains the best chance of minimising the false-positive results often obtained when trying to identify kinase substrates. The identification of residues that can rescue intolerant kinases means that, with modification, this method should be successful with any kinase investigated (Zhang *et al.* 2005), including LRRK2.

7.1.2.4 Protein interaction studies

The lack of antibodies able to recognise and immunoprecipitate endogenous protein is a problem for many areas in the PD field and indeed cell biology as a whole. As the results from experiments detailed here using the goat-polyclonal against LRRK2 (Everest), have shown (Figure 5.7), promising antibodies that work for some applications (Alegre-Abarrategui *et al.* 2008) do not always translate to success when used in other techniques. The issue of low LRRK2 expression is an important factor when attempting to immunoprecipitate endogenous protein, however these issues can be addressed through optimization of protocols to increase the amount of starting material used. Overexpression of tagged protein, has provided some good results for the LRRK2 field recently with the identification of the 14-3-3 proteins as LRRK2 interactors (Dzamko *et al*. 2010, Nichols *et al.* 2010, Li X. *et al.* 2011). As discussed above, this technique runs the risk of generating false-positive results, however when the right controls are used and interactions are verified using other models, use of overexpressed protein to dissect signaling pathways has been used with much success across a wide range of fields and as such may continue to prove useful in dissecting the role of LRRK2 in normal and pathogenic signaling.

7.2 CONCLUSIONS

7.2.1 Contribution of this work to our understanding of LRRK2 function and regulation

The experiments detailed in this thesis have provided support for many of the ideas proposed by other groups regarding the way LRRK2 self-regulates; autophosphorylation was shown to be important for complex formation (Figure 3.4) and the results of these experiments also support the idea that LRRK2 is able to dimerise (Greggio *et al.* 2008, Jorgensen *et al.* 2009 ,Sen *et al.* 2009, Berger *et al.* 2010). BN analysis of ΔN-LRRK2 and ROC domain quaternary structure, showed that, in the absence of interacting proteins, these fragments of LRRK2 are able to dimerise (Figures 3.1b, 4.1), suggesting that they have an intrinsic ability to do so, which is not mediated by other proteins. Investigation into the effect of familial mutations on LRRK2 quaternary structure using patient fibroblasts (Figure 4.2b), has shown that familial point-mutations are unlikely to affect binding of interacting proteins and subsequently the size of complex formation, as there was no difference in complex size between mutants and WT conditions (Figures 4.1d, 4.2b). The results of these experiments and those from other groups (Greggio *et al.* 2009), instead support the idea that mutations are acting enzymatically and are affecting the regulation mechanisms of LRRK2, perhaps disturbing the ability of LRRK2 to switch between an 'on' and 'off' state. G2019S has consistently been shown to increase LRRK2 kinase activity *in vitro* (reviewed in Greggio *et al.* 2009), however results from experiments in this thesis show that this is not always the case, as the difference in phosphorylation between WT and G2019S, depends on the substrate being used; for TUBB5 (Figure 6.5b) and DVLs 2 and 3 (Figure 6.6d, f), G2019S ΔN-LRRK2 did not show increased phosphorylation of these substrates compared to WT, despite showing significantly increased activity towards MBP (Figure 4.3c). This is also the case for G2019S autophosphorylation as experiments using TUBB5, and DVL2 and 3 did not show higher autophosphorylation than WT ΔN-LRRK2 in these conditions (Figures 6.5b, 6.6d, f). As such, these results support a model in which G2010S causes a dysregulation of enzymatic activation as opposed to a simple increase in the rate of kinase activity. Indeed, studies

characterising the kinase activity of G2019S ΔN-LRRK2 have shown that this mutant has a lower affinity for ATP than the WT version, and it has been suggested that kinase activity is higher as a result (Jaleel *et al.* 2007). In this case, the increase in kinase activity with some substrates such as MBP (Figure 4.3c) could be caused by a greater propensity for 'on' conformation.

Dephosphorylating recombinant ΔN-LRRK2 allowed the role of phosphorylation on LRRK2 dimer formation to be explored (Figures 3.3b, 3.4a). Results of these experiments suggest that phosphorylation is important for dimer formation and kinase activity. This data must be considered in the context of a protein tagged with GST, as GST is known to dimerise (Hayes *et al.* 1982), and as such, important questions still remain, such as whether LRRK2 would be able to dimerise *in vitro* without the tag. From the experiments described in this thesis, it can be concluded that dimerisation of LRRK2 could be mediated by phosphorylation at important residues (Figure 3.4a). These residues are more likely to be autophosphorylation targets, as kinase dead LRRK2 showed minimal phosphorylation in these experiments (Figure 3.3a) and in work done by other groups (Kamikawaji *et al.* 2009). From experiments done using affinity-purified ΔN-LRRK2, it is apparent that lower molecular weight species have little or no kinase activity (Figure 3.5b), results which agree with those published by other groups which also showed decreased kinase activity in lower molecular weight forms of LRRK2 (Sen *et al.* 2009, Berger *et al.* 2010). Further investigation as to the exact role of individual autophosphorylated residues will lead to a better understanding as to the sequence of events that result in LRRK2 activation.

Taken together, the results detailed here contribute towards a model of LRRK2 functioning whereby disruption of the finely-tuned mechanisms regulating enzymatic activity are disrupted by familial mutations. This disruption is likely to be caused largely by changes to enzymatic function, which may affect the ability of LRRK2 to modulate inputs from other proteins or to control subsequent outputs. This is likely to result in pathogenic changes to the homeostasis of signaling pathways that LRRK2 is involved in and eventually neuronal death.

7.2.2 Current understanding of LRRK2 functioning

In the time that has elapsed since starting this thesis, there have been many significant advances in the LRRK2 field, in terms of the tools available to researchers. A number of antibodies have been made available commercially and recently, access to phospho-antibodies has been made available (Nichols *et al.* 2010). Since finishing these experiments, a highly specific LRRK2 inhibitor has been designed (Deng X. *et al.* 2011) and there are currently numerous animal models now available for LRRK2. With the pace that techniques for LRRK2 experimentation are gathering, the next few years should prove to be extremely exciting for this area of PD research.

The likelihood that LRRK2 is dimeric (Greggio *et al.* 2008) was an important catalyst for understanding the sequence of events that lead to LRRK2 activation and it now seems likely that LRRK2 is monomeric in the cytosol, with low kinase activity, and dimeric when membrane bound, likely to be the active form of this protein (Sen *et al*. 2009, Berger *et al.* 2010). From these findings it would seem likely that LRRK2 is activated when cytosolic and recruited to the membrane where it becomes activated. The interaction of LRRK2 and the 14-3-3 proteins has been perhaps the most important finding in LRRK2 research to date, as it places LRRK2 in a dynamic signaling role, which likely encompasses a wide range of interactions and functions (Dzamko *et al*. 2010, Nichols *et al.* 2010, Li X. *et al*. 2011). Importantly, these experiments have also identified two phosphorylation sites in the N-terminus that mediate this interaction. These residues were shown to be targets for an interacting kinase (currently unknown) as opposed to autophosphorylation. Until this point, the majority of LRRK2 phosphorylation sites that had been identified were thought to be autophosphorylation sites.

Functionally, LRRK2 has been linked to MAPK signal transduction pathways (Carballo-Carbajal *et al.* 2010) and the downstream effectors of these pathways such as autophagy (Macleod *et al.* 2006, Plowey *et al.* 2008, Alegre-Abarrategui *et al.* 2009), and pathways involved in cytoskeletal dynamics (Gillardon, 2009a, b. Lin

et al. 2009, Parisiadou *et al.* 2009). Although the current role for LRRK2 is yet to be conclusively defined, the recent advances in research tools, suggest that the exact function of this protein will soon be defined.

7.2.3 PROPOSED FUNCTION OF LRRK2.

Kinase activity of LRRK2 is thought to be important for dimerisation (Sen *et al.* 2009) and is likely to mediate the toxic effects of this protein (Greggio *et al.* 2006, Smith *et al.* 2006). Despite this, the role of LRRK2 as a kinase is still heavily debated (Greggio *et al.* 2009). As shown in Table 7.1, numerous studies report kinase interactions of LRRK2 in animal models and human cell lines, however there is a large degree of disparity between these studies; papers are frequently being published with new suggestions for kinase substrates, yet no two studies in human models, seem to directly support other findings in the literature.

Substrate	Reference	Technique used
Moesin	Jaleel *et al*. 2008	Proteomic screen
4E-BP	Imai *et al*. 2008	*Drosophila* genetic interaction
MKKs	Gloeckner *et al*. 2009	Overexpression and immunoprecipitation. *C. Elegans* genetic interaction
β-Tubulin	Gillardon *et al*. 2009a, b	Endogenous mouse immunoprecipitation
α-Synuclein	Qing *et al*. 2009	Immunoprecipitation in human. *In vitro* kinase assay.
Foxo1	Kanao *et al*. 2010	*Drosophila* genetic interaction
Ste20 Kinases	Zach *et al*. 2010	Protein array

Table 7.1. Reported kinase substrates of LRRK2.

The variable pathology reported for LRRK2, and the numerous protein-protein interaction domains that it contains, make it likely that LRRK2 has a wide range of interactors and therefore make it possible that these wide-ranging results are not mutually exclusive, however more validation of individual substrates is needed. The robust interaction between LRRK2 and 4E-BP that has been shown in *drosophila*, has not been validated in humans and analysis of this interaction *in vitro* suggests that LRRK2 is less likely to be phosphorylating 4E-BP in humans (Kumar *et al.* 2010). The use of *in vitro* conditions to model physiological interactions has been discussed, however the issue of modelling human disease in animals will always be problematic as there is always the risk that individual components even of well-conserved pathways will differ between species.

A common finding in studies looking for LRRK2 kinase substrates is that the kinase activity of WT LRRK2 is negligible. Proteomic approaches using whole brain homogenates have shown that overexpressed, full-length WT LRRK2 kinase activity is undetectable (Jaleel *et al.* 2007). In this study, identification of a putative LRRK2 kinase substrate was only possible by using protein with the hyperactivating G2019S mutation, instead of WT. Similarly G2019S, as opposed to WT LRRK2, was used to identify the phosphorylation consensus motif **F/Y-x-T-x-R/K** as a likely target for LRRK2 kinase activity, for the same reasons (Pungaliya *et al.* 2010). The low level activity in WT LRRK2, has led to the suggestion that kinase activity could serve as a self-regulatory mechanism, as opposed to serving substrate phosphorylation (Greggio *et al.* 2009) with LRRK2 functioning mainly as a scaffold.

Whether LRRK2 is an authentic kinase or not, the role of this protein as a scaffold is likely to be central to its role in cellular functioning due to the numerous protein-protein interaction domains it contains. As this is the case, membrane localisation of LRRK2 may be important to its main functioning role (Hatano *et al.* 2007, Alegre-Abarrategui *et al.* 2009, Berger *et al.* 2010), suggesting the possibility of receptor-mediated signaling or even receptor interaction, resulting perhaps in phosphorylation of the Y707 residue. Indeed receptor involvement in signaling of

the closely related leucine-rich repeat protein LRRK1, has recently been shown with Grb2 interaction (Titz *et al.* 2010) and the discovery that LRRK1 mediates EGF receptor recycling and sorting, via Grb2 binding to PXXP sequences in the N-terminal region of the protein (Hanafusa *et al.* 2011). Given the close homology in sequence between LRRK1 and LRRK2, it is likely that they share some elements of signaling commonality, whether this is through shared interactions, or acting in common pathways. A proposed model of LRRK2 function is described here.

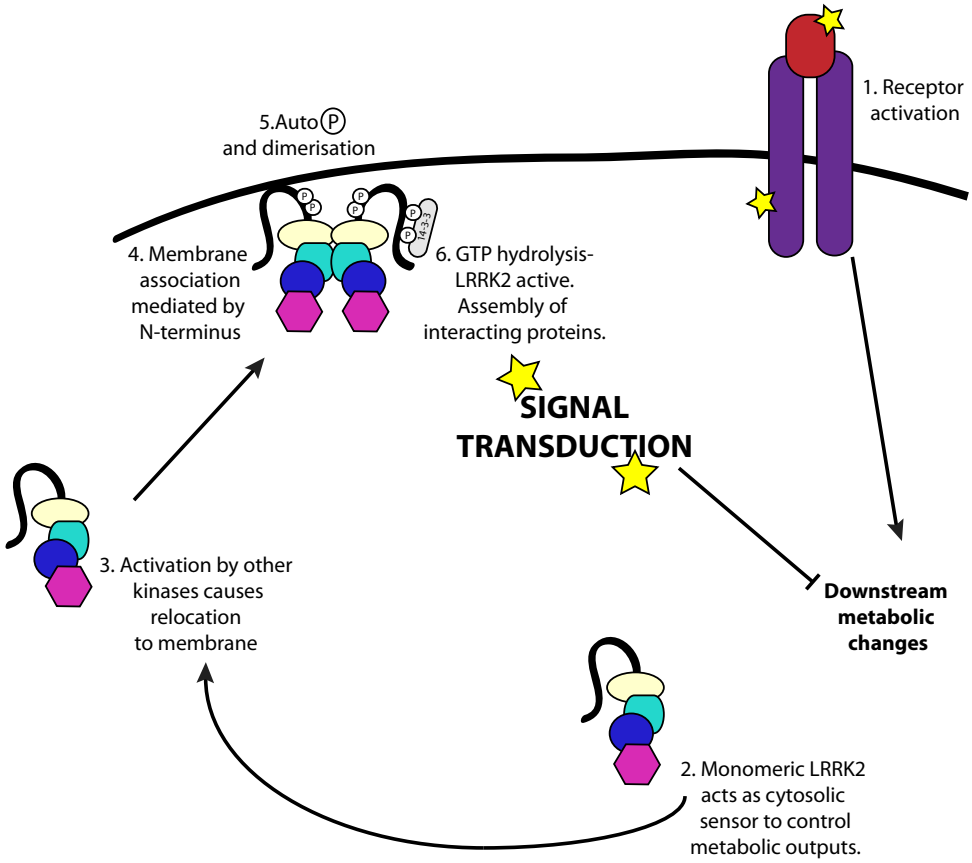

Figure 7.1. Proposed mechanism for LRRK2 functioning. 1. Receptor activation causes activation of receptor mediated signaling and metabolic responses to signaling. 2. LRRK2 acts as a cytosolic sensor to maintain homeostasis. 3. When signaling needs to be terminated, LRRK2 is activated by phosphorylation. 4. LRRK2 relocates to the membrane. 5. Autophosphorylation occurs and LRRK2 dimerises. Further phosphorylation by other kinases? 6. GTP binding activates kinase activity.

Interacting proteins bind and signal is transduced. Metabolic signaling downstream of the receptor is switched off.

7.3 GENERAL CONCLUSIONS

As a large protein with multiple domains in one molecule, LRRK2 is able to do the same work that perhaps three or four proteins do. The benefit of having multiple components and a 'cascade' of signaling is that each protein is subject to a high degree of regulation and so cumulatively, there are more quality control points. For LRRK2, having all these domains in one place means that dysregulation of functioning, for example by a point mutation, is more likely to be translated into the outputs of that cascade and thus upset a homeostatic balance. In this case, the likely effect of LRRK2 familial mutations would be an increase in outputs of this protein. If LRRK2 signaling is at the interface of proliferative signaling, then over-stimulation could result in an upregulation of factors aimed to counteract this (Plun-Favreau *et al.* 2010). This could cause problems with mitochondrial homeostasis, resulting in disruption of ATP production (Vander Heiden *et al.* 2000). Studies looking at putative functions of α-syn have shown that this protein may play a role in mitochondrial function (Elkon *et al.* 2002) and therefore it is plausible that dysregulation of LRRK2 leads to increased α-syn expression and signaling in response to mitochondrial damage. Downstream effects of this mitochondrial damage, such as proteasome inhibition and dyregulation of the cytoskeleton could be occurring as a knock-on effect of this mitochondrial damage.

Despite speculation however, the exact function of LRRK2 in the cell is currently unknown. This knowledge is vital in understanding how mutations in LRRK2 trigger the pathogenesis of PD. In the pursuit of this knowledge, the primary aim of research must be production of results that will ultimately result in therapeutic outcomes for patients. Although biochemical analyses of proteins implicated in disease is interesting, without understanding their contribution to normal cellular functioning, we cannot properly target the processes that are causing disease. Many papers discuss the possibility of LRRK2 inhibitors for therapeutic use, but at this point in time, there is no conclusive, measurable output of LRRK2 functioning and inhibition of LRRK2 may not necessarily be beneficial and may even be detrimental to cellular functioning. It seems more likely that the most beneficial

therapeutic approaches of the future will target the functional outputs of LRRK2 signaling, once these have been determined.

As with the majority of proteins of undetermined function, the proposed roles for LRRK2 are subject to a large amount of dogma, and there are a number of separate schools of thought that have emerged regarding the function of LRRK2. As a large protein with numerous protein-protein interaction domains, the function of this PD-associated protein may actually encompass many of these pathways. As such the most valuable contributions to this field are likely to be those that are able to consolidate existing and conflicting data, as well as adding something new to our understanding. In this way, a unified theory of LRRK2 function is needed to make sure that LRRK2 research is as effectual as possible in order to bring us a step closer to effective treatment regimes for this debilitating disease.

8. REFERENCES

Alegre-Abarrategui J, Ansorge O, Esiri M and Wade-Martins R (2008). LRRK2 is a component of granular alpha-synuclein pathology in the brainstem of Parkinson's disease. *Neuropathology and applied neurobiology*. **34**(3): 272-283.

Alegre-Abarrategui J, Christian H, Lufino MM, Mutihac R, Venda LL, Ansorge O and Wade-Martins R (2009). LRRK2 regulates autophagic activity and localizes to specific membrane microdomains in a novel human genomic reporter cellular model. *Hum Mol Genet*. **18**(21): 4022-4034.

Anand VS, Reichling LJ, Lipinski K, Stochaj W, Duan W, Kelleher K, Pungaliya P, Brown EL, Reinhart PH, Somberg R, Hirst WD, Riddle SM and Braithwaite SP (2009). Investigation of leucine-rich repeat kinase 2 : enzymological properties and novel assays. *Febs J*. **276**(2): 466-478.

Anden NE, Carlsson A, Kerstell J, Magnusson T, Olsson R, Roos BE, Steen B, Steg G, Svanborg A, Thieme G and Werdinius B (1970). Oral L-dopa treatment of parkinsonism. *Acta medica Scandinavica*. **187**(4): 247-255.

Anglade P, Vyas S, Javoy-Agid F, Herrero MT, Michel PP, Marquez J, Mouatt-Prigent A, Ruberg M, Hirsch EC and Agid Y (1997). Apoptosis and autophagy in nigral neurons of patients with Parkinson's disease. *Histol Histopathol*. **12**(1): 25-31.

Baer K, Al-Hasani H, Parvaresch S, Corona T, Rufer A, Nolle V, Bergschneider E and Klein HW (2001). Dimerization-induced activation of soluble insulin/IGF-1 receptor kinases: an alternative mechanism of activation. *Biochemistry*. **40**(47): 14268-14278.

Bence NF, Sampat RM and Kopito RR (2001). Impairment of the ubiquitin-proteasome system by protein aggregation. *Science*. **292**(5521): 1552-1555.

Bennett V (1982). The molecular basis for membrane - cytoskeleton association in human erythrocytes. *Journal of cellular biochemistry*. **18**(1): 49-65.

Berger Z, Smith KA and Lavoie MJ (2010). Membrane localization of LRRK2 is associated with increased formation of the highly active LRRK2 dimer and changes in its phosphorylation. *Biochemistry*. **49**(26): 5511-5523.

Berman SB and Hastings TG (1999). Dopamine oxidation alters mitochondrial respiration and induces permeability transition in brain mitochondria: implications for Parkinson's disease. *Journal of neurochemistry*. **73**(3): 1127-1137.

Beugnet A, Tee AR, Taylor PM and Proud CG (2003). Regulation of targets of mTOR (mammalian target of rapamycin) signalling by intracellular amino acid availability. *Biochem J*. **372**(Pt 2): 555-566.

Birkmayer W and Hornykiewicz O (1962). [The L-dihydroxyphenylalanine (L-DOPA) effect in Parkinson's syndrome in man: On the pathogenesis and treatment of Parkinson akinesis]. *Archiv fur Psychiatrie und Nervenkrankheiten, vereinigt mit Zeitschrift fur die gesamte Neurologie und Psychiatrie*. **203**(560-574.

Birkmayer W and Mentasti M (1967). [Further experimental studies on the catecholamine metabolism in extrapyramidal diseases (Parkinson and chorea syndromes)]. *Archiv fur Psychiatrie und Nervenkrankheiten*. **210**(1): 29-35.

Biskup S, Moore DJ, Celsi F, Higashi S, West AB, Andrabi SA, Kurkinen K, Yu SW, Savitt JM, Waldvogel HJ, Faull RL, Emson PC, Torp R, Ottersen OP, Dawson TM and Dawson VL (2006). Localization of LRRK2 to membranous and vesicular structures in mammalian brain. *Ann Neurol*. **60**(5): 557-569.

Biskup S, Moore DJ, Rea A, Lorenz-Deperieux B, Coombes CE, Dawson VL, Dawson TM and West AB (2007). Dynamic and redundant regulation of LRRK2 and LRRK1 expression. *BMC Neurosci*. **8**(102.

Bonetta L (2005). Prime time for real-time PCR. *Nature Methods*. **2**(305-312.

Bonifati V, Rizzu P, Squitieri F, Krieger E, Vanacore N, van Swieten JC, Brice A, van Duijn CM, Oostra B, Meco G and Heutink P (2003). DJ-1(PARK7), a novel gene for

autosomal recessive, early onset parkinsonism. *Neurological sciences : official journal of the Italian Neurological Society and of the Italian Society of Clinical Neurophysiology*. **24**(3): 159-160.

Bonifati V, Rohe CF, Breedveld GJ, Fabrizio E, De Mari M, Tassorelli C, Tavella A, Marconi R, Nicholl DJ, Chien HF, Fincati E, Abbruzzese G, Marini P, De Gaetano A, Horstink MW, Maat-Kievit JA, Sampaio C, Antonini A, Stocchi F, Montagna P, Toni V, Guidi M, Dalla Libera A, Tinazzi M, De Pandis F, Fabbrini G, Goldwurm S, de Klein A, Barbosa E, Lopiano L, Martignoni E, Lamberti P, Vanacore N, Meco G and Oostra BA (2005). Early-onset parkinsonism associated with PINK1 mutations: frequency, genotypes, and phenotypes. *Neurology*. **65**(1): 87-95.

Bosgraaf L and Van Haastert PJ (2003). Roc, a Ras/GTPase domain in complex proteins. *Biochimica et biophysica acta*. **1643**(1-3): 5-10.

Boulton TG, Nye SH, Robbins DJ, Ip NY, Radziejewska E, Morgenbesser SD, DePinho RA, Panayotatos N, Cobb MH and Yancopoulos GD (1991). ERKs: a family of protein-serine/threonine kinases that are activated and tyrosine phosphorylated in response to insulin and NGF. *Cell*. **65**(4): 663-675.

Braak H, Del Tredici K, Rub U, de Vos RA, Jansen Steur EN and Braak E (2003). Staging of brain pathology related to sporadic Parkinson's disease. *Neurobiol Aging*. **24**(2): 197-211.

Bras J, Singleton A, Cookson MR and Hardy J (2008). Emerging pathways in genetic Parkinson's disease: Potential role of ceramide metabolism in Lewy body disease. *Febs J*. **275**(23): 5767-5773.

Bridges D and Moorhead GB (2005). 14-3-3 proteins: a number of functions for a numbered protein. *Science's STKE : signal transduction knowledge environment*. **2005**(296): re10.

Brown EJ, Albers MW, Shin TB, Ichikawa K, Keith CT, Lane WS and Schreiber SL (1994). A mammalian protein targeted by G1-arresting rapamycin-receptor complex. *Nature*. **369**(6483): 756-758.

Brunn GJ, Williams J, Sabers C, Wiederrecht G, Lawrence JC, Jr. and Abraham RT (1996). Direct inhibition of the signaling functions of the mammalian target of rapamycin by the phosphoinositide 3-kinase inhibitors, wortmannin and LY294002. *Embo J*. **15**(19): 5256-5267.

Carballo-Carbajal I, Weber-Endress S, Rovelli G, Chan D, Wolozin B, Klein CL, Patenge N, Gasser T and Kahle PJ Leucine-rich repeat kinase 2 induces alpha-synuclein expression via the extracellular signal-regulated kinase pathway. *Cell Signal*.

Chandra S, Gallardo G, Fernandez-Chacon R, Schluter OM and Sudhof TC (2005). Alpha-synuclein cooperates with CSPalpha in preventing neurodegeneration. *Cell*. **123**(3): 383-396.

Chartier-Harlin MC, Kachergus J, Roumier C, Mouroux V, Douay X, Lincoln S, Levecque C, Larvor L, Andrieux J, Hulihan M, Waucquier N, Defebvre L, Amouyel P, Farrer M and Destee A (2004). Alpha-synuclein locus duplication as a cause of familial Parkinson's disease. *Lancet*. **364**(9440): 1167-1169.

Chen WY, Yang YM and Chuang NN (2002). Selective enhanced phosphorylation of shrimp beta-tubulin by PKC-delta with PEP(taxol), a synthetic peptide encoding the taxol binding region. *The Journal of experimental zoology*. **292**(4): 376-383.

Clark IE, Dodson MW, Jiang C, Cao JH, Huh JR, Seol JH, Yoo SJ, Hay BA and Guo M (2006). Drosophila pink1 is required for mitochondrial function and interacts genetically with parkin. *Nature*. **441**(7097): 1162-1166.

Cotzias GC, Papavasiliou PS and Gellene R (1968). Experimental treatment of parkinsonism with L-Dopa. *Neurology*. **18**(3): 276-277.

Covy JP and Giasson BI (2009). Identification of compounds that inhibit the kinase activity of leucine-rich repeat kinase 2. *Biochem Biophys Res Commun*. **378**(3): 473-477.

da Costa CA, Sunyach C, Giaime E, West A, Corti O, Brice A, Safe S, Abou-Sleiman PM, Wood NW, Takahashi H, Goldberg MS, Shen J and Checler F (2009). Transcriptional repression of p53 by parkin and impairment by mutations associated with autosomal recessive juvenile Parkinson's disease. *Nature cell biology*. **11**(11): 1370-1375.

Dachsel JC, Nishioka K, Vilarino-Guell C, Lincoln SJ, Soto-Ortolaza AI, Kachergus J, Hinkle KM, Heckman MG, Jasinska-Myga B, Taylor JP, Dickson DW, Gibson RA, Hentati F, Ross OA and Farrer MJ (2010). Heterodimerization of Lrrk1-Lrrk2: Implications for LRRK2-associated Parkinson disease. *Mechanisms of ageing and development*. **131**(3): 210-214.

Dachsel JC, Taylor JP, Mok SS, Ross OA, Hinkle KM, Bailey RM, Hines JH, Szutu J, Madden B, Petrucelli L and Farrer MJ (2007). Identification of potential protein interactors of Lrrk2. *Parkinsonism & related disorders*. **13**(7): 382-385.

Daniels V, Vancraenenbroeck R, Law BM, Greggio E, Lobbestael E, Gao F, De Maeyer M, Cookson MR, Harvey K, Baekelandt V and Taymans JM (2011). Insight into the mode of action of the LRRK2 Y1699C pathogenic mutant. *Journal of neurochemistry*. **116**(2): 304-315.

Davies P, Moualla D and Brown DR (2011). Alpha-synuclein is a cellular ferrireductase. *PLoS One*. **6**(1): e15814.

de Rijk MC, Breteler MM, Graveland GA, Ott A, Grobbee DE, van der Meche FG and Hofman A (1995). Prevalence of Parkinson's disease in the elderly: the Rotterdam Study. *Neurology*. **45**(12): 2143-2146.

Declercq W, Vanden Berghe T and Vandenabeele P (2009). RIP kinases at the crossroads of cell death and survival. *Cell*. **138**(2): 229-232.

Deng H, Le W, Huang M, Xie W, Pan T and Jankovic J (2007). Genetic analysis of LRRK2 P755L variant in Caucasian patients with Parkinson's disease. *Neuroscience letters*. **419**(2): 104-107.

Deng J, Lewis PA, Greggio E, Sluch E, Beilina A and Cookson MR (2008). Structure of the ROC domain from the Parkinson's disease-associated leucine-rich repeat kinase 2 reveals a dimeric GTPase. *Proc Natl Acad Sci U S A*. **105**(5): 1499-1504.

Deng X, Dzamko N, Prescott A, Davies P, Liu Q, Yang Q, Lee JD, Patricelli MP, Nomanbhoy TK, Alessi DR and Gray NS (2011). Characterization of a selective inhibitor of the Parkinson's disease kinase LRRK2. *Nature chemical biology*. **7**(4): 203-205.

Dexter DT, Wells FR, Agid F, Agid Y, Lees AJ, Jenner P and Marsden CD (1987). Increased nigral iron content in postmortem parkinsonian brain. *Lancet*. **2**(8569): 1219-1220.

Di Fonzo A, Chien HF, Socal M, Giraudo S, Tassorelli C, Iliceto G, Fabbrini G, Marconi R, Fincati E, Abbruzzese G, Marini P, Squitieri F, Horstink MW, Montagna P, Libera AD, Stocchi F, Goldwurm S, Ferreira JJ, Meco G, Martignoni E, Lopiano L, Jardim LB, Oostra BA, Barbosa ER and Bonifati V (2007). ATP13A2 missense mutations in juvenile parkinsonism and young onset Parkinson disease. *Neurology*. **68**(19): 1557-1562.

Diatlovitskaia EV, Valdnietse AT and Bergel'son LD (1977). [Lipid dependence of mitochondrial monoamine oxidase from rat hepatoma 27 with the use of rat liver lipid exchange proteins]. *Biokhimiia*. **42**(11): 2039-2043.

Diaz-Nido J, Serrano L and Avila J (1988). Differential phosphorylation of microtubule proteins by ATP and GTP. *Molecular and cellular biochemistry*. **79**(1): 73-79.

Duka T, Rusnak M, Drolet RE, Duka V, Wersinger C, Goudreau JL and Sidhu A (2006). Alpha-synuclein induces hyperphosphorylation of Tau in the MPTP model

of parkinsonism. *The FASEB journal : official publication of the Federation of American Societies for Experimental Biology*. **20**(13): 2302-2312.

Dzamko N, Deak M, Hentati F, Reith AD, Prescott AR, Alessi DR and Nichols RJ (2010). Inhibition of LRRK2 kinase activity leads to dephosphorylation of Ser(910)/Ser(935), disruption of 14-3-3 binding and altered cytoplasmic localization. *Biochem J*. **430**(3): 405-413.

Elkon H, Don J, Melamed E, Ziv I, Shirvan A and Offen D (2002). Mutant and wild-type alpha-synuclein interact with mitochondrial cytochrome C oxidase. *Journal of molecular neuroscience : MN*. **18**(3): 229-238.

Engelender S, Kaminsky Z, Guo X, Sharp AH, Amaravi RK, Kleiderlein JJ, Margolis RL, Troncoso JC, Lanahan AA, Worley PF, Dawson VL, Dawson TM and Ross CA (1999). Synphilin-1 associates with alpha-synuclein and promotes the formation of cytosolic inclusions. *Nature genetics*. **22**(1): 110-114.

Esposito D and Chatterjee DK (2006). Enhancement of soluble protein expression through the use of fusion tags. *Current opinion in biotechnology*. **17**(4): 353-358.

Eubel H, Braun HP and Millar AH (2005). Blue-native PAGE in plants: a tool in analysis of protein-protein interactions. *Plant methods*. **1**(1): 11.

Fahn S MC, Calne DB, Goldstein M, eds. (1987). Recent Developments in Parkinson's Disease. *Macmillan Health Care Information*. Florham Park, NJ. ,

Farrer M, Chan P, Chen R, Tan L, Lincoln S, Hernandez D, Forno L, Gwinn-Hardy K, Petrucelli L, Hussey J, Singleton A, Tanner C, Hardy J and Langston JW (2001). Lewy bodies and parkinsonism in families with parkin mutations. *Annals of neurology*. **50**(3): 293-300.

Farrer M, Stone J, Mata IF, Lincoln S, Kachergus J, Hulihan M, Strain KJ and Maraganore DM (2005). LRRK2 mutations in Parkinson disease. *Neurology*. **65**(5): 738-740.

Farrer MJ, Stone JT, Lin CH, Dachsel JC, Hulihan MM, Haugarvoll K, Ross OA and Wu RM (2007). Lrrk2 G2385R is an ancestral risk factor for Parkinson's disease in Asia. *Parkinsonism & related disorders*. **13**(2): 89-92.

Ferraro E and Cecconi F (2007). Autophagic and apoptotic response to stress signals in mammalian cells. *Archives of biochemistry and biophysics*. **462**(2): 210-219.

Feuerstein J, Goody RS and Webb MR (1989). The mechanism of guanosine nucleotide hydrolysis by p21 c-Ha-ras. The stereochemical course of the GTPase reaction. *The Journal of biological chemistry*. **264**(11): 6188-6190.

Fornai F, Schluter OM, Lenzi P, Gesi M, Ruffoli R, Ferrucci M, Lazzeri G, Busceti CL, Pontarelli F, Battaglia G, Pellegrini A, Nicoletti F, Ruggieri S, Paparelli A and Sudhof TC (2005). Parkinson-like syndrome induced by continuous MPTP infusion: convergent roles of the ubiquitin-proteasome system and alpha-synuclein. *Proc Natl Acad Sci U S A*. **102**(9): 3413-3418.

Fountaine TM, Venda LL, Warrick N, Christian HC, Brundin P, Channon KM and Wade-Martins R (2008). The effect of alpha-synuclein knockdown on MPP+ toxicity in models of human neurons. *Eur J Neurosci*. **28**(12): 2459-2473.

Fourest-Lieuvin A, Peris L, Gache V, Garcia-Saez I, Juillan-Binard C, Lantez V and Job D (2006). Microtubule regulation in mitosis: tubulin phosphorylation by the cyclin-dependent kinase Cdk1. *Molecular biology of the cell*. **17**(3): 1041-1050.

Francis SH and Corbin JD (1999). Cyclic nucleotide-dependent protein kinases: intracellular receptors for cAMP and cGMP action. *Critical reviews in clinical laboratory sciences*. **36**(4): 275-328.

Fujiwara M, Marusawa H, Wang HQ, Iwai A, Ikeuchi K, Imai Y, Kataoka A, Nukina N, Takahashi R and Chiba T (2008). Parkin as a tumor suppressor gene for hepatocellular carcinoma. *Oncogene*. **27**(46): 6002-6011.

Gandhi PN, Chen SG and Wilson-Delfosse AL (2009). Leucine-rich repeat kinase 2 (LRRK2): a key player in the pathogenesis of Parkinson's disease. *Journal of neuroscience research*. **87**(6): 1283-1295.

Gandhi PN, Wang X, Zhu X, Chen SG and Wilson-Delfosse AL (2008). The Roc domain of leucine-rich repeat kinase 2 is sufficient for interaction with microtubules. *Journal of neuroscience research*. **86**(8): 1711-1720.

Gandhi S, Wood-Kaczmar A, Yao Z, Plun-Favreau H, Deas E, Klupsch K, Downward J, Latchman DS, Tabrizi SJ, Wood NW, Duchen MR and Abramov AY (2009). PINK1-associated Parkinson's disease is caused by neuronal vulnerability to calcium-induced cell death. *Molecular cell*. **33**(5): 627-638.

Garcia-Marcos M, Ear J, Farquhar MG and Ghosh P (2011). A GDI (AGS3) and a GEF (GIV) regulate autophagy by balancing G protein activity and growth factor signals. *Molecular biology of the cell*. **22**(5): 673-686.

Gasper R, Meyer S, Gotthardt K, Sirajuddin M and Wittinghofer A (2009). It takes two to tango: regulation of G proteins by dimerization. *Nature reviews. Molecular cell biology*. **10**(6): 423-429.

Gehrke S, Imai Y, Sokol N and Lu B (2010). Pathogenic LRRK2 negatively regulates microRNA-mediated translational repression. *Nature*. **466**(7306): 637-641.

Gibb WR, Fearnley JM and Lees AJ (1990). The anatomy and pigmentation of the human substantia nigra in relation to selective neuronal vulnerability. *Advances in neurology*. **53**(31-34.

Gillardon F (2009a). Interaction of elongation factor 1-alpha with leucine-rich repeat kinase 2 impairs kinase activity and microtubule bundling in vitro. *Neuroscience*. **163**(2): 533-539.

Gillardon F (2009b). Leucine-rich repeat kinase 2 phosphorylates brain tubulin-beta isoforms and modulates microtubule stability--a point of convergence in parkinsonian neurodegeneration? *Journal of neurochemistry*. **110**(5): 1514-1522.

Gloeckner CJ, Boldt K, von Zweydorf F, Helm S, Wiesent L, Sarioglu H and Ueffing M (2010). Phosphopeptide analysis reveals two discrete clusters of phosphorylation in the N-terminus and the Roc domain of the Parkinson-disease associated protein kinase LRRK2. *Journal of proteome research*. **9**(4): 1738-1745.

Gloeckner CJ, Kinkl N, Schumacher A, Braun RJ, O'Neill E, Meitinger T, Kolch W, Prokisch H and Ueffing M (2006). The Parkinson disease causing LRRK2 mutation I2020T is associated with increased kinase activity. *Hum Mol Genet*. **15**(2): 223-232.

Gloeckner CJ, Schumacher A, Boldt K and Ueffing M (2009). The Parkinson disease-associated protein kinase LRRK2 exhibits MAPKKK activity and phosphorylates MKK3/6 and MKK4/7, in vitro. *J Neurochem*. **109**(4): 959-968.

Golbe LI, Di Iorio G, Sanges G, Lazzarini AM, La Sala S, Bonavita V and Duvoisin RC (1996). Clinical genetic analysis of Parkinson's disease in the Contursi kindred. *Annals of neurology*. **40**(5): 767-775.

Gosavi N, Lee HJ, Lee JS, Patel S and Lee SJ (2002). Golgi fragmentation occurs in the cells with prefibrillar alpha-synuclein aggregates and precedes the formation of fibrillar inclusion. *The Journal of biological chemistry*. **277**(50): 48984-48992.

Gotthardt K, Weyand M, Kortholt A, Van Haastert PJ and Wittinghofer A (2008). Structure of the Roc-COR domain tandem of C. tepidum, a prokaryotic homologue of the human LRRK2 Parkinson kinase. *Embo J*. **27**(17): 2352.

Graham DG, Tiffany SM, Bell WR, Jr. and Gutknecht WF (1978). Autoxidation versus covalent binding of quinones as the mechanism of toxicity of dopamine, 6-hydroxydopamine, and related compounds toward C1300 neuroblastoma cells in vitro. *Molecular pharmacology*. **14**(4): 644-653.

Greenamyre JT, MacKenzie G, Peng TI and Stephans SE (1999). Mitochondrial dysfunction in Parkinson's disease. *Biochem Soc Symp*. **66**(85-97.

Greenfield JG and Bosanquet FD (1953). The brain-stem lesions in Parkinsonism. *Journal of neurology, neurosurgery, and psychiatry*. **16**(4): 213-226.

Greggio E and Cookson MR (2009). Leucine-rich repeat kinase 2 mutations and Parkinson's disease: three questions. *ASN Neuro*. **1**(1):

Greggio E, Jain S, Kingsbury A, Bandopadhyay R, Lewis P, Kaganovich A, van der Brug MP, Beilina A, Blackinton J, Thomas KJ, Ahmad R, Miller DW, Kesavapany S, Singleton A, Lees A, Harvey RJ, Harvey K and Cookson MR (2006). Kinase activity is required for the toxic effects of mutant LRRK2/dardarin. *Neurobiol Dis*. **23**(2): 329-341.

Greggio E, Lewis PA, van der Brug MP, Ahmad R, Kaganovich A, Ding J, Beilina A, Baker AK and Cookson MR (2007). Mutations in LRRK2/dardarin associated with Parkinson disease are more toxic than equivalent mutations in the homologous kinase LRRK1. *J Neurochem*. **102**(1): 93-102.

Greggio E, Taymans JM, Zhen EY, Ryder J, Vancraenenbroeck R, Beilina A, Sun P, Deng J, Jaffe H, Baekelandt V, Merchant K and Cookson MR (2009). The Parkinson's disease kinase LRRK2 autophosphorylates its GTPase domain at multiple sites. *Biochem Biophys Res Commun*.

Greggio E, Zambrano I, Kaganovich A, Beilina A, Taymans JM, Daniels V, Lewis P, Jain S, Ding J, Syed A, Thomas KJ, Baekelandt V and Cookson MR (2008). The Parkinson disease-associated leucine-rich repeat kinase 2 (LRRK2) is a dimer that undergoes intramolecular autophosphorylation. *J Biol Chem*. **283**(24): 16906-16914.

Guo L, Gandhi PN, Wang W, Petersen RB, Wilson-Delfosse AL and Chen SG (2007). The Parkinson's disease-associated protein, leucine-rich repeat kinase 2 (LRRK2),

is an authentic GTPase that stimulates kinase activity. *Experimental cell research*. **313**(16): 3658-3670.

Habelhah H, Shah K, Huang L, Burlingame AL, Shokat KM and Ronai Z (2001). Identification of new JNK substrate using ATP pocket mutant JNK and a corresponding ATP analogue. *The Journal of biological chemistry*. **276**(21): 18090-18095.

Haebig K, Gloeckner CJ, Miralles MG, Gillardon F, Schulte C, Riess O, Ueffing M, Biskup S and Bonin M (2010). ARHGEF7 (Beta-PIX) acts as guanine nucleotide exchange factor for leucine-rich repeat kinase 2. *PLoS One*. **5**(10): e13762.

Halliwell B and Gutteridge JM (1985). The importance of free radicals and catalytic metal ions in human diseases. *Molecular aspects of medicine*. **8**(2): 89-193.

Hanafusa H, Ishikawa K, Kedashiro S, Saigo T, Iemura S, Natsume T, Komada M, Shibuya H, Nara A and Matsumoto K (2011). Leucine-rich repeat kinase LRRK1 regulates endosomal trafficking of the EGF receptor. *Nature communications*. **2**(158.

Harbour JW and Dean DC (2000). The Rb/E2F pathway: expanding roles and emerging paradigms. *Genes & development*. **14**(19): 2393-2409.

Hardy J, Cai H, Cookson MR, Gwinn-Hardy K and Singleton A (2006). Genetics of Parkinson's disease and parkinsonism. *Annals of neurology*. **60**(4): 389-398.

Harrison B, Kraus M, Burch L, Stevens C, Craig A, Gordon-Weeks P and Hupp TR (2008). DAPK-1 binding to a linear peptide motif in MAP1B stimulates autophagy and membrane blebbing. *The Journal of biological chemistry*. **283**(15): 9999-10014.

Hatano T, Kubo S, Imai S, Maeda M, Ishikawa K, Mizuno Y and Hattori N (2007). Leucine-rich repeat kinase 2 associates with lipid rafts. *Hum Mol Genet*. **16**(6): 678-690.

Hattori N, Shimura H, Kubo S, Kitada T, Wang M, Asakawa S, Minashima S, Shimizu N, Suzuki T, Tanaka K and Mizuno Y (2000). Autosomal recessive juvenile parkinsonism: a key to understanding nigral degeneration in sporadic Parkinson's disease. *Neuropathology : official journal of the Japanese Society of Neuropathology*. **20 Suppl**(S85-90.

Hayes JD and Clarkson GH (1982). Purification and characterization of three forms of glutathione S-transferase A. A comparative study of the major YaYa-, YbYb- and YcYc-containing glutathione S-transferases. *Biochem J*. **207**(3): 459-470.

Healy DG, Falchi M, O'Sullivan SS, Bonifati V, Durr A, Bressman S, Brice A, Aasly J, Zabetian CP, Goldwurm S, Ferreira JJ, Tolosa E, Kay DM, Klein C, Williams DR, Marras C, Lang AE, Wszolek ZK, Berciano J, Schapira AH, Lynch T, Bhatia KP, Gasser T, Lees AJ and Wood NW (2008). Phenotype, genotype, and worldwide genetic penetrance of LRRK2-associated Parkinson's disease: a case-control study. *Lancet neurology*. **7**(7): 583-590.

Hochstrasser M (1995). Ubiquitin, proteasomes, and the regulation of intracellular protein degradation. *Current opinion in cell biology*. **7**(2): 215-223.

Hoehn MM (1987). Parkinson's disease: progression and mortality. *Advances in neurology*. **45**(457-461.

Hoehn MM and Yahr MD (1967). Parkinsonism: onset, progression and mortality. *Neurology*. **17**(5): 427-442.

Hornykiewicz O (1962). [Dopamine (3-hydroxytyramine) in the central nervous system and its relation to the Parkinson syndrome in man]. *Deutsche medizinische Wochenschrift*. **87**(1807-1810.

Hsu CH, Chan D, Greggio E, Saha S, Guillily MD, Ferree A, Raghavan K, Shen GC, Segal L, Ryu H, Cookson MR and Wolozin B (2010). MKK6 binds and regulates expression of Parkinson's disease-related protein LRRK2. *Journal of neurochemistry*. **112**(6): 1593-1604.

Hughes AJ, Ben-Shlomo Y, Daniel SE and Lees AJ (1992). What features improve the accuracy of clinical diagnosis in Parkinson's disease: a clinicopathologic study. *Neurology*. **42**(6): 1142-1146.

Hurtado-Lorenzo A and Anand VS (2008). Heat shock protein 90 modulates LRRK2 stability: potential implications for Parkinson's disease treatment. *The Journal of neuroscience : the official journal of the Society for Neuroscience*. **28**(27): 6757-6759.

Hurtig HI, Trojanowski JQ, Galvin J, Ewbank D, Schmidt ML, Lee VM, Clark CM, Glosser G, Stern MB, Gollomp SM and Arnold SE (2000). Alpha-synuclein cortical Lewy bodies correlate with dementia in Parkinson's disease. *Neurology*. **54**(10): 1916-1921.

Iaccarino C, Crosio C, Vitale C, Sanna G, Carri MT and Barone P (2007). Apoptotic mechanisms in mutant LRRK2-mediated cell death. *Hum Mol Genet*. **16**(11): 1319-1326.

Ibanez P, Lesage S, Lohmann E, Thobois S, De Michele G, Borg M, Agid Y, Durr A and Brice A (2006). Mutational analysis of the PINK1 gene in early-onset parkinsonism in Europe and North Africa. *Brain : a journal of neurology*. **129**(Pt 3): 686-694.

Imai Y, Gehrke S, Wang HQ, Takahashi R, Hasegawa K, Oota E and Lu B (2008). Phosphorylation of 4E-BP by LRRK2 affects the maintenance of dopaminergic neurons in Drosophila. *Embo J*. **27**(18): 2432-2443.

Ito G, Okai T, Fujino G, Takeda K, Ichijo H, Katada T and Iwatsubo T (2007). GTP binding is essential to the protein kinase activity of LRRK2, a causative gene product for familial Parkinson's disease. *Biochemistry*. **46**(5): 1380-1388.

Jahreiss L, Menzies FM and Rubinsztein DC (2008). The itinerary of autophagosomes: from peripheral formation to kiss-and-run fusion with lysosomes. *Traffic*. **9**(4): 574-587.

Jaleel M, Nichols RJ, Deak M, Campbell DG, Gillardon F, Knebel A and Alessi DR (2007). LRRK2 phosphorylates moesin at threonine-558: characterization of how Parkinson's disease mutants affect kinase activity. *Biochem J*. **405**(2): 307-317.

Jao CC, Der-Sarkissian A, Chen J and Langen R (2004). Structure of membrane-bound alpha-synuclein studied by site-directed spin labeling. *Proceedings of the National Academy of Sciences of the United States of America*. **101**(22): 8331-8336.

Jenner P (2003). Dopamine agonists, receptor selectivity and dyskinesia induction in Parkinson's disease. *Curr Opin Neurol*. **16 Suppl 1**(S3-7.

Johnston JA, Ward CL and Kopito RR (1998). Aggresomes: a cellular response to misfolded proteins. *J Cell Biol*. **143**(7): 1883-1898.

Jorgensen ND, Peng Y, Ho CC, Rideout HJ, Petrey D, Liu P and Dauer WT (2009). The WD40 domain is required for LRRK2 neurotoxicity. *PLoS One*. **4**(12): e8463.

Junn E, Lee SS, Suhr UT and Mouradian MM (2002). Parkin accumulation in aggresomes due to proteasome impairment. *The Journal of biological chemistry*. **277**(49): 47870-47877.

Kahle PJ, Neumann M, Ozmen L, Muller V, Jacobsen H, Schindzielorz A, Okochi M, Leimer U, van Der Putten H, Probst A, Kremmer E, Kretzschmar HA and Haass C (2000). Subcellular localization of wild-type and Parkinson's disease-associated mutant alpha -synuclein in human and transgenic mouse brain. *The Journal of neuroscience : the official journal of the Society for Neuroscience*. **20**(17): 6365-6373.

Kamikawaji S, Ito G and Iwatsubo T (2009). Identification of the autophosphorylation sites of LRRK2. *Biochemistry*. **48**(46): 10963-10975.

Kanao T, Venderova K, Park DS, Unterman T, Lu B and Imai Y (2010). Activation of FoxO by LRRK2 induces expression of proapoptotic proteins and alters survival of

postmitotic dopaminergic neuron in Drosophila. *Hum Mol Genet*. **19**(19): 3747-3758.

Kay DM, Kramer P, Higgins D, Zabetian CP and Payami H (2005). Escaping Parkinson's disease: a neurologically healthy octogenarian with the LRRK2 G2019S mutation. *Movement disorders : official journal of the Movement Disorder Society*. **20**(8): 1077-1078.

Kay DM, Moran D, Moses L, Poorkaj P, Zabetian CP, Nutt J, Factor SA, Yu CE, Montimurro JS, Keefe RG, Schellenberg GD and Payami H (2007). Heterozygous parkin point mutations are as common in control subjects as in Parkinson's patients. *Annals of neurology*. **61**(1): 47-54.

Kitada T, Asakawa S, Hattori N, Matsumine H, Yamamura Y, Minoshima S, Yokochi M, Mizuno Y and Shimizu N (1998). Mutations in the parkin gene cause autosomal recessive juvenile parkinsonism. *Nature*. **392**(6676): 605-608.

Korr D, Toschi L, Donner P, Pohlenz HD, Kreft B and Weiss B (2006). LRRK1 protein kinase activity is stimulated upon binding of GTP to its Roc domain. *Cell Signal*. **18**(6): 910-920.

Kowall NW, Hantraye P, Brouillet E, Beal MF, McKee AC and Ferrante RJ (2000). MPTP induces alpha-synuclein aggregation in the substantia nigra of baboons. *Neuroreport*. **11**(1): 211-213.

Kruger R, Kuhn W, Muller T, Woitalla D, Graeber M, Kosel S, Przuntek H, Epplen JT, Schols L and Riess O (1998). Ala30Pro mutation in the gene encoding alpha-synuclein in Parkinson's disease. *Nature genetics*. **18**(2): 106-108.

Kumar A, Greggio E, Beilina A, Kaganovich A, Chan D, Taymans JM, Wolozin B and Cookson MR (2010). The Parkinson's disease associated LRRK2 exhibits weaker in vitro phosphorylation of 4E-BP compared to autophosphorylation. *PLoS One*. **5**(1): e8730.

Langston JW and Ballard P (1984). Parkinsonism induced by 1-methyl-4-phenyl-1,2,3,6-tetrahydropyridine (MPTP): implications for treatment and the pathogenesis of Parkinson's disease. *Can J Neurol Sci*. **11**(1 Suppl): 160-165.

Langston JW and Ballard PA, Jr. (1983). Parkinson's disease in a chemist working with 1-methyl-4-phenyl-1,2,5,6-tetrahydropyridine. *N Engl J Med*. **309**(5): 310.

Lashuel HA, Petre BM, Wall J, Simon M, Nowak RJ, Walz T and Lansbury PT, Jr. (2002). Alpha-synuclein, especially the Parkinson's disease-associated mutants, forms pore-like annular and tubular protofibrils. *Journal of molecular biology*. **322**(5): 1089-1102.

Lavedan C, Leroy E, Dehejia A, Buchholtz S, Dutra A, Nussbaum RL and Polymeropoulos MH (1998). Identification, localization and characterization of the human gamma-synuclein gene. *Human genetics*. **103**(1): 106-112.

Lees AJ (2007). Unresolved issues relating to the shaking palsy on the celebration of James Parkinson's 250th birthday. *Movement disorders : official journal of the Movement Disorder Society*. **22 Suppl 17**(S327-334.

Lees AJ, Hardy J and Revesz T (2009). Parkinson's disease. *Lancet*. **373**(9680): 2055-2066.

Lesage S, Ibanez P, Lohmann E, Pollak P, Tison F, Tazir M, Leutenegger AL, Guimaraes J, Bonnet AM, Agid Y, Durr A and Brice A (2005). G2019S LRRK2 mutation in French and North African families with Parkinson's disease. *Annals of neurology*. **58**(5): 784-787.

Lewis PA (2009). The function of ROCO proteins in health and disease. *Biology of the cell / under the auspices of the European Cell Biology Organization*. **101**(3): 183-191.

Lewis PA, Greggio E, Beilina A, Jain S, Baker A and Cookson MR (2007). The R1441C mutation of LRRK2 disrupts GTP hydrolysis. *Biochem Biophys Res Commun*. **357**(3): 668-671.

Lewy FH and Forster E (1912). "Paralysis agitans". *In Pathologische Anatomie. Handbuch der Neurologie (edited by M. Lewandowsky). Berlin: Springer*. 920-933.

Li J, Uversky VN and Fink AL (2002). Conformational behavior of human alpha-synuclein is modulated by familial Parkinson's disease point mutations A30P and A53T. *Neurotoxicology*. **23**(4-5): 553-567.

Li X, Moore DJ, Xiong Y, Dawson TM and Dawson VL (2010). Reevaluation of phosphorylation sites in the Parkinson disease-associated leucine-rich repeat kinase 2. *The Journal of biological chemistry*. **285**(38): 29569-29576.

Li X, Tan YC, Poulose S, Olanow CW, Huang XY and Yue Z (2007). Leucine-rich repeat kinase 2 (LRRK2)/PARK8 possesses GTPase activity that is altered in familial Parkinson's disease R1441C/G mutants. *J Neurochem*. **103**(1): 238-247.

Li X, Wang QJ, Pan N, Lee S, Zhao Y, Chait BT and Yue Z (2011). Phosphorylation-dependent 14-3-3 binding to LRRK2 is impaired by common mutations of familial Parkinson's disease. *PLoS One*. **6**(3): e17153.

Li Y, Dunn L, Greggio E, Krumm B, Jackson GS, Cookson MR, Lewis PA and Deng J (2009). The R1441C mutation alters the folding properties of the ROC domain of LRRK2. *Biochimica et biophysica acta*. **1792**(12): 1194-1197.

Lin X, Parisiadou L, Gu XL, Wang L, Shim H, Sun L, Xie C, Long CX, Yang WJ, Ding J, Chen ZZ, Gallant PE, Tao-Cheng JH, Rudow G, Troncoso JC, Liu Z, Li Z and Cai H (2009). Leucine-rich repeat kinase 2 regulates the progression of neuropathology induced by Parkinson's-disease-related mutant alpha-synuclein. *Neuron*. **64**(6): 807-827.

Lindecrona RH, Jensen TK, Andersen PH and Moller K (2002). Application of a 5' nuclease assay for detection of Lawsonia intracellularis in fecal samples from pigs. *Journal of clinical microbiology*. **40**(3): 984-987.

Liou AK, Leak RK, Li L and Zigmond MJ (2008). Wild-type LRRK2 but not its mutant attenuates stress-induced cell death via ERK pathway. *Neurobiol Dis*. **32**(1): 116-124.

Liu Y, Shah K, Yang F, Witucki L and Shokat KM (1998). A molecular gate which controls unnatural ATP analogue recognition by the tyrosine kinase v-Src. *Bioorganic & medicinal chemistry*. **6**(8): 1219-1226.

Lowe J, Stock D, Jap B, Zwickl P, Baumeister W and Huber R (1995). Crystal structure of the 20S proteasome from the archaeon T. acidophilum at 3.4 A resolution. *Science*. **268**(5210): 533-539.

Lucking CB, Durr A, Bonifati V, Vaughan J, De Michele G, Gasser T, Harhangi BS, Meco G, Denefle P, Wood NW, Agid Y and Brice A (2000). Association between early-onset Parkinson's disease and mutations in the parkin gene. *N Engl J Med*. **342**(21): 1560-1567.

Lwin A, Orvisky E, Goker-Alpan O, LaMarca ME and Sidransky E (2004). Glucocerebrosidase mutations in subjects with parkinsonism. *Molecular genetics and metabolism*. **81**(1): 70-73.

MacLeod D, Dowman J, Hammond R, Leete T, Inoue K and Abeliovich A (2006). The familial Parkinsonism gene LRRK2 regulates neurite process morphology. *Neuron*. **52**(4): 587-593.

Marin I (2006). The Parkinson disease gene LRRK2: evolutionary and structural insights. *Molecular biology and evolution*. **23**(12): 2423-2433.

Marongiu R, Ferraris A, Ialongo T, Michiorri S, Soleti F, Ferrari F, Elia AE, Ghezzi D, Albanese A, Altavista MC, Antonini A, Barone P, Brusa L, Cortelli P, Martinelli P,

Pellecchia MT, Pezzoli G, Scaglione C, Stanzione P, Tinazzi M, Zecchinelli A, Zeviani M, Cassetta E, Garavaglia B, Dallapiccola B, Bentivoglio AR and Valente EM (2008). PINK1 heterozygous rare variants: prevalence, significance and phenotypic spectrum. *Human mutation*. **29**(4): 565.

Martinez-Vicente M and Cuervo AM (2007). Autophagy and neurodegeneration: when the cleaning crew goes on strike. *Lancet neurology*. **6**(4): 352-361.

Maruta H and Burgess AW (1994). Regulation of the Ras signalling network. *BioEssays : news and reviews in molecular, cellular and developmental biology*. **16**(7): 489-496.

Mata IF, Wedemeyer WJ, Farrer MJ, Taylor JP and Gallo KA (2006). LRRK2 in Parkinson's disease: protein domains and functional insights. *Trends in neurosciences*. **29**(5): 286-293.

Matsui T, Maeda M, Doi Y, Yonemura S, Amano M, Kaibuchi K and Tsukita S (1998). Rho-kinase phosphorylates COOH-terminal threonines of ezrin/radixin/moesin (ERM) proteins and regulates their head-to-tail association. *J Cell Biol*. **140**(3): 647-657.

McNaught KS, Mytilineou C, Jnobaptiste R, Yabut J, Shashidharan P, Jennert P and Olanow CW (2002). Impairment of the ubiquitin-proteasome system causes dopaminergic cell death and inclusion body formation in ventral mesencephalic cultures. *J Neurochem*. **81**(2): 301-306.

Meixner A, Boldt K, Van Troys M, Askenazi M, Gloeckner CJ, Bauer M, Marto JA, Ampe C, Kinkl N and Ueffing M (2011). A QUICK screen for Lrrk2 interaction partners--leucine-rich repeat kinase 2 is involved in actin cytoskeleton dynamics. *Molecular & cellular proteomics : MCP*. **10**(1): M110 001172.

Melrose HL, Dachsel JC, Behrouz B, Lincoln SJ, Yue M, Hinkle KM, Kent CB, Korvatska E, Taylor JP, Witten L, Liang YQ, Beevers JE, Boules M, Dugger BN, Serna VA, Gaukhman A, Yu X, Castanedes-Casey M, Braithwaite AT, Ogholikhan S, Yu N,

Bass D, Tyndall G, Schellenberg GD, Dickson DW, Janus C and Farrer MJ (2010). Impaired dopaminergic neurotransmission and microtubule-associated protein tau alterations in human LRRK2 transgenic mice. *Neurobiol Dis*. **40**(3): 503-517.

Meyer G and Feldman EL (2002). Signaling mechanisms that regulate actin-based motility processes in the nervous system. *Journal of neurochemistry*. **83**(3): 490-503.

Meylan E and Tschopp J (2005). The RIP kinases: crucial integrators of cellular stress. *Trends in biochemical sciences*. **30**(3): 151-159.

Mira MT, Alcais A, Nguyen VT, Moraes MO, Di Flumeri C, Vu HT, Mai CP, Nguyen TH, Nguyen NB, Pham XK, Sarno EN, Alter A, Montpetit A, Moraes ME, Moraes JR, Dore C, Gallant CJ, Lepage P, Verner A, Van De Vosse E, Hudson TJ, Abel L and Schurr E (2004). Susceptibility to leprosy is associated with PARK2 and PACRG. *Nature*. **427**(6975): 636-640.

Morrison KE (2003). Parkin mutations and early onset parkinsonism. *Brain : a journal of neurology*. **126**(Pt 6): 1250-1251.

Naetzker S, Hagen N and Echten-Deckert G (2006). Activation of p38 mitogen-activated protein kinase and partial reactivation of the cell cycle by cis-4-methylsphingosine direct postmitotic neurons towards apoptosis. *Genes to cells : devoted to molecular & cellular mechanisms*. **11**(3): 269-279.

Nagakubo D, Taira T, Kitaura H, Ikeda M, Tamai K, Iguchi-Ariga SM and Ariga H (1997). DJ-1, a novel oncogene which transforms mouse NIH3T3 cells in cooperation with ras. *Biochemical and biophysical research communications*. **231**(2): 509-513.

Nalls MA, Plagnol V, Hernandez DG, Sharma M, Sheerin UM, Saad M, Simon-Sanchez J, Schulte C, Lesage S, Sveinbjornsdottir S, Stefansson K, Martinez M, Hardy J, Heutink P, Brice A, Gasser T, Singleton AB and Wood NW (2011). Imputation of

sequence variants for identification of genetic risks for Parkinson's disease: a meta-analysis of genome-wide association studies. *Lancet*. **377**(9766): 641-649.

Narendra D, Tanaka A, Suen DF and Youle RJ (2008). Parkin is recruited selectively to impaired mitochondria and promotes their autophagy. *J Cell Biol*. **183**(5): 795-803.

Nichols RJ, Dzamko N, Morrice NA, Campbell DG, Deak M, Ordureau A, Macartney T, Tong Y, Shen J, Prescott AR and Alessi DR (2010). 14-3-3 binding to LRRK2 is disrupted by multiple Parkinson's disease-associated mutations and regulates cytoplasmic localization. *Biochem J*. **430**(3): 393-404.

O'Sullivan SS, Evans AH and Lees AJ (2009). Dopamine dysregulation syndrome: an overview of its epidemiology, mechanisms and management. *CNS drugs*. **23**(2): 157-170.

Okochi M, Walter J, Koyama A, Nakajo S, Baba M, Iwatsubo T, Meijer L, Kahle PJ and Haass C (2000). Constitutive phosphorylation of the Parkinson's disease associated alpha-synuclein. *J Biol Chem*. **275**(1): 390-397.

Ostrerova N, Petrucelli L, Farrer M, Mehta N, Choi P, Hardy J and Wolozin B (1999). alpha-Synuclein shares physical and functional homology with 14-3-3 proteins. *The Journal of neuroscience : the official journal of the Society for Neuroscience*. **19**(14): 5782-5791.

Paisan-Ruiz C, Jain S, Evans EW, Gilks WP, Simon J, van der Brug M, Lopez de Munain A, Aparicio S, Gil AM, Khan N, Johnson J, Martinez JR, Nicholl D, Carrera IM, Pena AS, de Silva R, Lees A, Marti-Masso JF, Perez-Tur J, Wood NW and Singleton AB (2004). Cloning of the gene containing mutations that cause PARK8-linked Parkinson's disease. *Neuron*. **44**(4): 595-600.

Pandey N, Schmidt RE and Galvin JE (2006). The alpha-synuclein mutation E46K promotes aggregation in cultured cells. *Experimental neurology*. **197**(2): 515-520.

Pankratz N, Wilk JB, Latourelle JC, DeStefano AL, Halter C, Pugh EW, Doheny KF, Gusella JF, Nichols WC, Foroud T and Myers RH (2009). Genomewide association study for susceptibility genes contributing to familial Parkinson disease. *Human genetics*. **124**(6): 593-605.

Papavasiliou PS, Cotzias GC, Duby SE, Steck AJ, Fehling C and Bell MA (1972). Levodopa in Parkinsonism: potentiation of central effects with a peripheral inhibitor. *N Engl J Med*. **286**(1): 8-14.

Parisiadou L, Xie C, Cho HJ, Lin X, Gu XL, Long CX, Lobbestael E, Baekelandt V, Taymans JM, Sun L and Cai H (2009). Phosphorylation of ezrin/radixin/moesin proteins by LRRK2 promotes the rearrangement of actin cytoskeleton in neuronal morphogenesis. *The Journal of neuroscience : the official journal of the Society for Neuroscience*. **29**(44): 13971-13980.

Parkinson J (1817). An essay on the shaking palsy. *(London 1817). Published by Sherwood, Neely, and Jones*

Perez RG, Waymire JC, Lin E, Liu JJ, Guo F and Zigmond MJ (2002). A role for alpha-synuclein in the regulation of dopamine biosynthesis. *The Journal of neuroscience : the official journal of the Society for Neuroscience*. **22**(8): 3090-3099.

Pitcher JA, Hall RA, Daaka Y, Zhang J, Ferguson SS, Hester S, Miller S, Caron MG, Lefkowitz RJ and Barak LS (1998). The G protein-coupled receptor kinase 2 is a microtubule-associated protein kinase that phosphorylates tubulin. *The Journal of biological chemistry*. **273**(20): 12316-12324.

Plowey ED, Cherra SJ, 3rd, Liu YJ and Chu CT (2008). Role of autophagy in G2019S-LRRK2-associated neurite shortening in differentiated SH-SY5Y cells. *J Neurochem*. **105**(3): 1048-1056.

Plun-Favreau H, Klupsch K, Moisoi N, Gandhi S, Kjaer S, Frith D, Harvey K, Deas E, Harvey RJ, McDonald N, Wood NW, Martins LM and Downward J (2007). The

mitochondrial protease HtrA2 is regulated by Parkinson's disease-associated kinase PINK1. *Nature cell biology*. **9**(11): 1243-1252.

Plun-Favreau H, Lewis PA, Hardy J, Martins LM and Wood NW (2010). Cancer and neurodegeneration: between the devil and the deep blue sea. *PLoS genetics*. **6**(12): e1001257.

Polymeropoulos MH, Lavedan C, Leroy E, Ide SE, Dehejia A, Dutra A, Pike B, Root H, Rubenstein J, Boyer R, Stenroos ES, Chandrasekharappa S, Athanassiadou A, Papapetropoulos T, Johnson WG, Lazzarini AM, Duvoisin RC, Di Iorio G, Golbe LI and Nussbaum RL (1997). Mutation in the alpha-synuclein gene identified in families with Parkinson's disease. *Science*. **276**(5321): 2045-2047.

Pramstaller PP, Schlossmacher MG, Jacques TS, Scaravilli F, Eskelson C, Pepivani I, Hedrich K, Adel S, Gonzales-McNeal M, Hilker R, Kramer PL and Klein C (2005). Lewy body Parkinson's disease in a large pedigree with 77 Parkin mutation carriers. *Annals of neurology*. **58**(3): 411-422.

Pungaliya PP, Bai Y, Lipinski K, Anand VS, Sen S, Brown EL, Bates B, Reinhart PH, West AB, Hirst WD and Braithwaite SP (2010). Identification and characterization of a leucine-rich repeat kinase 2 (LRRK2) consensus phosphorylation motif. *PLoS One*. **5**(10): e13672.

Qing H, Wong W, McGeer EG and McGeer PL (2009a). Lrrk2 phosphorylates alpha synuclein at serine 129: Parkinson disease implications. *Biochem Biophys Res Commun*. **387**(1): 149-152.

Qing H, Zhang Y, Deng Y, McGeer EG and McGeer PL (2009b). Lrrk2 interaction with alpha-synuclein in diffuse Lewy body disease. *Biochem Biophys Res Commun*. **390**(4): 1229-1234.

Quinn NP (1997). Parkinson's disease: clinical features. *Bailliere's clinical neurology*. **6**(1): 1-13.

Rajput A, Dickson DW, Robinson CA, Ross OA, Dachsel JC, Lincoln SJ, Cobb SA, Rajput ML and Farrer MJ (2006). Parkinsonism, Lrrk2 G2019S, and tau neuropathology. *Neurology*. **67**(8): 1506-1508.

Ramirez A, Heimbach A, Grundemann J, Stiller B, Hampshire D, Cid LP, Goebel I, Mubaidin AF, Wriekat AL, Roeper J, Al-Din A, Hillmer AM, Karsak M, Liss B, Woods CG, Behrens MI and Kubisch C (2006). Hereditary parkinsonism with dementia is caused by mutations in ATP13A2, encoding a lysosomal type 5 P-type ATPase. *Nature genetics*. **38**(10): 1184-1191.

Ramsay RR and Singer TP (1986). Energy-dependent uptake of N-methyl-4-phenylpyridinium, the neurotoxic metabolite of 1-methyl-4-phenyl-1,2,3,6-tetrahydropyridine, by mitochondria. *The Journal of biological chemistry*. **261**(17): 7585-7587.

Rebrikov DV and Trofimov D (2006). [Real-time PCR: approaches to data analysis (a review)]. *Prikladnaia biokhimiia i mikrobiologiia*. **42**(5): 520-528.

Rogaeva E, Johnson J, Lang AE, Gulick C, Gwinn-Hardy K, Kawarai T, Sato C, Morgan A, Werner J, Nussbaum R, Petit A, Okun MS, McInerney A, Mandel R, Groen JL, Fernandez HH, Postuma R, Foote KD, Salehi-Rad S, Liang Y, Reimsnider S, Tandon A, Hardy J, St George-Hyslop P and Singleton AB (2004). Analysis of the PINK1 gene in a large cohort of cases with Parkinson disease. *Archives of neurology*. **61**(12): 1898-1904.

Roque AC and Lowe CR (2005). Lessons from nature: On the molecular recognition elements of the phosphoprotein binding-domains. *Biotechnology and bioengineering*. **91**(5): 546-555.

Rozengurt E (1986). Early signals in the mitogenic response. *Science*. **234**(4773): 161-166.

Rubinsztein DC (2006). The roles of intracellular protein-degradation pathways in neurodegeneration. *Nature*. **443**(7113): 780-786.

Rush J, Moritz A, Lee KA, Guo A, Goss VL, Spek EJ, Zhang H, Zha XM, Polakiewicz RD and Comb MJ (2005). Immunoaffinity profiling of tyrosine phosphorylation in cancer cells. *Nature biotechnology*. **23**(1): 94-101.

Sakanaka C, Sun TQ and Williams LT (2000). New steps in the Wnt/beta-catenin signal transduction pathway. *Recent progress in hormone research*. **55**(225-236.

Samaranch L, Lorenzo-Betancor O, Arbelo JM, Ferrer I, Lorenzo E, Irigoyen J, Pastor MA, Marrero C, Isla C, Herrera-Henriquez J and Pastor P (2010). PINK1-linked parkinsonism is associated with Lewy body pathology. *Brain : a journal of neurology*. **133**(Pt 4): 1128-1142.

Sancho RM, Law BM and Harvey K (2009). Mutations in the LRRK2 Roc-COR tandem domain link Parkinson's disease to Wnt signalling pathways. *Hum Mol Genet*. **18**(20): 3955-3968.

Sandal M, Valle F, Tessari I, Mammi S, Bergantino E, Musiani F, Brucale M, Bubacco L and Samori B (2008). Conformational equilibria in monomeric alpha-synuclein at the single-molecule level. *PLoS biology*. **6**(1): e6.

Sarnago S, Elorza A and Mayor F, Jr. (1999). Agonist-dependent phosphorylation of the G protein-coupled receptor kinase 2 (GRK2) by Src tyrosine kinase. *The Journal of biological chemistry*. **274**(48): 34411-34416.

Satake W, Nakabayashi Y, Mizuta I, Hirota Y, Ito C, Kubo M, Kawaguchi T, Tsunoda T, Watanabe M, Takeda A, Tomiyama H, Nakashima K, Hasegawa K, Obata F, Yoshikawa T, Kawakami H, Sakoda S, Yamamoto M, Hattori N, Murata M, Nakamura Y and Toda T (2009). Genome-wide association study identifies common variants at four loci as genetic risk factors for Parkinson's disease. *Nature genetics*. **41**(12): 1303-1307.

Saunders-Pullman R, Lipton RB, Senthil G, Katz M, Costan-Toth C, Derby C, Bressman S, Verghese J and Ozelius LJ (2006). Increased frequency of the LRRK2

G2019S mutation in an elderly Ashkenazi Jewish population is not associated with dementia. *Neuroscience letters*. **402**(1-2): 92-96.

Schagger H and von Jagow G (1991). Blue native electrophoresis for isolation of membrane protein complexes in enzymatically active form. *Analytical biochemistry*. **199**(2): 223-231.

Schapira AH, Cooper JM, Dexter D, Clark JB, Jenner P and Marsden CD (1990). Mitochondrial complex I deficiency in Parkinson's disease. *Journal of neurochemistry*. **54**(3): 823-827.

Schroeder A, Mueller O, Stocker S, Salowsky R, Leiber M, Gassmann M, Lightfoot S, Menzel W, Granzow M and Ragg T (2006). The RIN: an RNA integrity number for assigning integrity values to RNA measurements. *BMC molecular biology*. **7**(3.

Sen S, Webber PJ and West AB (2009). Dependence of leucine-rich repeat kinase 2 (LRRK2) kinase activity on dimerization. *The Journal of biological chemistry*. **284**(52): 36346-36356.

Shah K, Liu Y, Deirmengian C and Shokat KM (1997). Engineering unnatural nucleotide specificity for Rous sarcoma virus tyrosine kinase to uniquely label its direct substrates. *Proceedings of the National Academy of Sciences of the United States of America*. **94**(8): 3565-3570.

Shimura H, Hattori N, Kubo S, Mizuno Y, Asakawa S, Minoshima S, Shimizu N, Iwai K, Chiba T, Tanaka K and Suzuki T (2000). Familial Parkinson disease gene product, parkin, is a ubiquitin-protein ligase. *Nature genetics*. **25**(3): 302-305.

Silvestri L, Caputo V, Bellacchio E, Atorino L, Dallapiccola B, Valente EM and Casari G (2005). Mitochondrial import and enzymatic activity of PINK1 mutants associated to recessive parkinsonism. *Hum Mol Genet*. **14**(22): 3477-3492.

Simon-Sanchez J, Schulte C, Bras JM, Sharma M, Gibbs JR, Berg D, Paisan-Ruiz C, Lichtner P, Scholz SW, Hernandez DG, Kruger R, Federoff M, Klein C, Goate A,

Perlmutter J, Bonin M, Nalls MA, Illig T, Gieger C, Houlden H, Steffens M, Okun MS, Racette BA, Cookson MR, Foote KD, Fernandez HH, Traynor BJ, Schreiber S, Arepalli S, Zonozi R, Gwinn K, van der Brug M, Lopez G, Chanock SJ, Schatzkin A, Park Y, Hollenbeck A, Gao J, Huang X, Wood NW, Lorenz D, Deuschl G, Chen H, Riess O, Hardy JA, Singleton AB and Gasser T (2009). Genome-wide association study reveals genetic risk underlying Parkinson's disease. *Nature genetics*. **41**(12): 1308-1312.

Singh SV, Leal T, Ansari GA and Awasthi YC (1987). Purification and characterization of glutathione S-transferases of human kidney. *Biochem J*. **246**(1): 179-186.

Singleton AB (2005). Altered alpha-synuclein homeostasis causing Parkinson's disease: the potential roles of dardarin. *Trends in neurosciences*. **28**(8): 416-421.

Singleton AB, Farrer M, Johnson J, Singleton A, Hague S, Kachergus J, Hulihan M, Peuralinna T, Dutra A, Nussbaum R, Lincoln S, Crawley A, Hanson M, Maraganore D, Adler C, Cookson MR, Muenter M, Baptista M, Miller D, Blancato J, Hardy J and Gwinn-Hardy K (2003). alpha-Synuclein locus triplication causes Parkinson's disease. *Science*. **302**(5646): 841.

Sipe JD and Cohen AS (2000). Review: history of the amyloid fibril. *Journal of structural biology*. **130**(2-3): 88-98.

Smith WW, Margolis RL, Li X, Troncoso JC, Lee MK, Dawson VL, Dawson TM, Iwatsubo T and Ross CA (2005). Alpha-synuclein phosphorylation enhances eosinophilic cytoplasmic inclusion formation in SH-SY5Y cells. *The Journal of neuroscience : the official journal of the Society for Neuroscience*. **25**(23): 5544-5552.

Smith WW, Pei Z, Jiang H, Dawson VL, Dawson TM and Ross CA (2006). Kinase activity of mutant LRRK2 mediates neuronal toxicity. *Nat Neurosci*. **9**(10): 1231-1233.

Southgate RJ, Neill B, Prelovsek O, El-Osta A, Kamei Y, Miura S, Ezaki O, McLoughlin TJ, Zhang W, Unterman TG and Febbraio MA (2007). FOXO1 regulates the expression of 4E-BP1 and inhibits mTOR signaling in mammalian skeletal muscle. *The Journal of biological chemistry*. **282**(29): 21176-21186.

Specht KM and Shokat KM (2002). The emerging power of chemical genetics. *Current opinion in cell biology*. **14**(2): 155-159.

Spillantini MG, Schmidt ML, Lee VM, Trojanowski JQ, Jakes R and Goedert M (1997). Alpha-synuclein in Lewy bodies. *Nature*. **388**(6645): 839-840.

Stokes AH, Hastings TG and Vrana KE (1999). Cytotoxic and genotoxic potential of dopamine. *Journal of neuroscience research*. **55**(6): 659-665.

Surmeier DJ, Guzman JN, Sanchez-Padilla J and Goldberg JA (2011). The origins of oxidant stress in Parkinson's disease and therapeutic strategies. *Antioxidants & redox signaling*. **14**(7): 1289-1301.

Sussman DJ, Klingensmith J, Salinas P, Adams PS, Nusse R and Perrimon N (1994). Isolation and characterization of a mouse homolog of the Drosophila segment polarity gene dishevelled. *Developmental biology*. **166**(1): 73-86.

Tain LS, Chowdhury RB, Tao RN, Plun-Favreau H, Moisoi N, Martins LM, Downward J, Whitworth AJ and Tapon N (2009). Drosophila HtrA2 is dispensable for apoptosis but acts downstream of PINK1 independently from Parkin. *Cell death and differentiation*. **16**(8): 1118-1125.

Timm T, Matenia D, Li XY, Griesshaber B and Mandelkow EM (2006). Signaling from MARK to tau: regulation, cytoskeletal crosstalk, and pathological phosphorylation. *Neuro-degenerative diseases*. **3**(4-5): 207-217.

Titz B, Low T, Komisopoulou E, Chen SS, Rubbi L and Graeber TG (2010). The proximal signaling network of the BCR-ABL1 oncogene shows a modular organization. *Oncogene*. **29**(44): 5895-5910.

Ubersax JA, Woodbury EL, Quang PN, Paraz M, Blethrow JD, Shah K, Shokat KM and Morgan DO (2003). Targets of the cyclin-dependent kinase Cdk1. *Nature*. **425**(6960): 859-864.

Ueda K, Fukushima H, Masliah E, Xia Y, Iwai A, Yoshimoto M, Otero DA, Kondo J, Ihara Y and Saitoh T (1993). Molecular cloning of cDNA encoding an unrecognized component of amyloid in Alzheimer disease. *Proc Natl Acad Sci U S A*. **90**(23): 11282-11286.

Ugi S, Imamura T, Maegawa H, Egawa K, Yoshizaki T, Shi K, Obata T, Ebina Y, Kashiwagi A and Olefsky JM (2004). Protein phosphatase 2A negatively regulates insulin's metabolic signaling pathway by inhibiting Akt (protein kinase B) activity in 3T3-L1 adipocytes. *Molecular and cellular biology*. **24**(19): 8778-8789.

Urnov FD, Miller JC, Lee YL, Beausejour CM, Rock JM, Augustus S, Jamieson AC, Porteus MH, Gregory PD and Holmes MC (2005). Highly efficient endogenous human gene correction using designed zinc-finger nucleases. *Nature*. **435**(7042): 646-651.

Utley JD and Carlsson A (1965). Relative effects of L-DOPA and its methyl ester given orally or intraperitoneally to reserpine-treated mice. *Acta pharmacologica et toxicologica*. **23**(2): 189-193.

Valente EM, Abou-Sleiman PM, Caputo V, Muqit MM, Harvey K, Gispert S, Ali Z, Del Turco D, Bentivoglio AR, Healy DG, Albanese A, Nussbaum R, Gonzalez-Maldonado R, Deller T, Salvi S, Cortelli P, Gilks WP, Latchman DS, Harvey RJ, Dallapiccola B, Auburger G and Wood NW (2004). Hereditary early-onset Parkinson's disease caused by mutations in PINK1. *Science*. **304**(5674): 1158-1160.

van Egmond WN, Kortholt A, Plak K, Bosgraaf L, Bosgraaf S, Keizer-Gunnink I and van Haastert PJ (2008). Intramolecular activation mechanism of the Dictyostelium LRRK2 homolog Roco protein GbpC. *The Journal of biological chemistry*. **283**(44): 30412-30420.

Vander Heiden MG, Chandel NS, Li XX, Schumacker PT, Colombini M and Thompson CB (2000). Outer mitochondrial membrane permeability can regulate coupled respiration and cell survival. *Proceedings of the National Academy of Sciences of the United States of America*. **97**(9): 4666-4671.

Varanese S, Howard J and Di Rocco A (2010). NMDA antagonist memantine improves levodopa-induced dyskinesias and "on-off" phenomena in Parkinson's disease. *Movement disorders : official journal of the Movement Disorder Society*. **25**(4): 508-510.

Vila M, Vukosavic S, Jackson-Lewis V, Neystat M, Jakowec M and Przedborski S (2000). Alpha-synuclein up-regulation in substantia nigra dopaminergic neurons following administration of the parkinsonian toxin MPTP. *Journal of neurochemistry*. **74**(2): 721-729.

West AB, Moore DJ, Biskup S, Bugayenko A, Smith WW, Ross CA, Dawson VL and Dawson TM (2005). Parkinson's disease-associated mutations in leucine-rich repeat kinase 2 augment kinase activity. *Proc Natl Acad Sci U S A*. **102**(46): 16842-16847.

West AB, Moore DJ, Choi C, Andrabi SA, Li X, Dikeman D, Biskup S, Zhang Z, Lim KL, Dawson VL and Dawson TM (2007). Parkinson's disease-associated mutations in LRRK2 link enhanced GTP-binding and kinase activities to neuronal toxicity. *Hum Mol Genet*. **16**(2): 223-232.

Westerlund M, Ran C, Borgkvist A, Sterky FH, Lindqvist E, Lundstromer K, Pernold K, Brene S, Kallunki P, Fisone G, Olson L and Galter D (2008). Lrrk2 and alpha-synuclein are co-regulated in rodent striatum. *Mol Cell Neurosci*. **39**(4): 586-591.

White LR, Toft M, Kvam SN, Farrer MJ and Aasly JO (2007). MAPK-pathway activity, Lrrk2 G2019S, and Parkinson's disease. *Journal of neuroscience research*. **85**(6): 1288-1294.

Withers GS, George JM, Banker GA and Clayton DF (1997). Delayed localization of synelfin (synuclein, NACP) to presynaptic terminals in cultured rat hippocampal neurons. *Brain research. Developmental brain research*. **99**(1): 87-94.

Wittig I, Braun HP and Schagger H (2006). Blue native PAGE. *Nature protocols*. **1**(1): 418-428.

Yokota T, Sugawara K, Ito K, Takahashi R, Ariga H and Mizusawa H (2003). Down regulation of DJ-1 enhances cell death by oxidative stress, ER stress, and proteasome inhibition. *Biochemical and biophysical research communications*. **312**(4): 1342-1348.

Yoshida N, Haga K and Haga T (2003). Identification of sites of phosphorylation by G-protein-coupled receptor kinase 2 in beta-tubulin. *European journal of biochemistry / FEBS*. **270**(6): 1154-1163.

Zach S, Felk S and Gillardon F (2010). Signal transduction protein array analysis links LRRK2 to Ste20 kinases and PKC zeta that modulate neuronal plasticity. *PLoS One*. **5**(10): e13191.

Zarranz JJ, Alegre J, Gomez-Esteban JC, Lezcano E, Ros R, Ampuero I, Vidal L, Hoenicka J, Rodriguez O, Atares B, Llorens V, Gomez Tortosa E, del Ser T, Munoz DG and de Yebenes JG (2004). The new mutation, E46K, of alpha-synuclein causes Parkinson and Lewy body dementia. *Annals of neurology*. **55**(2): 164-173.

Zha J, Zhou Q, Xu LG, Chen D, Li L, Zhai Z and Shu HB (2004). RIP5 is a RIP-homologous inducer of cell death. *Biochem Biophys Res Commun*. **319**(2): 298-303.

Zhang C, Kenski DM, Paulson JL, Bonshtien A, Sessa G, Cross JV, Templeton DJ and Shokat KM (2005). A second-site suppressor strategy for chemical genetic analysis of diverse protein kinases. *Nature Methods*. **2**(6): 435-441.

Zhu M, Li J and Fink AL (2003). The association of alpha-synuclein with membranes affects bilayer structure, stability, and fibril formation. *The Journal of biological chemistry*. **278**(41): 40186-40197.

Zimprich A, Biskup S, Leitner P, Lichtner P, Farrer M, Lincoln S, Kachergus J, Hulihan M, Uitti RJ, Calne DB, Stoessl AJ, Pfeiffer RF, Patenge N, Carbajal IC, Vieregge P, Asmus F, Muller-Myhsok B, Dickson DW, Meitinger T, Strom TM, Wszolek ZK and Gasser T (2004). Mutations in LRRK2 cause autosomal-dominant parkinsonism with pleomorphic pathology. *Neuron*. **44**(4): 601-607.

Ziviani E, Tao RN and Whitworth AJ (2010). Drosophila parkin requires PINK1 for mitochondrial translocation and ubiquitinates mitofusin. *Proceedings of the National Academy of Sciences of the United States of America*. **107**(11): 5018-5023.

9. PUBLICATIONS ARISING FROM THIS THESIS

Journal Club

Editor's Note: These short, critical reviews of recent papers in the *Journal*, written exclusively by graduate students or postdoctoral fellows, are intended to summarize the important findings of the paper and provide additional insight and commentary. For more information on the format and purpose of the Journal Club, please see http://www.jneurosci.org/misc/ifa_features.shtml.

Unraveling LRRK2 Pathogenesis: Common Pathways for Complex Genes?

Emma Deas and Laura Dunn

Department of Molecular Neuroscience, UCL Institute of Neurology, University College London, London WC1N 3BG, United Kingdom

Review of Ng et al.

Parkinson's disease (PD) is the second most common neurodegenerative disease affecting the Western world. The disease in humans is characterized by the selective loss of dopaminergic neurons in the substantia nigra pars compacta; however, modeling this disease in transgenic animals has proven exceptionally difficult. Until recently, knock-out murine models for the PD-associated genes LRRK2, α-synuclein, Parkin, PINK1, and DJ-1 have typically failed to generate a comparable pathological setting to aid basic and therapeutic research into PD pathogenesis. Researchers have therefore used genetic manipulation in *Drosophila* to gain insight into the signaling pathways affected in PD. Typically, these fly models consist of either RNA-interference- or P-element-generated knock-outs and/or overexpression of the mutated genes associated with PD. One of the more recent proteins to be assessed in *Drosophila* is LRRK2, mutations of which can induce dominantly inherited, late-onset PD.

LRRK2 is a formidable protein, which can be difficult to express due to its large size (280 kDa) and is likely to influence a number of cellular functions due to its multidomain structure including a Roc (Ras of complex), COR (C terminal of Roc), serine/threonine kinase domain, and several WD40 repeat protein–protein interaction domains. Although the PD-associated mutations in LRRK2 are located throughout the protein, several studies have reported that an increase in kinase activity is associated with pathogenesis. Consequently, the identification of LRRK2 substrates and inhibitors has been a key focus of recent investigations (Nichols et al., 2009).

The recent publication by Ng et al. (2009) in *The Journal of Neuroscience* assessed the effects of overexpressing LRRK2 wild-type (wt) and PD-associated mutations on age-dependent dopaminergic (DA), tyrosine hydroxylase-positive (TH+) neuron loss, altered dopamine levels, and climbing defects in flies. Unlike most previous studies, in which the *Drosophila* LRRK2 homolog (dLRRK) was overexpressed or knocked out, Ng et al. (2009) specifically expressed the human wt, G2019S, Y1699C, and G2385R LRRK2 variant proteins in the wt fly eye and brain. The location of these mutations within the kinase, COR, and WD40 domains, respectively, permit the authors to determine whether mutations within the different protein domains of LRRK2 can induce similar phenotypes. Notably, Ng et al. (2009) are the first group to assess the functional consequences of mutations within the WD40 domains of LRRK2 in *Drosophila*.

Consistent with most studies (Lee et al., 2007; Imai et al., 2008), Ng et al. (2009) found no eye abnormalities in any of their LRRK2 wt or PD-mutant overexpressing flies. However, they observed a significant age-dependent loss of TH+ neurons specifically in the PPM (protocerebral posterior medial) 1 and 3 neural clusters in flies expressing PD-associated forms of LRRK2. This neuronal loss was associated with reduced lifespan, which was particularly prominent in the G2019S lines. Climbing deficits were also observed in the G2019S and Y1699C lines, but surprisingly, despite the loss of TH+ neurons, no locomotor abnormalities were identified in the G2385R mutant line.

Additional differences between the LRRK2 mutant lines were observed when the authors assessed the susceptibility of the flies' DA neurons to degeneration by administering the PD-associated toxin rotenone. Although, under normal conditions, all the LRRK2 mutant fly lines showed similar TH+ neuron loss in the PPM1 and PPM3 clusters with age, rotenone exposure accelerated TH+ neuron loss in the PPM3 cluster in both the G2019S and G2385R lines. Furthermore, rotenone treatment induced a novel set of TH+ neurons to die in the PPM2 cluster in both the G2019S and G2385R lines, and neuron loss was observed in the PPL1 and PAL clusters of the G2385R mutant. Strikingly, rotenone treatment had no effect on flies overexpressing Y1966C.

Finally, the authors demonstrated that co-overexpression of human Parkin (a neuroprotective E3 ubiquitin ligase associated with early-onset recessive PD)

Received Nov. 9, 2009; revised Dec. 14, 2009; accepted Dec. 15, 2009.

We thank Dr. Helene Plun-Favreau and Abi Li for critical appraisal of the article and helpful discussions.

Correspondence should be addressed to Dr. Emma Deas, UCL Institute of Neurology, University College London, Queen Square House, Queen Square, London WC1N 3BG, UK. E-mail: e.deas@ion.ucl.ac.uk.

DOI:10.1523/JNEUROSCI.5531-09.2010

 0270-6474/10/301577-03$15.00/0

in either the aged or rotenone-treated G2019S flies rescued the PPM1/3 and PPM2/3 TH+ neuronal death, respectively. The authors conclude that rotenone aggravates, whereas Parkin overexpression alleviates, the TH+ neuronal death induced by LRRK2 G2019S overexpression.

The finding that rotenone (a mitochondrial complex I inhibitor) accelerates TH+ neuron loss in a LRRK2 mutant model suggests that both environmental factors and genetics contribute to pathogenesis. The authors propose that these results, together with their previous work suggesting a direct interaction between LRRK2 and Parkin (Smith et al., 2005), indicate that interactions between LRRK2, Parkin, and mitochondria could have both therapeutic and mechanistic implications for PD.

Although the results reported by Ng et al. (2009) are intriguing and the mechanism underlying resistance to rotenone in their Y1699C line, is worthy of subsequent investigation, it is unfortunate that the experiments reported were not performed on all the LRRK2 mutant lines, to give a comprehensive assessment of all the phenotypes. Specifically, examination of dopamine levels in all fly lines, instead of just the G2019S line, may have provided an explanation for the lack of locomotor deficits, despite TH+ neuron loss, in the G2385R flies. These findings could open up an interesting possibility of compensatory mechanisms, perhaps similar to those occurring in patients, which could be investigated in this *Drosophila* model.

In addition, the increased sensitivity of the G2385R line to rotenone-induced TH+ neuronal death (compared to the G2019S line), particularly in neural clusters unaffected by aging, is worth noting. Previous studies have shown that the kinase activity of this LRRK2 mutant is not increased above wt levels, suggesting that pathogenesis is not induced by dysregulated kinase activity. However, expression of the G2385R protein induces cell death at comparable levels to the G2019S protein, which demonstrates increased kinase activity (West et al., 2007). Given these previous findings and the novel observations reported by Ng et al. (2009), showing that co-overexpression of Parkin can rescue TH+ neuron loss associated with age and rotenone treatment, it would have been interesting to assess the ability of Parkin co-overexpression to rescue the rotenone-induced G2385R phenotypes.

Another way Ng et al. (2009) could have gained insight into the differences in TH+ neuron loss in the aged or rotenone-treated fly lines would have been to assess 4E-BP phosphorylation levels. In 2008, it was shown that phosphorylation of 4E-BP on residues T37 and T46 are important for the pathogenic effects of mutant LRRK2 in *Drosophila* i.e., DA neuron loss, sensitivity to stress and reduced lifespan (Imai et al., 2008) (Fig. 1). Furthermore, a recent study by Tain et al. (2009) demonstrated that 4E-BP is hypophosphorylated in PINK1 and Parkin mutant fly lines and the pathogenesis observed in these lines can be rescued by either 4E-BP overexpression or rapamycin treatment (Fig. 1). The combination of these studies strongly suggests that 4E-BP phosphorylation levels are directly linked to the pathogenic phenotypes displayed in fly PD models and subsequent studies to dissect the involvement of the Akt/mTOR/4E-BP pathway in human pathogenesis should be an exciting area of future research. Given the differences in TH+ neuron loss, susceptibility to stress and increased mortality rates of their LRRK2 mutant lines, it is surprising that Ng et al. (2009) did not pursue this line of investigation, to gain mechanistic insights into their models. In particular, the group could have addressed (1) whether the prominent reduction in lifespan in the G2019S mutant flies was associated with increased phosphorylation of 4E-BP compared to the other fly lines, (2) whether the differential susceptibility to stress, observed in their fly lines, correlated with alterations in 4E-BP phosphorylation status, (3) whether the resistance to rotenone in their Y1699C line is associated with reduced 4E-BP phosphorylation levels, and finally (4) whether an alteration in 4E-BP phosphorylation state is induced in the rescued G2019S mutant line due to Parkin overexpression.

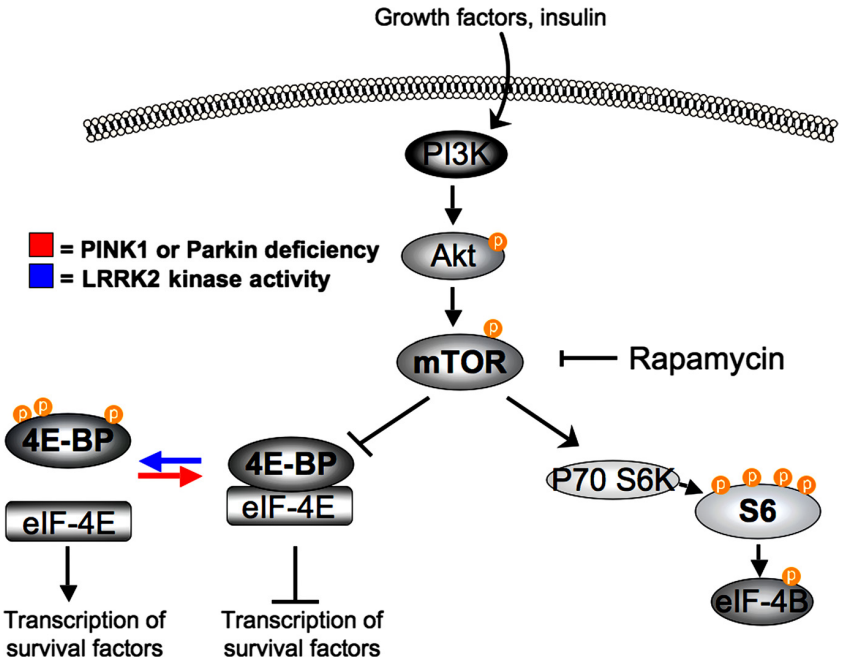

Figure 1. Modulation of 4E-BP phosphorylation status by PD-associated proteins. 4E-BP phosphorylation levels are regulated by the mTOR kinase, which acts downstream of Akt. In its hypophosphorylated state, 4E-BP binds to the transcription factor eIF-4E and inhibits the subsequent transcription of survival factors. Upon phosphorylation, 4E-BP dissociates from eIF-4E and permits transcription. Recently, the active LRRK2 kinase was shown to phosphorylate 4E-BP, whereas loss of either PINK1 or Parkin function was shown to result in hypophosphorylated 4E-BP.

Finally, it would have been interesting if additional aspects of the rescue phenotypes in the G2019S-Parkin coexpressing fly lines had been investigated. For example, Parkin overexpression has been shown to upregulate PINK1 protein levels in *Drosophila*, and recently, PINK1 was shown to phosphorylate Parkin, resulting in Parkin's relocalization to mitochondria (Yang et al., 2006; Kim et al., 2008). Since PINK1 can protect against oxidative stress, alleviate mitochondrial damage induced by complex I inhibitors and is tightly linked to Parkin (Deas et al., 2009), it seems premature for the authors to attribute all of the protective effects observed exclusively to Parkin.

In summary, Ng et al. (2009) have provided novel insights into the effects of the LRRK2 G2385R mutant protein *in vivo*, a PD-associated mutation which has received relatively little attention in the literature compared to mutations in the Roc

and COR domains. The location of this mutation in the protein–protein interaction WD40 domains, rather than an enzymatic domain of LRRK2, raises interesting questions about the mechanism by which mutant LRRK2 mediates PD pathogenesis. The generation of this particular fly model is therefore an important step toward advancing our overall understanding of LRRK2 function in PD. Furthermore, as the second comprehensive, detailed analysis of TH+ neuron loss in a combination of LRRK2 *Drosophila* models, these results finally allow a direct comparison between studies. The ability to compare studies is essential because several groups investigating the effects of PD-associated LRRK2 (or equivalent dLRRK) mutations on photoreceptor degeneration, TH+ neuron loss, muscle pathology, locomotor function, and lifespan have reported discrepancies in fly phenotypes (Lee et al., 2007; Imai et al., 2008; Liu et al., 2008; Vendarova et al., 2009). Specifically, LRRK2 wt and PD mutant fly lines range from having photoreceptor degeneration to having no abnormal eye phenotype, significant reductions in TH+ neuron numbers in all neuronal clusters to no apparent loss of TH+ neurons in any of the clusters, severe muscle pathology resulting in abnormal wing posture to no overt muscle phenotype, and either decreased, normal, or increased lifespan. On the surface, these discrepancies are confusing given that the authors all use the same GAL4 drivers, i.e., GMR (eye specific), elav (pan neuronal), Ddc (DA neuron specific), and TH (DA neuron specific), to selectively target LRRK2 wt or mutant protein expression to specific tissue regions. However, different phenotypes can be caused by insertion-site-specific effects on transgene expression levels or dosage effects caused by multiple transgene insertions in a single embryo (Spradling and Rubin, 1983). In addition, perhaps some of the discrepancy, specifically in measures of TH+ neuron loss, could be attributed to the fact that not all studies have assessed the same neural clusters. Moreover, in some cases, neurons assigned to different clusters by some groups have been combined and examined as a single cluster by others, and this may have resulted in the TH+ neuron loss dropping below the level of significance. However, before any of the phenotypes are potentially ignored (based on a consensus between studies), it is important to remember that the pathology of LRRK2 patients carrying the same pathogenic mutation is also varied (Giasson et al., 2006). Given these observations in patients, it is perhaps not surprising that a range of phenotypes have been observed in fly models recapitulating the disease. As a consequence, further assessments of LRRK2 pathogenic function in *Drosophila* will be required to address these issues.

References

Deas E, Plun-Favreau H, Wood NW (2009) PINK1 function in health and disease. EMBO Mol Med 1:152–165.

Giasson BI, Covy JP, Bonini NM, Hurtig HI, Farrer MJ, Trojanowski JQ, Van Deerlin VM (2006) Biochemical and pathological characterization of Lrrk2. Ann Neurol 59:315–322.

Imai Y, Gehrke S, Wang HQ, Takahashi R, Hasegawa K, Oota E, Lu B (2008) Phosphorylation of 4E-BP by LRRK2 affects the maintenance of dopaminergic neurons in *Drosophila*. EMBO J 27:2432–2443.

Kim Y, Park J, Kim S, Song S, Kwon SK, Lee SH, Kitada T, Kim JM, Chung J (2008) PINK1 controls mitochondrial localization of Parkin through direct phosphorylation. Biochem Biophys Res Commun 377:975–980.

Lee SB, Kim W, Lee S, Chung J (2007) Loss of LRRK2/PARK8 induces degeneration of dopaminergic neurons in *Drosophila*. Biochem Biophys Res Commun 358:534–539.

Liu Z, Wang X, Yu Y, Li X, Wang T, Jiang H, Ren Q, Jiao Y, Sawa A, Moran T, Ross CA, Montell C, Smith WW (2008) A *Drosophila* model for LRRK2-linked parkinsonism. Proc Natl Acad Sci U S A 105:2693–2698.

Ng CH, Mok SZ, Koh C, Ouyang X, Fivaz ML, Tan EK, Dawson VL, Dawson TM, Yu F, Lim KL (2009) Parkin protects against LRRK2 G2019S mutant-induced dopaminergic neurodegeneration in *Drosophila*. J Neurosci 29:11257–11262.

Nichols RJ, Dzamko N, Hutti JE, Cantley LC, Deak M, Moran J, Bamborough P, Reith AD, Alessi DR (2009) Substrate specificity and inhibitors of LRRK2, a protein kinase mutated in Parkinson's disease. Biochem J 424:47–60.

Smith WW, Pei Z, Jiang H, Moore DJ, Liang Y, West AB, Dawson VL, Dawson TM, Ross CA (2005) Leucine-rich repeat kinase 2 (LRRK2) interacts with parkin, and mutant LRRK2 induces neuronal degeneration. Proc Natl Acad Sci U S A 102:18676–18681.

Spradling AC, Rubin GM (1983) The effect of chromosomal position on the expression of the *Drosophila* xanthine dehydrogenase gene. Cell 34:47–57.

Tain LS, Mortiboys H, Tao RN, Ziviani E, Bandmann O, Whitworth AJ (2009) Rapamycin activation of 4E-BP prevents parkinsonian dopaminergic neuron loss. Nat Neurosci 12:1129–1135.

Venderova K, Kabbach G, Abdel-Messih E, Zhang Y, Parks RJ, Imai Y, Gehrke S, Ngsee J, Lavoie MJ, Slack RS, Rao Y, Zhang Z, Lu B, Haque ME, Park DS (2009) Leucine-rich repeat kinase 2 interacts with Parkin, DJ-1 and PINK-1 in a *Drosophila melanogaster* model of Parkinson's disease. Hum Mol Genet 18:4390–4404.

West AB, Moore DJ, Choi C, Andrabi SA, Li X, Dikeman D, Biskup S, Zhang Z, Lim KL, Dawson VL, Dawson TM (2007) Parkinson's disease-associated mutations in LRRK2 link enhanced GTP-binding and kinase activities to neuronal toxicity. Hum Mol Genet 16:223–232.

Yang Y, Gehrke S, Imai Y, Huang Z, Ouyang Y, Wang JW, Yang L, Beal MF, Vogel H, Lu B (2006) Mitochondrial pathology and muscle and dopaminergic neuron degeneration caused by inactivation of *Drosophila* Pink1 is rescued by Parkin. Proc Natl Acad Sci U S A 103:10793–10798.